(12) INTERNATIONAL APPLICATION PUBLISHED UNDER THE PATENT COOPERATION TREATY (PCT)

(19) World Intellectual Property Organization
International Bureau

(43) International Publication Date
28 February 2002 (28.02.2002)

PCT

(10) International Publication Number
WO 02/16865 A2

(51) International Patent Classification[7]: G01B 11/00

(21) International Application Number: PCT/DK01/00564

(22) International Filing Date: 24 August 2001 (24.08.2001)

(25) Filing Language: English

(26) Publication Language: English

(30) Priority Data:
PA 2000 01258 25 August 2000 (25.08.2000) DK
60/244561 31 October 2000 (31.10.2000) US

(71) Applicant *(for all designated States except US)*: **3SHAPE APS** [DK/DK]; Bredgade 58, 2-3.sal, DK-1260 Copenhagen K (DK).

(72) Inventors; and
(75) Inventors/Applicants *(for US only)*: **DEICHMANN, Nikolaj** [DK/DK]; Kirsteinsgade 12, 1.sal, DK-2100 Copenhagen Ø (DK). **CLAUSEN, Tais** [DK/DK]; Viborggade 72A, 1.tv., DK-2100 København Ø (DK).

(74) Agent: **HØIBERG APS**; St. Kongensgade 59B, 4.sal, DK-1264 Copenhagen K (DK).

(81) Designated States *(national)*: AE, AG, AL, AM, AT, AT (utility model), AU, AZ, BA, BB, BG, BR, BY, BZ, CA, CH, CN, CO, CR, CU, CZ, CZ (utility model), DE, DE (utility model), DK, DK (utility model), DM, DZ, EC, EE, EE (utility model), ES, FI, FI (utility model), GB, GD, GE, GH, GM, HR, HU, ID, IL, IN, IS, JP, KE, KG, KP, KR, KZ, LC, LK, LR, LS, LT, LU, LV, MA, MD, MG, MK, MN, MW, MX, MZ, NO, NZ, PH, PL, PT, RO, RU, SD, SE, SG, SI, SK, SK (utility model), SL, TJ, TM, TR, TT, TZ, UA, UG, US, UZ, VN, YU, ZA, ZW.

(84) Designated States *(regional)*: ARIPO patent (GH, GM, KE, LS, MW, MZ, SD, SL, SZ, TZ, UG, ZW), Eurasian patent (AM, AZ, BY, KG, KZ, MD, RU, TJ, TM), European patent (AT, BE, CH, CY, DE, DK, ES, FI, FR, GB, GR, IE, IT, LU, MC, NL, PT, SE, TR), OAPI patent (BF, BJ, CF, CG, CI, CM, GA, GN, GQ, GW, ML, MR, NE, SN, TD, TG).

Published:
— *without international search report and to be republished upon receipt of that report*

For two-letter codes and other abbreviations, refer to the "Guidance Notes on Codes and Abbreviations" appearing at the beginning of each regular issue of the PCT Gazette.

WO 02/16865 A2

(54) Title: OBJECT AND METHOD FOR CALIBRATION OF A THREE-DIMENSIONAL LIGHT SCANNER

(57) Abstract: The invention relates to the field of precision calibration of three-dimensional light scanners. The invention specifically concerns a calibration object for calibration of all parameters of a three-dimensional light scanning system, the calibration object having at least one plane of symmetry and whereby at least one 3D object feature curve of each symmetric part is a continuous curve. The invention further relates to a method for calibration of a three-dimensional light scanner and a method for three-dimensional light scanning. Further specific embodiments for scanning of and modelling of objects for the ear and/or ear canal, and for scanning and modelling of dental implants are described.

Object and method for calibration of a three-dimensional light scanner.

Technical field

The invention relates to the field of precision calibration of three-dimensional light scanners. The invention specifically concerns a calibration object for calibration of all parameters of a three-dimensional light scanning system, a method for calibration of a three-dimensional light scanner and a method for three-dimensional light scanning. Furthermore, the invention relates to specific embodiments for scanning of and modelling of objects for the ear and/or ear canal, and for scanning and modelling of dental implants.

Prior art

System for three-dimensional light scanning are well known in the prior art. They typically comprise one or more light sources projecting a light sheet on the object to be scanned, one or more cameras and data processing equipment to convert the recorded image co-ordinates to three dimensional co-ordinates using state of the art software. The precision of the light sources and cameras are very high today as are also the software developed to detect the intersection of the light sheet with the object and convert the two-dimensional data to three dimensional co-ordinates. Therefore differences in and hence improvement of the precision primarily resides in the calibration of the systems.

Precision is of utmost importance in the applications where the scan data are used for modelling an object which must fit precisely into or onto another object. Such applications are e.g. objects for the ear canal such as hearing aids, dental implants and other prostheses for the body. For hearing aid shells sub-millimetre precision is required or the shell will cause irritation and possibly infection to the epidermis of the ear canal. For dental implants the precision requirement is even greater, since a human being can detect differences less than 1/10 of a millimetre when biting. Therefore systematic or random errors in the calibration of scanners for these uses can be fatal. This has hitherto limited the use of scanning in the modelling of such implants and shells.

Methods and object for calibration of three-dimensional light scanners are known from the prior art. The majority of such calibration methods are composed of several steps often using different calibration objects for calibrating different parameters. One general drawback is that the known methods do not allow an accurate calibration of the light sheet offset.

US 5,978,092 (BROWN) teaches a number of steps necessary for calibration of the system according to the publication. According to the disclosure several different objects of different shape are needed for calibration of the different parameters of the system.

US 5,870,220 (REAL-TIME GEOMETRY CORP) also concerns the calibration of a scanner. Calibration for camera lens distortion is carried out by scanning a flat reference surface with a repeated and evenly spaced pattern of laser-lines. As an alternative an image of a rectilinear grid pattern on a flat reference surface can be scanned for calibration. Calibration of focal point value of the camera is carried out by scanning a flat reference surface on which an equilateral triangle of known dimensions is drawn. It therefore appears that several steps and several calibration objects are needed to calibrate the scanner.

US 5,561,526 (LOCKHEED MISSILES & SPACE COMPANY INC.) concerns a calibration object and a method for calibration of a three dimensional scanner. The object shown in Figures 8, 9, and 10 is a plate with a plurality of substantially identical truncated pyramids each having countersunk pins During calibration the surface of the calibration object is first accurately measured by conventional traceable mechanical methods. Thereafter the object is placed in the scanner and scanned. The intersections of the plane surfaces of the pyramids are calculated and the three dimensional co-ordinates for the intersections are calculated. To this end approximate values of the system parameters of the scanner are used. Finally the calibration is carried out by varying the system parameters in order to minimise the difference between the mechanically measured co-ordinates and the estimated co-ordinates. This is done in a least squares sense. Calibration precision using this method is primarily determined by the accuracy of the initial mechanical measurement of the calibration object. The disclosed calibration object does not have a plane of symme-

try to calibrate the laser sheet displacement and angle and furthermore has very few feature co-ordinates to use in the calibration.

US 5,661,667 (VIRTEK VISION CORP) concerns a three-dimensional scanner wherein calibration is carried out by placing reflection targets on pre-determined locations on the object to be scanned so that the co-ordinates of the reflection targets are known. The scanner can then be calibrated using these reference points.

US 5,991,437 (REAL-TIME GEOMETRY CORPORATION) concerns a system for high accuracy calibration of a three-dimensional light scanning system, which provides an object for calibration of a known geometry, such as a plane or a sphere. Upon that object is marked a pattern of points or geometric shapes, such as a set of equilateral triangles or their vertices. A set of computer programmed elements process photographic images of the object (containing a depiction of the pattern of geometric objects) and scanned images of the object to calibrate to high precision parameters, including a focal point relationship value for scanning systems which use a camera as an image collector (which describes the relationships between the focal point of the lens and the light/image collection device of the camera), a set of values to correct for distortion of the lens, the relative distance between the image collector and the scanner light source and also an initial angle to determine light position scanning. The known geometric constraints of the object allow the location of the object to be determined by photographic images. By scanning the object and computing 3D X,Y,Z co-ordinates for those points against a constraint that the X,Y,Z co-ordinates fit onto the surface of the object, the system calibrates parameters pertaining to the relative distances between the image collector and light source, an initial angle of rotation for systems which employ movable light sources and other parameters. The system is applied to multiple camera scanning systems to calibrate rotation matrices and translation vectors which facilitate the joining of the scanned data.

Specific examples of pre-determined geometric shapes are one or several equilateral or right triangles. The calibration object may be a flat plane or a ball. According to the publication there is no need to know the distance between the different geometric shapes on the calibration object. Only the exact size of the geometric shapes need to be known. A disadvantage of such calibration is that the disclosed calibra-

tion object does not have a plane of symmetry to calibrate the laser sheet displacement and angle and furthermore has very few feature co-ordinates to use in the calibration.

WO 98/59300 (REAL TIME GEOMETRY CORP.) concerns a system and method for modelling 3D objects and 2D images by wire frame mesh constructions having data points that combine both spatial data and surface information such as colour or texture data. The use of the complex data points (e.g., X, Y, Z, R, G, B in 3D and x, y, R, G, B in 2D) allows the modelling system to incorporate both the spatial features of the object or image as well as its colour or other surface features into the wire-frame mesh. According to one embodiment the system is adapted to determine the distance of each data point to a pre-selected reference object. Calibration is performed using a pre-selected reference object, which may be in the shape of a sphere or a plane.

WO 00/04506 (GEOMETRIX INC.) concerns a system and a method for computer modelling of 3D objects and 2D images by mesh constructions that incorporate non-spatial data such as colour or texture.

According to one disclosed embodiment the system is automatically calibrated. The disclosed calibration object is of round shape. For calibration the disc shaped object of known size is secured to a turntable and it is viewed by the camera in an angle so that the image seen by the camera is of ellipse shape. The system subsequently determines the axes of the ellipse and calibrates the following parameters of the system

a) the angle between the rotation axis of the disc and the ray connection the centre of the disc with the camera;
b) the viewing angle subtended by a pair of image rays extending to the two end points of the minor axis;
c) the angle of the image plane subtended by the axis of rotation of the disc target and the vertical image direction, and
d) the distance and height of the camera.

According to the disclosure it is not necessary for the camera to capture a view of the whole disc as long as one of the minor and both major axes can be seen. A

drawback of such a calibration method is primarily that very few data points are used and the points used do not cover the scanned area. Therefore the calibration precision is not great enough to allow for sub-millimetre calibration.

US 6,044,170 (REAL-TIME GEOMETRY CORP.) concerns a system and a method for rapid shape digitising and adaptive mesh generation. According to the publication the system can be calibrated using an auto-calibration procedure. During auto-calibration the camera scans a flat reference surface such as a wall covered by a white sheet of paper. Scanning of a two-dimensional object of known dimensions for calibration will not yield a satisfactory calibration for three-dimensional purposes.

US 5,988,862 (CYRA TECHNOLOGIES INC.) concerns an integrated system for imaging and modelling three dimensional objects. In order to calibrate the lens distortion, this distortion is removed by comparing the image the camera produces when aimed at a carefully designed and printed calibration target image. The difference in the anticipated image and the recorded image provides the information needed to warp subsequently acquired images to eliminate the distortion. The publication provides no details about the shape of the target image. Since the comparison of the image and the printed image of the calibration target takes place in two dimensions – the image of the calibration target being printed – the method does not allow for precision calibration for three-dimensional purposes.

US 5,999,840 (MASSACHUSETTS INSTITUTE OF TECHNOLOGY) concerns a method and a system for registration of three dimensional data sets, calibration of the laser scanning unit including the laser striping unit and the cameras is performed using scan data from a precisely machined shape referred to as a gauge. This known shape, along with the images of the laser scans from it, can be used to precisely calibrate the laser instrument such that all subsequent measurements, anywhere in the operating range of the scanning unit will result in accurate 3D measurements as measured relative to some fixed reference frame. The shape of the gauge is not disclosed.

US 6,081,273 (MICHIGAN STATE UNIVERSITY) concerns a method and a system for building three-dimensional object models such as virtual reality object models. Prior to scanning the system needs to be calibrated. This is done by scanning a

calibration reference object having a special 3D calibration pattern. The pattern shown as an example is a cube. For high accuracy, the 3D calibration pattern should be similar to the size of the object to be scanned. As an alternative to a calibration reference object, the object to be scanned may be used for calibration. This merely requires that the 3D co-ordinates of a number of reference points on the object are determined by measurement prior to calibration.

Using the object to be scanned for calibration of the scanning system is a cumbersome way to perform the calibration, since measurement of reference points and calibration is required prior to every scan of a new object. Furthermore, since the disclosure provides no information as to where to select the reference points it is not possible to determine the precision of the calibration method.

US 5,753,931 (NIKE INC.) features a method for capturing surface information regarding the surface shape of an object, such as the underside of a human foot or other extremity. Also disclosed is a solid calibration gauge manufactured from aluminium and having a sawtooth-type pattern. The surface of the calibration gauge comprises a plurality of nodes and ridges. The method for calibration includes comparison of the "real" X, Y, and Z co-ordinates with the estimated co-ordinates and adjustment of the calibration parameters accordingly. The process is repeated until the difference between "real" and scanned co-ordinates is below a pre-determined threshold.

US 5,549,476 (Stern) relates to a method of making dental restorations including temporarily repairing a tooth area to be restored to desired final shape, taking a first impression of the tooth area to be restored, preparing the tooth to be restored and forming a second impression within first impression with material that is non-adherent to the first impression material. The first impression and the second impression are separated. The second impression is scanned to obtain a digital image of the final restoration. A model of the dental restoration can the be made using 3-D milling. The publication concerns no information about calibration of the scanner.

US 5,121,333, US 5,121,334, US 5,128,870, US 5,184,306, US 5,027,281, and US 5,257,203 (REGENTS OF THE UNIVERSITY OF MINNESOTA) describe a method and apparatus for the automated reproduction of three dimensional objects of com-

plex and unique geometry. A computer acquires data describing an object and its surroundings, constructs a computer-based three dimensional model of the object from that data, superimposes an ideal geometry on the computer-based model, alters the ideal geometry to fit the form and function required of the reproduction, and then guides a milling machine in the fabrication of the reproduction.

The publications primarily concern the manufacture of dental prostheses. It is mentioned that the system can be used for the manufacture of in-the-ear hearing aid housings and moulds or implants to replace damaged bones but there are no examples of such use.

US 4,575,805 (MOREMANN ET AL.) also concerns a method and an apparatus for the fabrication of custom-shaped implants. The surface characteristics of an organ that needs restoration, for example, a tooth which has been prepared for an inlay insertion, are read by means of a non-contact scan-head. The three-dimensional shape parameters of the implant required to restore the tooth in function and appearance are computed on the basis of the recorded contour data. These parameters are then used in a program sequence which controls a milling, cutting or erosive process in order to manufacture the restorative inlay while the patient waits.

The publication further describes that the scanner can be calibrated by mapping a standard object, which has been measured utilising conventional techniques e.g. callipers.

WO 00/34739 (FAGAN ET AL.) concerns a method for manufacturing hearing aid shells involving the use of a specially adapted ultrasonic probe head to safely measure the contours of the ear canal without contact with the surface being measured. The recording of the data in the ear canal is made possible by filling the canal with a liquid and inserting the ultrasonic probe. The scan data are processed by a computer and the data are used with a rapid prototyping set-up such as stereo lithography, selective laser sintering, laminate object modelling, inkjet modelling, fused depositing modelling, 3DP or any other system that produces real models from computer mathematical models to manufacture the hearing aid shell. One disadvantage of the system is the need for filling the patient's ear completely with water. This can extremely annoying to patients and they may experience symptoms of

nausea during and after such treatment. Furthermore it is doubtful whether it is really possible to determine the three dimensional co-ordinates of the surface of the ear canal with the required precision using an ultra sonic probe. An ultrasonic sound signal emitted does not travel in just one direction in the liquid in the ear canal. As the ultrasonic waves are reflected by the surface of the ear canal they travel in many different directions. Thus the transducers of the ultrasonic probe will detect a number of signals of varying size with different delays after the emission of one sound signal. It must be extremely difficult for the underlying software to determine which of the signals to use in the determination of the co-ordinates. The disclosure provides no information on how to perform this operation.

EP 0 516 808 (TØPHOLM & WESTERMANN APS) concerns a method for computer assisted manufacture of otoplastic individually fitted to the contours of the ear canal. According to the described method a digital representation of the internal contours of the ear canal are used for milling or 3D printing of a hearing aid shell. A computer is used to optimise the location of the components of the hearing aid and the thickness of the walls of the shell. The disclosure does not suggest the solution of scanning the internal contours of the ear canal or a model of the ear canal using a laser scanner.

US 5,056,204 (ASCOM AUDIOSYS AG) concerns a method for milling of hearing aids whereby the internal contours of the ear canal are allegedly recorded by a laser apparatus located outside the ear of the patient. The disclosure contains no means to direct the laser light into the ear canal. Due to occlusion effects only part of the ear canal can be scanned according to the disclosed method. Furthermore, the disclosure fails to take regard to the fact that the individual is likely to move while the image is recorded.

Definitions

For the purposes of the present invention, the following definitions are provided. For a graphical representation of the terms, reference is made to the accompanying drawings especially Figure 22:

3-D object feature curves 2201

3-D object feature curves are lines or curves on a calibration object. The 3D object feature curves are characterised by real world 3D co-ordinates. When illuminated with a light contour such as that formed by a laser sheet, points on the 3D object feature curves are visible by a detection device such as a camera, a CCD or a CMOS. 3D object feature curves can be made by painting the lines on the calibration object, so that they differ in colour from the other surface of the calibration object. In this case a colour sensitive detection device is required. More preferably they are edges formed on the calibration object, by e.g. milling away part of the object. In this case the feature points are detected as corners on the intersection contour created by the sheet of light on the object.

2D- image feature curves 2202

2D-image feature curves are created by a sheet of light on an object and are detected in the images recorded by the detection device (e.g. camera, CMOS, CCD). The detection comprises state of the art algorithms. One sheet of light may produce a number of 2D image feature curves. Where these multiple 2D image feature curves intersect image feature points are located having a 2D x and y image co-ordinate in the image in which it is recorded. The image feature points are representations of the 3D object feature curves.

It is to be understood in the foregoing and in the following that when the term image is used, this also encompasses the term picture, which describes a 2-D image recorded by a camera.

Summary of the invention

According to a first embodiment of the invention is provided a three dimensional calibration object having at least one plane of symmetry and whereby at least part of at least one 3D object feature curve of each symmetric part is a continuous curve. By providing the calibration object with a plane of symmetry, it becomes possible to calibrate all parameters, including the laser sheet parameters and the offset of an optional rotational angle. The continuous symmetric 3D object feature curves of the object assist in the calibration of the laser sheet parameters and angle offset by pro-

viding an exceptionally precise estimate for the plane of symmetry of the object. Furthermore, they provide numerous calibration points for use in the transformation of image co-ordinates to laser sheet co-ordinates and thereby to real-world co-ordinates.

Preferably the object is rigid, such as being manufactured from metal, preferably aluminium or from a material selected from the group consisting of alloy, stainless steel, a plastic polymer, kevlar®, carbon, wood. The rigidity of the object makes it more stable and the materials listed above all have excellent properties in respect of hardness, temperature expansion and workability.

According to an especially preferred embodiment at least part of the surface of the object is rough or non-glossy. Ideally the surface of the calibration object should have the characteristics of a perfect *lambertian* surface to minimise the specular and diffuse reflection of light from its surface during calibration.

The continuous curves of the at least part of the at least one 3D object feature curve are preferably described by continuous mathematical functions. Thereby the calculation of points on the curves becomes especially easy, since this can be done merely by using the mathematical functions. This technical feature is also an advantage if the object is milled using an automatic high precision milling machine, since the functions can simply be entered into the milling program. Preferably the functions describe part of a spiral, an ellipse, or a circle, or those that comprise trigonometric functions such as sinus, cosinus, tangens, cotangens. These mathematical functions have the advantage that the 3D object feature curves cover a large part of the camera field of view so that the calibration becomes precise over the whole field of view.

Each symmetric part may have two, three, four, six or more 3D object feature curves being symmetric over the plane of symmetry. The presence of multiple 3D object feature curves improves the estimation of laser sheet parameters and angle offset. Preferably the distance between two 3D object feature curves of each symmetric part is constant, and more preferably all distances between 3D object feature curves of each symmetric part are constant.

The object may have an axis of rotation such as an essentially vertical or horizontal axis of rotation. By recording numerous images of the object during rotation and/or translation the calibration performance is greatly improved.

Improved calibration is obtained by having two axes of rotation or three, four, five or more axes of rotation.

A mathematical combination of image feature points or features derived from these points plotted as a function of the angle of rotation φ or the translation preferably produces an estimable mathematical function. When this condition is fulfilled it becomes easier to estimate the plane of symmetry of the object. Note that the image feature points are projections of 3D object feature curves and detected in images of the object recorded by a camera at discrete values of angle of rotation and/or translation. The plotted mathematical combination may be the image feature point x co-ordinate, the image feature point y co-ordinate, the sum of the x and y co-ordinates, the product of the x and y co-ordinates, any other function of the x and y co-ordinates such as $x^n + y^n$, $x^n - y^n$, $y^n - x^n$, $x^n * y^n$, x/y, y/x, x^n/y^n, y^n/x^n, sinus $(x^n + y^n)$, cosinus $(x^n + y^n)$, tangens $(x^n + y^n)$, cotangens $(x^n + y^n)$, sinus $(x^n * y^n)$, cosinus $(x^n * y^n)$, tangens $(x^n * y^n)$, cotangens $(x^n * y^n)$, exp $(x^n * y^n)$, hyp $(x^n * y^n)$ or features derived from these points, e.g. the difference in rotation angle or translation between symmetric points.

The estimable mathematical function obtained by the plot of the mathematical combination of image feature points or derived features as a function of rotational angle or translation preferably can be modelled with a first order approximation, a second order approximation, a third, fourth, fifth, sixth, seventh, eighth, ninth, tenth, or n^{th} order approximation. These functions are easily estimated using state of the art mathematical software.

Preferably the object has a size corresponding to the size of the objects to be scanned later. Thereby a precise calibration of the three-dimensional room housing the object to be scanned later is obtained. The linear size of the object could be between 50 and 150 % of the linear size of the object to be scanned later, such as between 60 and 140 %, for example between 70 and 130 %, such as between 75 and 125 %, such as between 80 and 120 %.

The object may also have a size corresponding to the camera field of view. Thereby the whole field of view can be calibrated and irregularities in e.g. the lens can be compensated for during calibration. The linear size of the object may be at least 10% of the camera field of view, such as at least 20%, for example at least 30%, such as at least 40%, for example at least 50%, such as at least 60%, for example at least 70%, such as at least 75%, for example at least 80%, such as at least 85%, for example at least 90%, such as at least 95%.

For certain applications, such as for scanners for ear scanning it is advantageous that the calibration object is hollow and has the 3D object feature curves on the inside.

To provide improved precision, the calibration object may be provided with fastening means to secure it to the scanner or the table of the scanner.

According to a second aspect of the invention is provided a method for calibration of a three dimensional light scanner comprising the steps of providing a three dimensional light scanner, providing a calibration object according to the invention, scanning the calibration object, determining image feature co-ordinates being representations of at least one pair of 3D object feature curves for each of a discrete number of values of an angle of rotation and/or a translation, a pair consisting of one 3D object feature curve in each symmetric part of the calibration object, changing the calibration parameters to fit the calibration object. Due to the presence of the 3D object feature curves and plane of symmetry, a very accurate estimation of the laser sheet parameters can be obtained in one calibration step.

Preferably, a sheet of laser light is projected onto the calibration object to produce image feature curves.

When preferred, the image feature lines may also be determined using the Hough transformation, filter search, max intensity, threshold, centre of gravity, derivatives or other procedures.

The image feature co-ordinates are found as the intersection between image feature curves. These intersections could be seen in the images as corners or sharp edges of the image feature curves. The image feature co-ordinates may be found as the intersection between image feature curves such as the intersection between two n^{th} order curves, as the intersection between two first order curves, as the intersection between two second order curves, as the intersection between two third order curves, as the intersection between a fist order curve and a second order curve, as the intersection between a first order curve and a third order curve, or as the intersection between a second order curve and a third order curve or as the intersection between any other possible combination of curves.

Preferably, the calibration method further comprises plotting of a mathematical combination of image feature points or features derived from these points against the angle of rotation φ or the translation of the calibration object. By plotting this function and optionally estimating a mathematical function describing the relationship between the function of an image co-ordinate and the angle of rotation, estimation of the laser sheet parameters and angle of rotation becomes especially precise. The method may further comprise determination of the mean plane of symmetry in the plot.

The mean plane of symmetry can be determined by calculating the mean angle of rotation / mean translation for pairs of image feature points having the same value in the mathematical combination. Doing this produces multiple estimates for the encoder offset and laser sheet displacement allowing also for the estimate of the laser sheet angle.

Alternatively mathematical formulas can be derived for the curves, which appear in some of the plots of the mathematical combination as a function of the angle of rotation or the translation. Given these curves and the corresponding formulas the encoder offset, the laser sheet displacement and the laser sheet angle can be estimated.

Preferably laser sheet co-ordinates of the 3D object feature curves are estimated corresponding to a discrete number of values of angle of rotation and/or translations.

These values should preferably cover the whole circumference and/or length of the calibration object.

2D co-ordinates of the 3D object feature curves corresponding to a discrete number of values of angle of rotation and/or translation may be calculated from mathematical functions determining the 3D object feature curves. In order to determine the calibration parameters such as camera position, camera orientation, and camera optic parameters, pairs of 2D laser sheet co-ordinates are compared to calculated 2D co-ordinates for a discrete number of values of angle of rotation. This comparison preferably comprises using the Tsai or the Heikkilä algorithm. The advantage of the Tsai and the Heikkilä algorithm in this context is that it provides rapid and precise estimation of the calibration parameters such as radial lens distortion.

Alternative methods for calibration comprise direct linear transformation, and direct non-linear matrix transformation optionally in combination with an optimisation procedure such as least squares means to minimise the error. In these cases initial calibration parameters may be estimated to facilitate the convergence of the parameters during optimisation.

To improve calibration precision outliers may be excluded from the calibration. Outliers can e.g. be identified in the plot of the mathematical combination of image feature co-ordinates against the angle of rotation / the translation or by back projection of co-ordinates after an initial calibration.

2% of the feature points deviating most from the back-projected 2D image feature curves may be excluded from the calibration or at least 3%, such as at least 5%, for example at least 10%, for example at least 12%, such as at least 15% for example at least 20, preferably at least 25%, for example at least 30 %, more preferably at least 33 % may be excluded to improve calibration precision.

In order to cover the whole circumference and/or length of the calibration object the discrete number of values for angle of rotation / translation may be at least 100, preferably at least 240, for example at least 500, such as at least 750, for example at least 1000, such as at least 1200, for example at least 1500, such as at least 1800, for example at least 2000, such as at least 2400, for example at least 3000,

for example at least 3600, such as at least 4200. The higher the discrete number of values of angle of rotation / translation, the higher the calibration precision.

According to a third aspect of the invention is provided a method for three-dimensional scanning comprising the steps of providing a three-dimensional light scanner, calibrating the system, scanning an object determining image co-ordinates on the light contour for each of a discrete number of values of an angle of rotation/ a translation, calculating three dimensional real world co-ordinates describing the surface of the object. The advantages of a scanning method according to the invention is the improved precision compared to prior art scanning methods. The precision normally lies in the sub-millimetre range.

Preferably calibration is performed using a calibration object according to the invention using the calibration method according to the invention.

The three-dimensional real world co-ordinates may be calculated from the image co-ordinates using the Tsai algorithm, the Heikkilä algorithm, direct linear transformation or be estimated using direct non-linear matrix transformation. Image co-ordinates may be determined using Hough transformation, filter search, max intensity, threshold, centre of gravity, and derivatives or similar known algorithms.

The three-dimensional light scanner preferably comprises at least one light sources and at least one cameras such as at least two light sources and at least two cameras such as at least three light sources and at least three cameras, for example three light sources and six cameras. By increasing the number of cameras and light sources, occlusion effects are minimised and a more precise scanning of the whole three-dimensional room housing the object to be scanned is obtained.

The object to be scanned may be rotated and/or translated during scanning or the camera and the light source may be rotated and/or translated around the object during scanning. The actual motion may advantageously be planned by an automatic motion planner, which creates the optimal motion for the individual object, camera and light source. One advantage associated with this embodiment is that occlusion effects can be minimised and in some cases eliminated.

The object to be scanned may advantageously be aligned manually to the centre of a rotating plate using the cross section between two laser sheets as a guiding reference. Thereby very precise placement of the object in the centre is possible. It is not possible to centre the object using a marking on the rotation plate, since this marking will be covered by the object.

More preferably, the object is mounted on e.g. a spike, which may be located at the rotational centre. This elevates the object and minimises occlusion effects caused by the rotating plate. This embodiment is especially advantageous for small objects and objects where the whole surface needs to be scanned.

Preferably the light source comprises laser light and/or structured light. The camera used for the scanner may be a video camera, a CCD or a CMOS.

In order to cover the whole circumference and/or length of the object the discrete number of values for angle of rotation / translation may be at least 100, preferably at least 240, for example at least 500, such as at least 750, for example at least 1000, such as at least 1200, for example at least 1500, such as at least 1800, for example at least 2000, such as at least 2400, for example at least 3000, for example at least 3600, such as at least 4200. The higher the discrete number of values of angle of rotation / translation, the higher the scanning precision.

According to a fourth embodiment of the invention is provided a method for manufacturing a shell comprising a device for the ear of an individual comprising the steps of providing three dimensional co-ordinates describing the surface of the ear canal using three-dimensional scanning, and subsequently modelling a three-dimensional model. The ear and ear canal differ from individual to individual and therefore a precise measurement of each person's ear is required to get a satisfactory fit of a device to be carried in the ear. Therefore, a measurement of the dimensions of each individual's ear and ear canal is required. The advantage over prior art techniques for modelling devices for the ear is that the production time is significantly reduced combined with an improvement in the quality.

The data describing the dimensions of the individual's ear and/or ear canal may be provided by scanning a model of the ear canal of an individual. To improve the scanning precision the surface of the model preferably is non-glossy or rough.

The data are more preferably provided by scanning the ear canal of an individual. Thereby, the steps for manufacturing the device are reduced to the absolute minimum and an especially perfect fit of the device can be obtained. The ear and/or ear canal may be scanned a number of times, such as under different conditions affecting the geometry of the ear canal of the individual. Thereby the variations in the dimensions of the ear and the ear canal can be recorded. This is impossible using the prior art techniques. Methods and apparatus for scanning the ear canal are disclosed in PCT/DK01/ (Method and apparatus for three-dimensional optical scanning of interior surfaces, 3-Shape) filed on 24. August 2001.

When the variations in the ear canal have been recorded, computer modelling of the device for the ear by adjusting the model for the dynamic changes in the geometry of the ear canal using scan data from different scans can be carried out and a device which will fit under all circumstances as a compromise between the varying dimensions of the ear and ear canal.

Especially precise scanning is obtained when carried out according to the method described above.

Once the data are recorded the device may be manufactured using any automatic manufacturing technique such as milling. More preferably the modelling technique comprises 3-dimensional printing, stereo lithography, selective laser sintering, laminated object modelling, inkjet modelling, fused deposition modelling, nano-printing. Common for these techniques is that only the required amount of material is used and that it is easier to model complicated models such as devices for the ear and/or ear canal.

The device may comprises a hearing aid, a mobile phone, a loud speaker, a microphone, communication devices, a tinnitus masker or a tinnitus masking device such as the ones described and US 5,325,872, WO 91/17638.

The invention also encompasses the devices manufactured according to the method described.

The invention furthermore features a method for manufacturing a dental implant for an individual comprising the steps of providing three dimensional co-ordinates describing the surface of the dental implant using three-dimensional scanning, modelling a three-dimensional dental implant.

The data describing the surface of the dental implant may be provided by scanning a model of the dental implant for the individual, the model preferably being non-glossy or rough. But the data can also be provided by scanning the tooth in situ in the patient. In addition data from a tooth scanned in situ can be combined with data obtained from a scan of the surface to which the dental implant is to be attached.

The dental implant can be manufactured according to any of the methods described above for the ear device using different materials. Preferably the data describing the surface of the dental implant are obtained by scanning according to the method described above.

Brief figure description

Figure 1 illustrates a CAD model of a scanner according to the invention.

Figure 2 shows a camera image of the setup shown in Figure 1.

Figure 3 illustrates an embodiment of the scanner with two cameras, one laser and a rotation plate.

Figure 4 illustrates an embodiment of the scanner with four cameras, two lasers and a rotation plate.

Figure 5 illustrates an embodiment of the scanner with six cameras, three lasers and a rotation plate.

Figure 6 show how occlusion effects can be reduced by placing the object on a spike.

Figure 7 illustrates a laser source projecting multiple laser sheets on the rotational plate.

Figure 8 shows two laser sources projecting laser sheets on the rotational table to produce a cross section. The cross section can be used to guide the placement of the scan object.

Figure 9 illustrates an embodiment of the scanner with six cameras, three lasers, a rotation plate and a linear axis.

Figure 10 shows the object movement during shutter and image transfer.

Figure 11 shows a CAD model of the rotating plate mounting system.

Figure 12 illustrates the specular, diffuse specular and uniform diffuse reflections from the object surface.

Figure 13 shows the relation between Hough and image space.

Figure 14 shows an image of an object intersecting the laser sheet (left) and a number of negative images of the contour (right).

Figure 15 illustrates the results of transformation in Hough space.

Figure 16 gives an overview of the co-ordinate system for which a transformation needs to be found and calibrated.

Figure 17 show a possible configuration of a calibration object.

Figure 18 illustrates the laser sheet co-ordinate system relative to the object co-ordinate system. (a) the definition of $\varphi=0$ (encoder position=0). (b) rotation relative to the zero angle.

Figure 19 shows three CAD models of different calibration objects. 1901 prior art calibration object. 1902. object according to the invention. 1903 preferred embodiment of the calibration object according to the invention.

Figure 20 shows a CAD model of a preferred calibration object according to the invention as seen from the camera.

Figure 21 illustrates a graphic representation of eight 3D object feature curves of a preferred calibration object.

Figure 22 shows an image of the milled calibration object from camera 1.

Figure 23 shows two images (negative) captured from the calibration program.

Figure 24 illustrates two screen dumps from the calibration point processor program. (a) raw corner detected during one full rotation. (b) selected 2D image feature curves corresponding to the calibration object 3D object feature curves.

Figure 25 shows X-co-ordinates of extracted corner features plotted as a function of the encoder position (proportional to the rotation angle φ).

Figure 26 shows identical feature location in image space.

Figure 27 illustrates the extraction of encoder offset and laser sheet parameters from encoder mean position of symmetric image features.

Figure 28 illustrates the geometrical relations used for estimation of the laser sheet parameters, d – laser sheet displacement, φ_0 - encoder offset, α - laser sheet angle.

Figure 29 shows three camera images of an ear impression.

Figure 30 shows the result of scanning of the ear impression in figure 29.

Figure 31 illustrates a scanner according to the invention adapted for scanning of the ear and ear canal.

Figure 32 illustrates another embodiment of the scanner for the ear and ear canal.

Figure 33 shows an embodiment of the ear scanner, where a lens system is used as image guide.

Figure 34 shows an embodiment of the ear scanner, where fiber optics are used as image guide.

Figure 35 shows an embodiment of the ear scanner, where the camera is placed on the head of the scanner.

Detailed description of the invention

In the following a description of the preferred embodiment is provided.

Mechanical construction

The mechanical construction shown in Figure 1 was designed using SolidWorks, a modern CAD modelling tool. Most of the mechanical parts have been customised exclusively to fulfil the requirements of the scanner. The actual milling was done partly manual and partly using MasterCam, a modern CAM (Computer Aided Manufacturing) system.

The laser scanner of Figure 1 comprises a light source 101, a camera 102) a rotational plate 103) and a frame 104. During scanning and calibration, the object to be scanned is placed and secured to the rotational plate, a sheet of laser light is projected onto the surface of the object and images are recorded by the camera as the object moves.

In Figure 2 is shown a photograph of the built laser scanner with a preferred calibration object 201 in place on the rotational table.

The following series of figures illustrate variations in the laser scanner hardware. Figure 3 shows an embodiment with two cameras 301 positioned on either side of the laser source 302 above the rotational table 303. In Figure 4 is shown an embodiment with four cameras 401, 401', 401", and 401"' together with two laser sources 402, 402'. With this setup occlusion effect are minimised. Even better minimisation of occlusion is obtained with the setup in Figure 5 with two series of each three cameras 501 located on either side of a series of three laser sources 502. A number of extra bars 503 have also been added to increase the flexibility and stability of the construction. Another way of reducing the occlusion effects of the scan object itself and of the rotational plate is shown in Figure 6, where the scan object 601 is located on a spike 602 or similar means above the rotational plate 603. Two laser sources 604 project laser sheets on the object 601 and images are recorded by four cameras 605. In Figure 7 a laser source projecting multiple laser sheets 701 on the rotational plate are shown. With this setup more effective scanning is obtained since more features can be extracted at any one time. In Figure 8 two laser sources project laser sheets on the rotational table to produce a cross section. The cross section can be used to guide the placement of the scan object or calibration object on the rotational plate. Figure 9 shows an embodiment with both a rotation 901 and a translation axis 902. This embodiment makes it possible to rotate as well as translate the object with respect to the camera. The construction can easily be expanded to include two, three, four, five, six or more rotation and/or translation axis.

The construction is based on a desire for flexibility-, size- and stability-constraints. Though the actual size is not considered important, scalability of the developed and adopted solutions have been paid attention to, in order to enable scale up of the complete system. The diameter of the rotation plate was chosen to be 120 mm, enabling a relatively small and handy construction. Another reason for which to keep the construction as small as possible was to enable customised parts to be created with a customary milling machine (medium size CNC milling machine and turning lathe).

The absolute precision of the CNC machine (OKUMA O700) is assumed to be better than 0.02 mm (based on the milling machine parameter setup), whereas the relative precision is assumed to be better than 0.01 mm, depending on the desired milling

speed. Some parts have been latched, and then milled (e.g. the rotating plate), requiring a "manual" origin calibration between the two operations. This will obviously introduce some extra inaccuracy to the created object.

Figure 1 to Figure 9 show the hardware construction, which is designed to be as flexible as possible, yet maintaining a stable and rugged design. The cameras can be translated and rotated in all direction in order to optimise the FOV (Field of view), focus, depth of field, etc. Furthermore, a special laser-mounting device has been developed to allow fine adjustment to the laser sheet position. Another important issue, paid special attention during the design phase, was stability of the construction. Connectors and mounting devices was designed and made in hardened steel and high quality aluminium. All manually movable parts are designed with multiple bolt fixtures enabling a stable and noise immune static setup.

Test of mechanical stability

To test the stability of the construction a μ-watch was attached to one of the cameras, and selected features where manually bent or forced to move.

It was possible to change the relative camera position approximately +/-0.1 mm, by applying a somewhat large manual force (approximately 10-20 kg). Fortunately the camera stabilises to its original position (within the resolution of the watch, 2μm = 0.002 mm) as the force is removed, and the basis mechanical construction was therefore considered sufficiently accurate and stable. Moreover, if a more stable steel construction is required, it will increase the weight further (with the disclosed construction the total weight is approximately 50 kg).

The lens itself was also tested for mechanical stability. It was found that it could be moved +/-0.2 mm in all directions, if the lens fixtures have not been tightened. As discussed later it is therefore necessary to fix both focus and lens aperture.

Temperature expansion

The linear temperature expansion at 25 °C is approximately $23 \cdot 10^{-6}$ K^{-1} for aluminium and $6 \cdot 10^{-6}$ K^{-1} for the used steel (i.e. one meter steel expands approximately 0.006mm pr. °C). Approximately 90% of the construction is made of steel, thus the combined expansion is assumed to be approximately $7 \cdot 10^{-6}$ K^{-1}. The distance be-

tween the laser and the camera in the implemented setup is approximately 0.16 m, resulting in 0.001mm displacement pr. K. The "*steel*" distance from the rotating plate to the camera is approximately 0.6 m, resulting in a maximal displacement of 0.004 mm/K. Using the scanner at normal conditions the temperature will only vary a few Kelvin and the expansion is not considered to be a problem.

Laser

The following factors constitutes to the choice of laser:

- Lasers compatible with line generating optics.
- Visible by the camera. (i.e. The wavelength of the laser must be sensible by the camera)
- Line width and intensity distribution.
- Depth of field, focus range within the limits of the construction.
- Focus adjustable high quality laser.

The laser chosen was a 10mW laser from Lasiris. The laser wavelength 635 nm (smallest possible) was chosen to obtain optimal camera sensitivity. At 630 nm the relative camera CCD sensitivity is 65% (65% relative camera sensitivity at 630nm, according to the camera specification sheet provided by JAI). The laser is mounted with a pattern head generating a laser line with a fan angle (FA) of 20 degrees. The distribution along the laser line is linear whereas the light distribution across the laser line is Gaussian. The laser was mounted on a customised CAD modelled design, allowing the laser to be moved, in order to change the distance and angle to the scanned object. By moving the laser, the focus and depth of field can be optimised.

The line thickness is measured at the $1/e^2$ point of the Gaussian distribution. Depth of field is defined as twice the Rayleigh range, the distance at which the line thickness has increased to $\sqrt{2}$ times of its minimum width.

In the implemented setup the object distance can be varied between 300 and 500 mm, consequently the minimal laser thickness will be approximately 0.2 mm. The laser thickness will limit the possibility of scanning small details. However, it will be Gaussian distributed on continuous surfaces, and it is possible to estimate the peak

with an accuracy much higher than 0.2 mm. In another example, a laser source was used, which provided a laser thickness of approximately 0.09 mm for improved precision.

The depth of field corresponding to object range in the implemented setup is approximately 200 mm, sufficiently large to cover the scan area.

The fan angle (FA) determined by the chosen pattern head, must be large enough to cover the desired scan area. The laser angle (LA) can be adjusted manually to minimise occlusion effects.

The CAD modelled laser mounting system was design to enable fine adjustment of the laser line position at the object being scanned. The laser line forms a laser sheet, ideally equal the ZY-plane (zero rotational angle), featuring a simple transform of co-ordinates. The screws are chosen very small (Ø3 mm) to obtain a fine pitch, thereby enabling accurate adjustment capabilities. However it is practically impossible to adjust the laser sheet to exactly equal the ZY-plane. This is obvious considering the following: If the object range is 500mm the relative screw adjustment distance is 10 times smaller (Ø/2=50mm). A small adjustment (e.g. 0.01 mm) of the laser position will thus result in a 10 times larger (0.1mm) movement of the laser sheet at object range. Furthermore it is hard to tell whether the sheet is right positioned using manual inspection. Therefor a calibration of the laser sheet is required.

Camera and grabber

Choice of camera

The choice of camera(s) is obviously crucial to the performance of the scanner, and the following key parameters constitutes to the choice of camera:

- Progressive scan and asynchronous reset, featuring triggered grabs.
- Cost, resolution, frame rate and sensitivity.
- General quality (e.g. S/N-ratio) and ability to interface with a standard grabber card.

To limit the number of options and optimise cost-benefit, a monochrome camera solution was chosen.

JAI M1, monochrome high resolution camera

It was found that the only progressive scan camera featuring high resolution and frame rate at a relatively low cost was CV-M1, a high performance camera from JAI. The camera is based on a 2/3-inch progressive scan CCD image sensor from SONY. The monochrome (8-bit) censor has a resolution of 1300x1030 pixel elements and it features approximately 12 frames pr. second in continuous mode. In asynchronous reset mode the frame rate is somewhat lower, depending on the shutter time. In the adopted setup the optimal shutter time was found to be 1/24 second. In asynchronous reset mode the frame is transferred to the grabber in a 1/12 seconds period succeeding the shutter time, resulting in a maximum frame rate of approximately 24/3=8 frames pr. second.

The chosen grabber card was a Matrox Meteor II/MC (Multi Channel), likewise supplied by JAI. The grabber was chosen based on its ability to handle the large amount of image data, and the support of asynchronous triggering. The setup adopted, features computer controlled asynchronous triggered grabs from one of the two software selectable cameras.

Camera mounting system

The mechanical camera mounting system was designed to enable manual translations and rotations. The system is thereby made flexible in terms of scan area and it is possible to adjust the cameras to a specific assignment (featuring a special object geometry), thereby minimising occlusion effects, and maximising the accuracy. Besides the dynamic requirements, it was designed to have a maximal static stability, and immunity to external forces and noise. This was reached using hardened steel and multiple bolt fixtures.

Lens

Another crucial part of the vision system is the camera lens. The following basic demands, concerning the lens, are important in order to obtain the highest possible image quality within the scope of the construction:

- Appropriate FOV (field of view). To obtain the highest static resolution the FOV should only cover the area of interest (the scan area).
- Optimal resolution and sharpness
- Standard (off-the-shelf) lens
- Focus at short range (approximately 0.2 mm), to minimise the size of the construction and enable a customised short-range setup.
- Large DOF (depth of field). To obtain sharp images a large DOF is needed.
- Appropriate focal length. In order to minimise lens distortion, the focal length should not be very small.
- C-Mount, compatible with the cameras.

Based on the initial construction setup and the demands above, a number of lens restriction parameters can be listed. Some of the parameters are determined by the camera and cannot be changed, others are rough estimates based on the initial setup and therefore changeable within a certain range.

- $W_{FOV} \approx 120$ mm (Initial scan area with)
- $H_{FOV} \approx 100$ mm (Initial scan area height)
- $lo \in [300; 400]$ mm (distance from the lens to the object)
- $k \approx 11\text{-}22$ (aperture stop, for which the laser is visible)
- $W_{ccd} = 8.7$ mm (CCD width)
- $H_{ccd} = 6.9$ mm (CCD height)
- $W_{pixel} = 6.7$ µm (CCD pixel element size)
- $f \in [16; 50]$ (focal length, restricted to standard lenses)
- $\lambda \approx 635$ nm (wave length of the laser light)

Tilting the cameras might optimise W_{FOV} and H_{FOV}.

Field of view

The object distance *lo,* the image plane distance *li,* and the focal length *f* are connected with the FOV and the CCD size, by the lens low, and the magnification ratio (*m*) [2].

$$Lens\ low: \frac{1}{f} = \frac{1}{lo} + \frac{1}{li} \cong \frac{1}{li} \Rightarrow f \cong li \quad , magnification: \ m = \frac{W_{CCD}}{W_{FOV}} = \frac{li}{lo} \cong \frac{f}{lo}$$

Depth of field

In order to obtain optimal quality of the laser contour, the captured images have to be as sharp as possible. The depth range of which the image must be sharp is dependent on many factors, mainly the scan area, the laser sheet position and the relative laser-camera angle. Ideally the intersection between the scan area and the laser sheet equals the FOV, and the image must be sharp in that area. A sharp image is obtained with the right focus and a large DOF (depth of field). Where DOF is the depth range in which the image is not *blurred* more than a maximum defined limit [2].

$$\delta = \left| \frac{\left(\frac{lo}{l} - 1\right) f^2}{(lo - f)k} \right|$$

Where δ is the diameter of the *circle of confusion* or *blur* measured on the CCD plane. *l* is the distance to the plane of interest (i.e. the most focussed, or sharpest plane), and $k = \frac{f}{aperture}$. DOF is defined as the range of *l* given a constant circle of confusion with diameter δ.

$$\delta < \text{constant} \Rightarrow \left|\frac{lo}{l} - 1\right| < \text{constant}$$

$$\left|\frac{lo}{l} - 1\right| = \left|\frac{lo}{lo - lx_1} - 1\right| = \left|\frac{lo}{lo + lx_2} - 1\right| \quad \text{, where } |lx_1 - lx_2| = DOF$$

$$\Downarrow$$

$$\delta = \left|\frac{\left(\left(\frac{lo}{lo - DOF/2} - 1\right) - \left(\frac{lo}{lo + DOF/2} - 1\right)\right)/2 \times f^2}{(lo - f)\,k}\right| = \left|\frac{f^2}{\left(\frac{2lo}{DOF} - \frac{DOF}{2lo}\right)(lo - f)k}\right|$$

$$\Downarrow$$

$$\delta \cong \frac{f^2 DOF}{2lo(lo - f)k} \quad \Rightarrow \quad DOF \cong \frac{2\delta lo(lo - f)k}{f^2}$$

Choice of lens

Due to the fact that DOF is proportional to the aperture stop (k), it is preferable to have a large aperture stop (16-22). The drawback of a large aperture stop is that the amount of light passing trough the lens is reduced. To compensate for this, it might be necessary to increase the shutter time of the camera, thus introducing a new drawback due to object movement during the shutter time. In figure 10 object movement during shutter (t1, typically 1/24 second) and image transfer (t2, 1/12 second) as a function of angular speed and scan area size are shown. In the implemented setup, the typical magnitude of x1 is 0.02 mm, the typical magnitude of x2 is 0.05 mm to 1.5 mm depending on the rotational speed.

To find the optimal choice of lens the following table was made.

δ_{MAX} = n pixel = n × 6.7 µm

lo [mm]	*f* [mm]	k (aperture stop)	DOF [mm]
300	21.8	11	n × 27
350	25.4	16	n × 39
400	29.0	22	n × 54
450	32.6	16	n × 39
500	36.3	16	n × 39

The object distance in the initial implemented setup was 300 - 400 mm, thus a lens with 25 mm focal length will be suitable. A 25mm standard lens from Pentax was therefore chosen.

Changing focus and aperture

If the camera is moved and the relative object distance thereby changes, the lens focus will obviously have to be updated, and thus the whole scanner system must be re-calibrated. If only the aperture stop is changed (e.g. when scanning objects reflecting the laser light differently), it might not be necessary to recalibrate. However it was found that a manual adjustment of the aperture, might well cause the imaged frame to be misaligned or moved more than ½ pixel. Although it might not seem to be a large error source, it will actually result in an error of more than 0.04 mm on the final scan result. To prevent the error, focus and aperture stop was locked with the provided bolt fixtures. The drawback of fixing the aperture is that it will not be possible to scan a bright object (e.g. white) using the same setup as for scanning a black light absorbing object. To solve the problem the laser illumination was made adjustable.

Motor, encoder and gear

To enable a precise calculation of the laser sheet position relative to the object coordinate system the rotation angle of the round plate must be known with high accuracy. Furthermore the rotation angle should be steady during the camera shutter time to avoid multiple feature detection, and blurred laser contour. It was considered to buy a reassembled high precision rotary table, but due to high pricing and unnecessary complexity, it was decided to design and create a customised solution. First of all a suitable motor is needed to enable the actual motion, secondly the angular position must be available. Two solutions were considered:

- Stepper motor with gear.
- Linear motor with gear and encoder.

A linear motor solution was chosen for the following reasons:

- Possibility of high speed scanning (pre-scan).
- Accurate and absolute position readout, without the risk of "loosing" steps.
- Limited demands to the controlling system.
- Smooth nonstop motion, preventing gear and motor backlash problems.

Nonstop movement

To prevent backslash in the gear and faulty position readout it was decided to let the motor run at constant speed during the scanning. Furthermore the smooth motion enables a constant synchronism between the captured image and the angular position recorded. The drawback of continuous motion is that the object moves during the camera shutter time, thus small errors proportional to the angular speed might appear. The geometric relations shown in Figure 10 and below contribute to the final choice of motor speed, gear ratio and encoder resolution.

$$x1 = \frac{D}{2} \cdot \omega_{plate} \cdot t1 \quad , \qquad x2 = \frac{D}{2} \cdot \omega_{plate} \cdot t2$$

$$\omega_{motor} = \omega_{plate} \cdot Gear\ Ratio$$

$$f_{encoder} = \omega_{motor} \cdot Encoder\ tics\ pr.\ revolution$$

Table 1 describes the motor, gear and encoder that were chosen. The components were supplied by LMT-Transmission and Danbit:

Component	Name / Vendor	Key-parameters
Motor	Penta 5X / Motor Power Company	Linear DC-motor, Speed=100-3000 rpm, Operating toque=0.32 Nm
Gear 1	Reg 42/ Eisele	Precision planetary gear. Ratio=1:30. Straight.
Gear 2	BW-W / Brown Group	Precision planetary gear. Ratio=1:30. 90 degree.
Encoder	2RHI / Scancon	Incremental (A,B) output, Max speed=3000, 400 tics pr. round, resulting on 352,000

		encoder pulses pr. rotation of the rotational plate.
Motor control	400 / Sprint Electric	One quadrant one phase linear DC motor speed controller. (i.e. only one way). Speed proportional to input voltage (0-10 voltage)
Encoder card	PLC833 / Advantech	Encoder tics to absolute position converter. 24 bit resolution.
DAC	AD16S12 / DanBit	Digital to analogue converter, used to control the motor speed.

Table 1: Components chosen to control the rotation of the plate.

The choice of encoder and gear ratio leads to the following angular resolution on the rotation plate:

$$\text{Angular resolution} = \frac{360\text{ degrees}}{\text{Encoder tics pr. round} \times \text{gear ratio}} = \frac{360\text{ degrees}}{400 \times 30 \times 30} = 0.001\text{ degree}$$

The linear resolution on the plate movement 50 mm from the centre axis, is consequently:

$$\text{Linear movement 50 mm from center axis} = \frac{\pi \times D}{\text{tics/round}} = \frac{\pi \times 100\text{ mm}}{360000\text{ tics/round}} = 0.00087\text{ mm} = 0.87\mu\text{m}$$

The actual angular resolution may well be less accurate than the theoretical resolution, due to non-linearity in the gear and encoder.

Object movement during shutter and image transfer, with the chosen motor and gear

The object movement (x1 and x2) 50 mm from the centre axis during the shutter time (t1) and the image transfer time (t2), was calculated with slow (100 rpm) and fast (3000 rpm) motor speed (see Figure 10). In addition the scanning time was estimated.

Slowest speed (least angular movement)

$$\omega_{motor} = \frac{2\pi \times 100\,\text{rpm}}{60\,\text{scc}} = 10{,}5\,\text{sec}^{-1}$$

$$\Downarrow$$

$$x1 = \frac{D}{2}\omega_{motor} \times Gear\ Ratio \times t1 = \frac{100\,\text{mm}}{2} 10{,}5\,\text{sec}^{-1} \times \frac{1}{30} \times \frac{1}{30} \times 1/24\,\text{sec} = \underline{0.024\,\text{mm}}$$

$$x2 = \frac{D}{2}\omega_{motor} \times Gear\ Ratio \times t2 = \frac{100\,\text{mm}}{2} 20{,}9\,\text{sec}^{-1} \times \frac{1}{30} \times \frac{1}{30} \times 1/12\,\text{sec} = \underline{0.048\,\text{mm}}$$

$$\text{Scanning time} = \frac{2\pi}{\omega_{plate}} = \frac{2\pi}{\omega_{motor}} \times \frac{1}{Gear\ Ratio} = \frac{2\pi}{10{,}5} 30 \times 30 = 539\,\text{seconds} \approx \underline{9\,\text{minutes}}$$

Fastest speed (maximal angular movement)

$$\omega_{motor} = \frac{2\pi \times 3000\,\text{rpm}}{60\,\text{sec}} = 314{,}2\,\text{sec}^{-1}$$

$$\Downarrow$$

$$x1 = \frac{D}{2}\omega_{motor} \times Gear\ Ratio \times t1 = \frac{100\,\text{mm}}{2} 314{,}2\,\text{sec}^{-1} \times \frac{1}{30} \times \frac{1}{30} \times 1/24\,\text{sec} = \underline{0.73\,\text{mm}}$$

$$x2 = \frac{D}{2}\omega_{motor} \times Gear\ Ratio \times t2 = \frac{100\,\text{mm}}{2} 314{,}2\,\text{sec}^{-1} \times \frac{1}{30} \times \frac{1}{30} \times 1/12\,\text{sec} = \underline{1.45\,\text{mm}}$$

$$\text{Scanning time} = \frac{2\pi}{\omega_{plate}} = \frac{2\pi}{\omega_{motor}} \times \frac{1}{Gear\ Ratio} = \frac{2\pi}{314{,}2} 30 \times 30 = \underline{18\,\text{seconds}}$$

If the surface scanned is a continuous varying surface the induced error during the shutter time may not be a problem, but is the surface consist of sudden changes the accuracy will obviously be limited by the angular movement.

Scanning smaller objects (diameter less than 100 mm) the movement during shutter and image transfer will obviously be smaller, and more accurate results might be obtainable. Furthermore, when capturing an image, the corresponding position is

recorded as the encoder position in the middle of the shutter time interval, thus bisecting the possible error.

The rotation plate

To minimise errors induced by dynamic mechanics, the rotation plate mounting system must be stable and accurate. The surface of the rotation plane must be totally flat, and the axis of rotation must be perpendicular to the plane. Furthermore the mounting system on which the plate is fixed must be well designed to obtain a high mechanical precision. To enable precise calibration of the system, fixtures were designed and milled directly in the plate surface. Although the four fixtures are accurately positioned relative to each other (+/- 5μm), the absolute accuracy is not expected to be better than +/- 10 μm (0.01 mm), due to the "manual" origin calibration (using a μ-watch).

In the process of finding the best solution, for the rotating plate and the mounting system, two different approaches were implemented. In the first solution tested, the plate was mounted directly on the gear. The stability and mechanical accuracy was measured using a micron watch.

The relative horizontal and vertical movement during one rotation was measured 50 mm from the centre axis. Furthermore the vertical displacement caused by adding an external force was measured. The result (as shown in table 2) was not satisfactory and it was decided to create a more stable solution. To control and minimise the effect of horizontal and vertical forces the rotating plate was mounted using two bearings. Figure 11 shows a CAD model of the rotating plate mounting system consisting of a rotating plate 1101, large axial bearing 1102, dust protector and axial bearing holder 1103, bottom plate 1104, conventional bearing 1105, bolt fixture 1106 and gear connector 1107. The bearings used are high precision SKF bearings (bearing ball roundness = 0.4 μm).

The stability and accuracy of the new construction was measured, using the same technique as for the "direct gear mounting" approach (shown in table 2). As shown in the table, the new construction is very stable and indifferent to external forces, compared to the first approach.

Construction	Maximal vertical displacement during one rotation.	Maximal horizontal displacement during one rotation.	Relative vertical displacement caused by an external force of 1kg =10N.
Direct gear mounting	190μm	240μm	75μm
Customized design	8μm	4μm	<1μm

Table 2: Direct gear mounting versus customised design. Measurement of stability and accuracy was performed using a micron watch.

Steel deformation

The new plate mounting system was tested at various speeds for approximately ½ hour. Then the construction was disassembled to investigate possible damages and changes. The axial bearing and its contact faces were investigated. The axial bearing had created a visible path, about 0.02 mm in depth 0.2 mm wide. The path was constant (of equal size all around) and therefore not considered as a serious problem degrading the tolerance or accuracy. The path is caused by the softness of the steel material used for the bottom plate. The contact surface between the plate and the baring balls are infinitely small and therefore the theoretic pressure goes to infinity. The possibility of using a hardened steel bottom plate was considered. The idea of hardened steel was rejected because it could cause the bearing balls to be deformed. In that case it is preferable to have soft steel surrounding the bearing balls.

Clutch

A play free clutch was installed between the rotating plate and the gear axis. The coupling must be flexible though it must still be precise and able to transmit the force from the gear to the rotating plate.

Image processing

The profile generated by the laser light beamed onto the object is captured by a high resolution CCD camera, and the resulting image is processed and analysed in order to locate the lightened contour. This chapter describes a number of different methods and techniques to locate points on the laser-generated contour. The majority of

described methods features sub pixel detection; thereby it is possible to enhance the accuracy of scanned data beyond the resolution of the CCD. Conventional methods are investigated, and a fast accurate and stable method is presented.

Image convention

Most of the presented images are captured using the actual scanner cameras, but in order to enhance the visual impression the aperture has been changed to make the object visible. Furthermore some contour images have been negated to economize with the printer toner.

The reflected laser contour

The shape and "quality" of the laser contour imaged by the camera is highly dependent of the surface of the object scanned. Ideally the surface is planar and diffuse reflective causing the intensity level along the contour to be constant and the intensity across to be Gaussian distributed, corresponding to the laser specification sheet. Although some objects might satisfy the ideal criteria, it is far from assumable that all objects do. If the scanned object is made of blank steel, the reflection pattern is much different from the pattern reflected from black plastic. Another factor causing large intensity variations in the imaged laser contour is the angle of the surface relative to the laser beam direction and the camera. If the laser-beam direction is perpendicular to the surface exposed, and the surface is assumed to be an *ideal lambertian surface*, the imaged contour intensity is relatively high, corresponding to the *Bi-directional Reflectance Distribution Function* (BRDF) for the *ideal lambertian surface*, whereas the reflected light intensity from a surface parallel (or close to parallel) to the laser direction will vanish. On an ideal *lambertian* surface, the surface appears equally bright from all viewing direction. Its brightness is entirely dependent on the angle between the light source and the surface normal. BRDF is used to describe the ratio between radiance and irradiance from a surface patch, as a function of light source direction and observer position, relative to the surface patch.Three different reflection types are used to describe the scatter pattern from a given surface. Figure 12 shows a graphic interpretation of the three different reflection phenomena, specular, diffuse specular and uniform diffuse reflections from the object surface.

If the object surface scatter-pattern equals a perfect mirror (only specular reflection), the laser light is reflected in only one direction, and the object is obviously not suitable for scanning. For the scanning purpose the ideal surface is the *lambertian surface*. Thus the reflected light is uniform diffuse (see Figure 12), causing the laser light to be spread equally in all directions. Thereby discontinuous light emission and ghost points (e.g. caused by secular laser light reflections in the surface) are avoided. Later in the overall performance test, the reflection pattern from different object surfaces will be discussed.

In addition to the changing light conditions, variations in object shape influences the choice and development of a stable contour detection method. Some objects consist entirely of planar surfaces (e.g. milled cube), whereas others consist of continuous varying surfaces (e.g. clay modelled figure).

Based on the analysis of scatter patterns from different objects with various shapes, the optimal contour detector must be indifferent to the following artefacts and phenomena.

- External light from various natural light sources (e.g. lamp or sun-light).
- Changing contour width, and scatter pattern. (e.g. contour on black, white, or metal surface)
- Ghost points from reflected laser light.

It is practically impossible to handle severe artifacts from highly reflective objects (e.g. mirror). Coating the object surface (e.g. with spray paint) might solve the problem, however under some conditions it may ruin the object appearance. Furthermore the coating will add a thin layer of material to the surface causing the accuracy to decline. Under some conditions it may be advantageous to coat the surface and thereby obtain a better detection of the laser contour. The thickness of the paint can be subtracted in the computer after the computer model has been made. The thickness of the layer of paint can be measured by scanning a known object with a *lambertian* surface with and without paint. The paint used to spray the surface may be commercial products like Magnaflux ®, Spotocheck ®, or SKD-S2. It may also be possible to obtain the desired surface by milling or polishing the surface.

Considered contour detectors

A number of edge and contour detecting methods were considered and tested in the search for a suitable solution.

- Edge detectors based on derivatives.
- Transformation (Hough and radon).
- Line-by-line search (peak detection, interval midpoint, moment based methods and line filtering).

The edge detectors (based on derivatives) and the Hough transform, do not assume prior knowledge of the contour direction, whereas the line-by-line methods implemented assume knowledge of the laser contour direction.

Edge detectors

The edge detectors that were reviewed and tested are based on zero crossing contours of first and second derivatives in the different image directions (x and y). The tested methods are:

- First derivative
- Second derivative

Using derivatives, two edges are detected, one on each side of the contour and thus the centre must be interpolated. The two methods were tested in the early phase of the project using Matlab, and the tracked contour(s) were unusable. Furthermore the methods are sensitive to noise resulting in multiple contour detection, was observed. Prior threshold of the image to remove noise and dark was tried, but the resulting zero crossing contours was still not satisfactory. In addition the methods were found to be relatively time consuming.

Hough transformation

Contour and line detection performed using a Hough transform was investigated and tested on a number of different laser-contour images. The idea behind the Hough transform is to enable a simple identification of known image features. In this case

the Hough transform was used to identify lines in the image, using the following parameterisation to connect image space (x, y) with the Hough space (θ, r): $x \cdot Cos\theta + y \cdot Sin\theta = r$. Figure 13 shows a graphic representation of the relation between lines 1301 in the Hough and image space.

To find lines in an image (image space) all points must be transformed into Hough space using the relation above. Co-ordinates constituting to the same line equation in image space will sum-up the same co-ordinate in Hough space, enabling the line to be found using a simple peak detector. The Hough transform is visualised in Figure 14 and Figure 15, showing the transform applied to the selected area 1401. On the left of Figure 14 is shown a selected area and on the right, negative images of the contour. To visualise the force and the drawbacks of Hough transform, it was applied to the three contours 1402, 1403, and 1404 in the right side of Figure 14. The results of the Hough transformation are shown in Figure 15.

Line-by-line search

As the camera position relative to the laser is fixed, the laser-beam angle is known, and the contour direction can be estimated. If the laser contour direction (search direction) is known, the contour position can be detected from the cross section profile (search line profile). This is a simple and easy way to detect the laser contour.

The search step distance and the profile step (dr) can be varied to optimise for speed and accuracy, although it should be noticed that the image pixel intensities are discrete values. Pixel intensities corresponding to floating point image co-ordinates can be estimated using an interpolation scheme (e.g. bilinear or bicubic interpolation). In the implemented solutions bilinear interpolation was used to estimate pixel intensities, corresponding to floating point image co-ordinates.

The search direction should ideally be changed according to the laser-beam fan angle, to obtain the most correct laser cross-section profile, and to avoid multiple peak detection. However, it is possible to find a search direction that does not cause multiple peak detection. It is noticed that the direction of the various bending contour cannot be constantly equal to the search direction, using this type of search.

The following methods where considered to detect the peak of the search line profile:

- Max intensity
- Centre of gravity
- Filter search

Max intensity

The simplest way of detecting the profile peak is to find the global maximum. However it is not possible to gain sub-pixel accuracy, in the discrete image.

Centre of gravity

A more accurate way to locate the peak, is to calculate the centre of gravity for the profile. The estimated peak position can be calculated as:

$$r_{peek} = \frac{\sum_{r=0}^{N_r-1} r \cdot I(r)}{\sum_{r=0}^{N_r-1} I(r)}$$

Although it is possible to gain sub pixel accuracy using this method, it is highly sensitive to image noise, and dark current in the CCD-chip. If the peak is not located in the middle of the watched interval, the image noise sum up unsymmetrical and the peak detection might be pulled aside. To remove noise and dark current, a prior threshold of the image can be performed, thus introducing a new problem: finding the right threshold level. The threshold level must be high enough to remove the noise, and still be small enough to enable sub pixel accuracy.

Filter search

Another method that can be used to locate the profile peak is filter search. By multiplying a pre-constructed window filter with the image along the search line, the peak is found where the maximum response is present. The method is somewhat insensitive to noise in the image, and the preliminary threshold is thereby avoided. As the laser contour cross-section intensity profile is assumed Gaussian distributed, it is logical to choose a Gauss filter to search for the peak centre.

In some cases it might be preferable to have a circular window filter, but to ease the implementation all filters were implemented as rectangular window filters.

Calibration and transformation

In the following a number of different calibration techniques are discussed and disclosed. A calibration object according to the invention being designed exclusively for the calibration purpose is disclosed. The calibration leads to the direct transformation of co-ordinates between the defined co-ordinate systems. A method for direct calibration according to the invention is thereby also disclosed.

To obtain a 3D point cloud representing the scanned object, the contour points detected in 2D (the image co-ordinates) must be transformed into real world 3D co-ordinates, and rotated according to the plate rotational angle. To simplify the transformation and enable use of well-known methods to calibrate the camera and lens (e.g. DLT, Heikkilä or Tsai), the transformation is performed in two steps, namely:

- Image co-ordinates (2D) → Laser sheet co-ordinates
- Laser sheet co-ordinates → World co-ordinates (3D)

To assure correct transformation of points between the different co-ordinate systems, the involved transformations must be calibrated prior to the actual scanning. In this case the calibration is performed beaming the laser line onto a known physical object, thus obtaining knowledge on the relationship between the different co-ordinate systems.

Co-ordinate systems

As shown in Figure 16 three co-ordinate systems are introduced to describe the transformation from image co-ordinates to 3D world co-ordinates. Those are the image co-ordinates system (X_I ,Y_I) 1601, the laser sheet co-ordinates system (X_L ,Y_L) 1602 and the 3D real world co-ordinates system 1603 (X, Y, Z), also referred to as the main co-ordinate system or object co-ordinate system. Note that there is a one to one mapping 1604 between 3D coordinates 1605 in the laser plane 1606 and 2D image coordinates 1607 through a pinhole (lens) 1608. As said earlier the

transformation is performed in two steps; from image co-ordinates to laser sheet co-ordinates and then from laser sheet co-ordinates to real world co-ordinates. In the following sections the two transformation steps are treated individually, although they are based on the same basis geometric assumptions, of which the most important are:

- The Y-axis of the main co-ordinate system (O) is assumed equal to the axis of rotation for the plate, and thus the Y-axis vector equals the plate surface normal.
- The plate surface is assumed totally flat.
- The laser sheet is assumed totally flat.
- The CCD array (image plane) is assumed totally flat.
- To assure a one to one and onto (One to one and onto: A co-ordinate in image space corresponds to one and only one co-ordinate in the laser sheet plane, and vice versa) transformation between image and laser sheet co-ordinates, the image plane normal cannot be perpendicular to the laser sheet normal (i.e. the camera must be angled relative to the laser).
- To assure a one to one and onto transformation between laser sheet and world co-ordinates, the laser sheet normal must be somewhat perpendicular to the (Z, Y) plane.

Image plane ↔ Laser sheet

This section deals with the transformation of co-ordinates from image plane to the laser sheet, and the prior calibration needed for the transform to be correct and accurate. Four methods have been considered:

- Direct linear transformation (DLT).
- Tsai algorithm [1] proposed by Rodger Y. Tsai.
- Heikkilä algorithm [3] proposed by Janne Heikkilä.
- Direct non-linear matrix transformation.

As light rays travels from the laser sheet (intersection with the scanned object) to the image plane (CCD) they may well be distorted in the camera lens system, or hit a wrong CCD pixel element due to inhomogeneous pixel size and pixel spacing on the CCD. Neglecting these distortion effects, the transformation of co-ordinates between

the image plane and the laser sheet can be modelled using the so-called pinhole model. The pinhole model describes the central perspective projection (as shown in Figure 16), of co-ordinates in space onto the image plane. The pinhole model assumes all light to pass trough an infinitely small hole 1608, which is obviously not practically possible. To avoid long exposure time due to the limited pinhole size, a lens is inserted at the pinhole position thus redirecting all light-rays from the same point in space to hit the same co-ordinate on the image plane. Although the ideal lens will redirect all light rays towards the right CCD pixel element, it is not assumable that a standard off-the-shelf lens will be able to do so. For this reason the lens distortion must be handled in order to obtain a precise model for the transformation.

Direct linear transform

Neglecting non-linear lens distortion the transformation of co-ordinates from laser plane to image plane can be formulated as a direct linear transform (DLT).

$$\begin{bmatrix} wX_i \\ wY_i \\ w \end{bmatrix} = \begin{bmatrix} a_{11} & a_{12} & a_{13} \\ a_{21} & a_{22} & a_{23} \\ a_{31} & a_{32} & a_{33} \end{bmatrix} \begin{bmatrix} X_L \\ Y_L \\ 1 \end{bmatrix}$$

Where w is an arbitrary scaling factor allowing the image perspective to be modelled. $a_{i,j}$ are constants that must be calibrated (determined) prior to the actual scanning. Restricting one of the constants (a_{33}=1), the existing constants in the linear equation system can be calibrated (determined) from a minimum of 4 corresponding point sets (see Figure 16). Using more than four points to calibrate the transformation constants a least squares approach is used. A comprehensive description of the mathematics constituting to the equation set-up can be found elsewhere, e.g. a standard computer vision text book or www.icaen.uiowa.edu/~dip/ LECTURE/3DVisionP1_2.html. Results and accuracy of the transformation are presented and discussed below.

Tsai

To obtain a more accurate transformation of co-ordinates, Rodger Y. Tsai has formulated a calibration method [1] often referred to as the two-stage Tsai calibration technique, allowing first order radial lens distortion to be modelled[1]. Furthermore the technique includes a calibration method optimised for coplanar observations,

which is specially suited for this application (the laser sheet is assumed coplanar). Although the Tsai calibration method and transformation is used, the mathematics behind it will not be described in application. The method has been described in a number of publications and can be found elsewhere [1]. The implementation by Reg Wilson (TSai calibration, implementation by Reg Wilson: www.mmm.com), found on the web was adopted and a DDL (Dynamic Link Liberay, used to interface between different windows based programming platforms (e.g. C++ and Delphi). interface was created to enable Delphi to call the functions and procedures written in C. Results and accuracy estimates are presented and discussed below.

Heikkilä

An alternative calibration method along the same line as the Tsai is proposed by Heikkilä [3]. Compared to the Tsai algorithm the Heikkilä calibration method consists of a four-step procedure, where all the calibration parameters are simultaneous optimised using a bundle adjustment approach including a non-linear optimisation algorithm. For details about the algorithm refer to [3].

Direct non-linear matrix transform

Assuming the transformation from image co-ordinates to laser sheet co-ordinates to be one to one and onto (One to one and onto: A co-ordinate in image space corresponds to one and only one co-ordinate in the laser sheet plane, and vice versa), the following relationship can be formulated:

$$X_L = f(X_i, Y_i) \text{ , for one and only one combination of } X_i \text{ and } Y_i$$
$$Y_L = g(X_i, Y_i) \text{ , for one and only one combination of } X_i \text{ and } Y_i$$

Instead of using a simplified model of the real world (as modelled by the DLT, Heikkilä and Tsai algorithm) to solve the transformation, one can "expand" the transformation functions (*f* and *g*) to be "infinitely" accurate, using a matrix transformation (lookup table) for each function. Obviously the transformation matrix must be filled with values that are more accurate than what can be calculated using DLT, Heikkilä or Tsai (the idea is not just to create lookup tables reflecting simplified models of the real world). Consequently it is required that function values of *f* and *g* must be found for all image co-ordinates, resulting in two infinitely large matrices (2D). In practice this is not possible, but it should be possible to get sufficiently close using our prior

knowledge about the system, and limiting our demand for accuracy. First of all the transformation is assumed to be continuously defined, for all image co-ordinates (i.e. Sudden changes in the lens surface or the CCD array is not expected). As the function is continuous, adequately accurate results can be obtained using interpolation between neighbouring matrix cells (e.g. bilinear or bi-cubic interpolation), thus limiting the size of the matrix (lookup table) describing each transformation *f* and *g*. Furthermore the matrix can be limited to include only co-ordinates on the laser sheet that are visible to the camera. Using the CCD rows and columns to limit the resolution of the array and bilinear interpolation to determine the function values in non-discrete image co-ordinates; the transformation functions can be expressed as follows:

$$\begin{aligned} X_L = f(X_i, Y_i) \quad &= (1-dx)\cdot(1-dy)\cdot f_{array}\left[X_i^{trunc}, Y_i^{trunc}\right] \\ &+ dx\cdot(1-dy)\cdot f_{array}\left[X_i^{trunc}+1, Y_i^{trunc}\right] \\ &+ dy\cdot(1-dx)\cdot f_{array}\left[X_i^{trunc}, Y_i^{trunc}+1\right] \\ &+ dx\cdot dy\cdot f_{array}\left[X_i^{trunc}+1, Y_i^{trunc}+1\right] \end{aligned}$$

$$\begin{aligned} Y_L = g(X_i, Y_i) \quad &= (1-dx)\cdot(1-dy)\cdot g_{array}\left[X_i^{trunc}, Y_i^{trunc}\right] \\ &+ dx\cdot(1-dy)\cdot g_{array}\left[X_i^{trunc}+1, Y_i^{trunc}\right] \\ &+ dy\cdot(1-dx)\cdot g_{array}\left[X_i^{trunc}, Y_i^{trunc}+1\right] \\ &+ dx\cdot dy\cdot g_{array}\left[X_i^{trunc}+1, Y_i^{trunc}+1\right] \end{aligned}$$

Where X_i^{trunc} and Y_i^{trunc} are the integer parts of the X_i and Y_i. $dx = X_i - X_i^{trunc}$ and $dy = Y_i - Y_i^{trunc}$. The size of f_{array} and g_{array} matrices equals the camera CCD size (1300 x 1025 pixels), and thus the memory needed to store the each lookup table (matrix) is: $1300 \cdot 1025 \cdot 4 \approx 5Mb$ (4 byte float = 7-8 significant digits).

Although a suitable transformation have been defined, one has to fill in correct and accurate values in every cell of the transformation matrix (lookup table), to make it work. Theoretically 1300x1025≈1.4 million correct placed and corresponding co-ordinate sets connecting the two systems, is needed to fill the matrices. However it may well be possible to reach a sufficiently accurate result using a reduced number of observations, thus using interpolation to fill in the "holes", based on the continuity

assumption. To obtain the actual co-ordinate sets, it one may use a translating calibration object as shown in Figure 17, thereby recording multiple corresponding co-ordinate sets extracted from the known corner features 1701. The object in Figure 17 is used to calibrate a system to a matrix transform.

Laser sheet ↔ real world

To complete the overall transformation of image co-ordinates to 3D world co-ordinates, the relationship between co-ordinates in the laser sheet (X_L,Y_L) and the main co-ordinate system (X,Y,Z) must be defined. As the object is rotating it includes a rotation around the Y-axis. Figure 18 illustrates the relationship between the two co-ordinate systems. In Figure 18 (a) is shown the definition of φ=0 (encoder position = 0). In Figure 18 (b) is shown the rotation relative to the zero angle.

The transformation from laser sheet co-ordinates (X_L, Y_L) to real world co-ordinates (X,Y,Z) can thus be defined by the following equation:

$$\begin{bmatrix} X \\ Y \\ Z \end{bmatrix} = \begin{bmatrix} \cos(\varphi) & 0 & \sin(\varphi) \\ 0 & 1 & 0 \\ -\sin(\varphi) & 0 & \cos(\varphi) \end{bmatrix} \begin{bmatrix} k_1 \cdot Y_L - d \\ k_2 \cdot Y_L \\ X_L \end{bmatrix}$$

where $k_1 = \tan(\alpha)$, $k_2 = \cos(\alpha)$.

Ideally the laser sheet equals the (Z, Y)-plane, consequently the transformation can be expressed as a simple counter clockwise rotation around the Y-axis (i.e. α=0 and d=0 $\Rightarrow$ k_1=0, k_2=1). However it is practically impossible to adjust the laser sheet to be that accurate, even using the fine adjustment mechanics, therefore d and α must be calibrated (found) or at least estimated prior to the transformation. In addition the transformation can be used in a multiple laser setup, with several laser sheets.

Choice of calibration object

To calibrate the adopted transformations, image features corresponding to known laser sheet co-ordinates must be recorded.

$$(X_i, Y_i) \leftrightarrow (X_L, Y_L)$$

In addition the laser sheet parameters (d and α) must be calibrated based on the same feature detection or additional calibration. To enhance calibration performance image features must be detected within sub pixel accuracy (the resolution of the used CCD is relatively coarse, approximately 0.1mm pr. pixel using a 25mm lens at 400-500mm distance). Corresponding co-ordinates of different systems can be obtained using a calibration object placed on the rotating table. The following constitutes to the design and choice of calibration object:

- Ability to calibrate the whole system, both transform from image co-ordinates to laser sheet co-ordinates, and the transform from laser sheet co-ordinates to object co-ordinates.
- Features detected in image space must be known in world co-ordinates.
- Feature should be easy to detect using the desired lens aperture stop.
- The feature detection should be stable and versatile.
- The designed object must be feasible, even at high accuracy.
- The calibration object should have as many accurately detectable and known features as possible, spread out on the area of interest.

Based on the stated demands, a number of different calibration objects may be considered; the most important ones are shown in Figure 19. Figure 19, 1901 shows a prior art calibration object known as the traditional dot matrix. 1902 shows a calibration object in which the laser line is used to generate the features thus enabling calibration of both laser, camera and lens system. In 1903 is shown a preferred embodiment of the inventive calibration object comprising two symmetric and continuous winding staircases.

To calibrate a camera-lens system the dot matrix 1901 is commonly used. The dot matrix is available as an off-the-shelf component from a number of vendors (e.g. Melles Griot), and the accuracy is high (typ. 5 μm). Furthermore, the dots are easy and accurately detected using a simple blob detection algorithm. Despite these advantages of the dot matrix, it does not allow the laser sheet to be calibrated simultaneously. Consequently the laser sheet position relative to the world co-ordinate

system must be calibrated subsequently (e.g. using another object). Furthermore it might be necessary to determine the axis of rotation thus introducing a number of error sources. Another crucial problem is the fact that the lens-aperture stop is likely to be changed subsequent to the calibration to compensate the laser light intensity.

Exploiting the geometry of the rotational plate and linear axis combined with the fact that all essential co-ordinates are located in the same plane (the laser sheet), four alternative calibration objects according to the invention were designed (i.e.1902, 1903, 1904 and 1905). 1903, 1904 and 1905 is a preferable embodiment of the calibration object since it has the following advantages (compared to 1902):

- Continuous geometry enabling, sub-sub pixel accuracy.
- Limited occlusion (continuous geometry compared to the stairs)
- The symmetric geometry enables the laser sheet parameters to be calibrated using the same object $\varphi = 0, d, \alpha$. (see Figure 18 and Figure 28).
- Feasible and somewhat easy to produce object.
- Surface features (3D object feature curves) defined by known mathematical functions facilitate the calculation of co-ordinates for calibration.

Calibration object geometry

The calibration object 1903 was designed to provide known co-ordinate features as a function of the rotational angle throughout the desired scan area. Although it is preferable to have feature points throughout the scan area, it is possible to calibrate with the same object using a larger FOV (field of view). Utilising the geometry of a winding staircase (continuous), the features detected at the intersection between object and laser sheet will follow continuous known curves (assuming $d \approx \alpha \approx 0$, the features are lines). Thus enabling a simple and accurate feature extraction process. Furthermore the object is symmetrically designed to allow the laser sheet parameters to be calibrated simultaneously. Figure 20 shows how feature points 2001 can be extracted from a captured image given the invented calibration object 2002 and the laser sheet 2003. Figure 22 shows the corresponding image where 3D object feature curves 2201, 2D image feature curves 2202 and image feature points 2203 are visible.

As illustrated in Figure 20 the feature co-ordinates in image space can be calculated from the intersection of two lines. The corresponding laser sheet co-ordinates are calculated from the rotational angle, φ, provided by the encoder.

The calibration object was modelled in a CAD system the object by connecting a number of mathematically defined spirals, forming a solid body. The eight 3D object feature curves 2101 were created from the definitions below and are plotted in Figure 21.

$$r_1(\varphi) = 59 - 10\frac{|\varphi|}{\pi} \quad , \quad y'_1(\varphi) = y_{off} + 80\frac{|\varphi|}{\pi}$$

$$r_2(\varphi) = -52.5 + 10 - 10\frac{|\varphi|}{\pi} \quad , \quad y'_2(\varphi) = y_{off} + 80 - 80\frac{|\varphi|}{\pi}$$

$$r_3(\varphi) = 48 - 10\frac{|\varphi|}{\pi} \quad , \quad y'_3(\varphi) = y_{off} + 80\frac{|\varphi|}{\pi}$$

$$r_4(\varphi) = -41.5 + 10 - 10\frac{|\varphi|}{\pi} \quad , \quad y'_4(\varphi) = y_{off} + 80 - 80\frac{|\varphi|}{\pi}$$

$$r_5(\varphi) = 37 - 10\frac{|\varphi|}{\pi} \quad , \quad y'_5(\varphi) = y_{off} + 80\frac{|\varphi|}{\pi}$$

$$r_6(\varphi) = -30.5 + 10 - 10\frac{|\varphi|}{\pi} \quad , \quad y'_6(\varphi) = y_{off} + 80 - 80\frac{|\varphi|}{\pi}$$

$$r_7(\varphi) = 26 + 10\frac{|\varphi|}{\pi} \quad , \quad y'_7(\varphi) = y_{off} + 80\frac{|\varphi|}{\pi}$$

$$r_8(\varphi) = -\text{Not used} -$$

$$\text{for } \varphi \in [-\pi;\pi]$$

As will be immediately evident for the skilled person, numerous variations of the mathematical functions describing the 3D object feature curves can be constructed, keeping the basic requirements of the object in mind: continuous and symmetric geometry, limited occlusion, coverage of the whole camera field of view.

Another advantage of the present calibration object is that it is possible to construct the object in a CAD and make it using automatic milling controlled by the CAD. Thereby great precision of the individual 3D object feature curves is obtained.

Assuming d=0 and α=0 (see Figure 18), the laser sheet co-ordinates corresponding to detected feature points can be found directly from the rotational angle using the 3D object feature curve definitions:

$$X_{L,i} = r_i(\varphi) \quad , \quad Y_{L,i} = y'_i(\varphi)$$

However it is practically impossible to obtain d=0 and α=0, consequently a small angular displacement is included, resulting in the following update of the equations:

$$X_{L,i} = r_i(\varphi + d\varphi(d,\alpha,\varphi)) \quad , \quad Y_{L,i} = y'_i(\varphi + d\varphi(d,\alpha,\varphi))$$

Assuming the $d \approx \alpha \approx 0$ (very small) the angular displacement $d\varphi$ can be approximated.

$$\tan(d\varphi) \approx \frac{d - \tan(\alpha) \cdot y'_i(\varphi)}{r_i(\varphi)}$$

Shiny surface

The initial result of the milling, was a "*steel glossy*" calibration object with a mirror like surface. To improve object reflectance, the calibration object was treated with an etching liquid (NaOH). The resulting object surface (see Figure 22) was less specular and almost optimally diffuse reflective. As a result of the treatment the feature detection stability and accuracy improved significantly, however it did also remove approximately 0.04 mm of the object surface and thus the feature parameter description had to be adjusted. The object shown in Figure 22 was milled using a high speed CNC milling machine. The milling time was approximately 1 hour with an absolute accuracy better than +/- 0.02 mm. Such high precision is required for accurate calibration precision.

Another way of dealing with this problem is to spray the surface with paint, charcoal dust, chalk powder or other similar materials that cover the surface and provide the surface with the desired *lambertian* characteristics. Whereas it is important for all surfaces to be scanned to have the desired surface characteristics it is especially important for the calibration object, since errors in the calibration affect all subsequent measurements done by the scanner.

Feature detection

With the accomplished design of calibration object, the feature extraction is reduced to line and corner detection. Contour points can be found using the Hough or Radon

transform. The corners are found as the points where the contour points change direction. In Figure 23 is illustrated how contour points 2301, and corners 2302 are detected with sub-pixel accuracy.

Multiple features

Figure 24 shows the corner features detected during a full rotation of the calibration object (suppose that the object in Figure 22 rotates, while corner features are detected and recorded). Figure 24 shows a screen dump from the calibration point processor program. In Figure 24 (a) are shown raw corner features 2401 detected during one full rotation of the calibration object (seen from camera 1). In Figure 24 (b) are shown manually selected 2D image feature curves, which correspond to the calibration object 3D object feature curves. In the shown example the rotation was performed in one minute, resulting in approximately 1300 valid feature points (6 frames per second, 7 valid points per frame) with corresponding rotational angles (encoder position).

Although corners are detected using sub pixel accuracy, there are still a number of outliers and undefined corners that does not correspond to the parametric feature definition in Figure 21 (especially at angles close to 0 or +/-π). These corner features must be deleted, before the actual calibration can take place. Furthermore the correspondence between "corner lines" (see lines in Figure 24) and the parametrically described 3D object feature curves (see Figure 21) must be determined. In the implemented setup the reduction and identification was performed using a semi-automatic user interface, requiring the user to point out the approximate position of the different 2D image feature curves (i.e. using a mouse).

Displaying the detected corner features x-co-ordinate (image space) as a function of the encoder position reveals the result shown in Figure 25. The symmetry points 2501 will be used in the next step to find the encoder position corresponding to φ=0 (see Figure 21), and calibration of the defined laser sheet parameters (see Figure 18).

During the first half of one rotation (-π to 0), the calibration object is facing against the camera, and thus corners are easily and accurately detected. At the second half

of one rotation (0 to π) some features may not be detectable due to occlusion, and faulty detection might occur (front and back facing see Figure 26). However some corners detected during the second half (0 to π) are necessary to calibrate the laser sheet (exploitation of symmetry). When the laser sheet parameters have been determined, the camera-lens calibration can be completed (DLT, Heikkilä or Tsai), using only the corners detected during the first half round ($-\pi$ to 0), thereby avoiding that inaccurately detected feature points spoils the calibration result.

Laser sheet calibration

The laser sheet parameters can be calibrated by analysing the encoder position corresponding to coexisting (symmetric) image features 2501 as shown in Figure 25 and 26. Recording a number of likewise symmetrical coordinates, enables the calibration of the laser sheet position (d and α), relative to the coordinate system (see Figure 18). Notice that the object features may be occluded by the object itself.

The laser sheet may be parameterised by the following parameters (see Figure 18):

- Encoder offset, φ_0, corresponding to $\varphi=0$, locking the co-ordinate system.
- Laser sheet displacement, d.
- Laser sheet angle, α.

To obtain a good estimate of the encoder offset, φ_0, corresponding to $\varphi=0$,and enable estimation of d, the mean encoder position 2701 was calculated for all symmetrical points (shown in Figure 27). In the Figure encoder offset and laser sheet parameters are extracted from encoder mean position of symmetric image features (see Figure 25).

Using the sinus relation, d can be approximated by:

$$\frac{(r_i - r_{i+2})}{\sin(\nu)} = \frac{r_{i+2}}{\sin(\theta)} \quad \Rightarrow \quad d \approx \frac{r_{i+2} \cdot \sin(\nu)}{(r_i - r_{i+2})} \cdot r_i$$

where r_i are defined in figure 28. Note the laser plane 2801 and the rotation centre 2802. When *d* is known (approximated), the encoder offset corresponding to φ=0 can be approximated:

$$\text{Encoder offset} = \text{pos}\_r_i - \frac{\theta \cdot \text{Tics per round}}{2\pi}$$

The laser sheet angle α is roughly estimated from the slope of the first order approximations 2702 (Figure 27), using *d* as the distance reference.

Using the formulas above the laser sheet parameters were estimated to d≈0.1 mm, φ_0≈146210, α≈0.11°. The noise level on each mean value is seen to be relatively high (100 pulses corresponds to a relative change in the 2D image feature curve position y direction of approximately 0.045 mm). Furthermore it can be seen that the noise on the corner features located far from the camera (line 2) is much higher than the noise on features close to the camera (e.g. line 1).

Furthermore a first order approximation was calculated to determine the relative movement of symmetrical points and thus enabling approximation of the laser sheet angle α.

An alternative method for estimation of the laser sheet parameters based on pairs of symmetric points is to create a φ-θ plot, where φ is the rotation angle / translation for the first symmetric point and θ is the difference in the rotation angle / translation between the symmetric points. For each of the visible feature curves on the calibration object a corresponding line will appear in the φ-θ plot. It can be shown that these lines usually correspond to straight lines for α and *d* close to zero. Likewise mathematical formulas can be derived for these lines, where the only unknown parameters are α, *d and* φ_0. Given two or more lines in the φ-θ plot the laser sheet parameters can be estimated using the derived formulas.

Laser intensity calibration

The laser intensities are preferably varied depending on the surface and colour of the object to be scanned. Preferably the intensity should be determined automatically using automatic laser intensity calibration.

The intensity calibration may be performed by inserting the object into the scanner and calculate a number of histograms from the acquired images. First a histogram is calculated with the laser turned off. A second histogram is the calculated when the laser is turned on with an arbitrary intensity. The first histogram is then subtracted from the second to remove the background intensity. The intensity is then adjusted until the selected quantile corresponds to a predefined intensity. The background could also be removed by subtracting the image corresponding to the laser turned off from the image with laser light. The histogram used to determine the intensity could then be calculated from this difference image.

Calibration performance

To investigate calibration performance, feature points (X_i, Y_i) are back projected to the laser sheet, and compared with their original counterparts (X_L, Y_L):

$$\text{Tsai/DLT}(X_i, Y_i) = (X_{L,Tsai}, Y_{L,Tsai}) \text{ compared to } (X_L, Y_L)$$

Three feature sets (e.g. 685 corresponding image and laser sheet co-ordinates) were recorded using the same camera-laser setup. DLT, Heikkilä and Tsai calibration was performed, and the image co-ordinates were backprojeced to measure the model accuracy. The result shown in table 3 was obtained with camera 1, positioned relative to the laser as shown in Figure 22. Calibrating camera 2 leads to approximately the same results, although it is obviously somewhat dependent on the camera position relative to the laser.

Feature set nr.	d	α	Method	Removed outliers	Points	Mean deviation	Std. deviation	Max deviation
1	0	0	DLT	0%	685	0.63	0.41	1.3
2	0	0	DLT	0%	1470	0.58	0.38	1.8
3	0	0	DLT	0%	1295	0.62	0.40	1.8
1	0	0	Tsai	0%	685	0.0227	0.0190	0.12
1	0.08	0.11	Tsai	0%	685	0.0211	0.0188	0.10
1	0.08	0.11	Tsai	26%	503	0.0072	0.0056	0.03
2	0	0	Tsai	0%	1470	0.0249	0.0194	0.16
2	0.08	0.11	Tsai	0%	1470	0.0235	0.0190	0.14
2	0.08	0.11	Tsai	33%	982	0.0073	0.0063	0.04
3	0	0	Tsai	0%	1295	0.0221	0.0166	0.18
3	0.08	0.11	Tsai	0%	1295	0.0219	0.0173	0.13
3	0.08	0.11	Tsai	30%	982	0.0075	0.0059	0.03

Table 3: Errors on backprojected image features compared with their original counterparts (data have been captured using camera 1). Calibration of camera 2 revealed somewhat the same results. Removing outliers, improves the result, although it may not correspond to real improvements in terms of more accurate transformation parameters. All measurements are in mm.

As shown in Table 3 the standard deviation using the TSai calibration technique is approximately 0.01 mm, corresponding to a standard deviation in image space of approximately 0.1 pixels (measured on backprojected laser sheet co-ordinates). Considering the accuracy of the milled calibration object, the potential mechanical error sources and non-modelled lens distortion etc. it is an extremely high accuracy. However, the calculated errors are relative and based on the same points as used for the actual calibration, thus the measured error cannot be used as a direct qualifier for the scanner accuracy.

Instead the error can be used as an indicator of the calibration model accuracy (Tsai versus DLT), and the magnitude of the feature detection noise. As shown in table 3 the Tsai calibration and transformation technique, models the camera and lens distortion much better than the direct linear transformation. Consequently the main error source using the DLT transform, is assumed to be the DLT transformation model itself (i.e. the perspective projection does not model non-linear lens distortion).

Using a Tsai calibration to model the camera-lens system the error is much smaller.

Removing the worst outliers (25-30%) and then re-calibrating, obviously reduces the error on back projected points, although it may not correspond to more accurate calibration parameters. Small changes of the laser sheet parameters (d and α) does not influence the back projection result significantly, although it changes the calibration parameters and thereby the overall transformation accuracy.

For each camera in the setup, the TSai/DLT calibration needs to be repeated. It is straightforward to add additional cameras, thus reducing occlusion effects and enhance scanning accuracy.

Overall performance

The overall performance of the scanner system has been tested by a number of relevant scanner jobs, and has proved to yield result of very high quality, surpassing competitive solutions.

Ear model

The developed system's, ability to scan ear models was investigated.

Figure 29 shows Camera images (2D) of an ear impression supplied by a hearing aid manufacturer. The model corresponds to the inside of a human ear, and it is used to create a fitting hearing aid, customised especially for the patient. Currently the hearing aid is created in a silicon mould, made with the ear clay model.

Result of scanning the ear model shown in Figure 30. The shown 3D model consists of 332,955 triangles spanned between 166,843 points. The 3D model was created from two sub scans that have been registered and merged. Another setup more suitable for such scanning is the scanner disclosed in Figure 4,5 and 9. Using one of these scanner set-ups it is possible to scan the model in one scan. Improved scanning is especially obtained when the model is placed on a spike as in Figure 6.

The shown 3D model was scanned and processed in approximately 3 minutes, however it is possible to complete the 3D model in less than 1 minutes if the registration process is automated, or avoided (e.g. by introduction of one or more cameras).

As shown by the figures it is possible to scan and create very detailed and accurate copies of ear clay models with the developed system.

In order to improve the detection of surface features during the scan, it may be advantageous to treat the surface of the clay model as described above to obtain a *lambertian* surface.

As described, hearing aids are normally made by taking an impression of the ear canal. This is normally done by educated staff. The impression is then sent to the hearing aid manufacturer, who casts a mould around the impression and moulds the shell inside. Thereby, at least 3 impressions are made, each of which contribute to the error of the hearing aid shell. The scanning methods disclosed in this application are very useful for comparing the size of the impression to the size of the moulded or hand made hearing aid shell as a quality control, before the hearing aid shell is sent to the patient. The comparison can be made in a computer, where the result of a scan of the impression is compared to the result of the scan of the hearing aid shell. A colour code can be used to identify the areas where the differences differ more than a pre-determined tolerance.

In many cases, the hearing aid shells are returned by the patient to the hearing aid manufacturer due to lack of fit. In these cases it is advantageous for the manufacturer to be able to compare the actual size of the impression to the size of the hand made hearing aid shell.

Devices for the ear

Other devices that could advantageously be incorporated into a shell manufactured according to the disclosed method include mobile phones, communication devices, loud speakers, tinnitus masking devices, or devices recording vibrations in the skull and transforming these into an audio signal.

Devices that may be incorporated into a shell in the ear also comprise devices related to Man Machine Interface (MMI) products, such as custom made ear microphone/receivers that enable reliable and clear communication even in the noisiest environments, or products related to wireless internet applications.

Speech not only creates sound waves, it also generates vibrations within the skull of the speaker. These vibrations can be picked up in the ear (they may be picked up other places too, but by far the most convenient method is to do it in the ear). In one piece, a device thus may comprise a microphone to pick up the speech of the person wearing it, and a loudspeaker to transmit the speech of the communication partner. It is important that such devices are made to fit the ear.

The devices based detection of vibration instead of sound can be used in the noisiest environments, since they only pick up the speech of the wearer and they allow for quiet communication, since the speaker can speak with a low voice when needed. The devices allow for completely hand-free communication.

Such a device is naturally also devoid of any kind of acoustic feed-back.

Scanning the ear canal

Another possibility according to the invention, is to scan the ear canal directly. This can be done by building the components of the scanner into an apparatus, which can be inserted into the ear of the patient. Embodiments of this scanner are shown in Figure 31. Preferably, the light source, e.g. the laser, and the camera are located outside the ear. The laser light can be carried into the scanner by light guides 3101 such as optical fibers, and similarly, the reflected signals are carried to a camera by image guide 3102 such as optical fibers. During the scan, the scanner preferably rests on the edge of the ear canal, most preferably in those places where bones are closest to the skin surface. This is in order to obtain the highest stability and is very important, since the scanner itself works with an accuracy less than 0.05 mm. The length of the ear canal can be scanned by moving the scanner in or out and record a series of overlapping images of the ear canal. The scanner may comprise only one laser source and one camera as the one shown in the left of Figure 31. In that case the scanner has to rotate while the camera records images. Preferably, the scanner comprises multiple laser sources such as four as shown in the scanner in the right part of Figure 31. The presence of multiple laser sources and cameras removes the need for rotation of the scanner in the ear canal. In the laser scanner disclosed in

Figure 31, the laser source or sources project a ray of laser light on the surface of the ear canal.

Another type of ear canal laser scanner is shown in Figure 32. Here the laser light is projected as laser sheets producing a laser contour on the surface of the ear canal. Thereby, more rapid scanning can be performed compared to the above laser scanner. In the scanner shown in the right part of Figure 32, four laser sheets 3201 and four cameras 3202 are present. Thereby the laser sheets cover the whole circumference and rotation of the scanner is not required.

A third type of ear canal scanner is shown in Figure 33. The scanner is shown in the ear canal 3301 and consists of a rigid probe/pipe 3302, a box 3303, light guides 3304 such as optical fibers, a light source 3305 such as a laser, a position sensor device 3306, a camera 3307, optics 3308 and a collision detector / distance measure 3309. This scanner works by projection a structured light pattern such as a grid of spots on the whole circumference. The light is generated by the light source and travels through the light guides. At the end of the light guides optics and mirrors creates the desired pattern. The light beams 3310 for a dot pattern are illustrated in Figure 33. By locating this pattern the corresponding 3D surface positions can be reconstructed adopting the techniques described above. The rigid canal scanner has the advantage that light guides such as optical fibers are not required for the camera. Note that light guides degrade the image quality. Another advantage of the rigid scanner is that the position sensor can be placed outside the ear, e.g. in the box, and not on the head of the probe/pipe. Examples of position sensor are magnetic sensors, optical sensors, sonic sensors and mechanic sensors. An alternative to measuring the positions is to register each local scan of the subsurface to form the full surface. This technique is feasible since only the relative positions of the subscans are required to form the full surface.

The disadvantage of the rigid scanner is the lack of flexibility to move inside the ear canal, which can be obtained by a flexible probe/pipe. The embodiment of a flexible scanner in the ear canal 3301 is shown in Figure 34. The scanner consists of a flexible probe/pipe 3302, a box 3303, light guides 3304, image guides 3401 such as optical fibers, a light source 3305 such as a laser, a position sensor device 3306, a camera 3307, optics 3308 and a collision detector 3309.

A design that improves the image quality of the flexible ear scanner is shown in Figure 35. The difference is that the camera 3307 is moved to the head of the probe/pipe to avoid degrading of the image quality through the light guides. In a similar way the camera can be moved to the front of the probe/pipe for the rigid scanner.

The same types of variation of the ear canal scanner can be used as in other cases of three-dimensional scanners according to this invention. Thus, preferably the scanner comprises at least two cameras, more preferably 4 cameras such as for example 6 cameras. Likewise, there may be several laser sources such as for example 2 lasers creating laser sheets with an offset of 180°, preferably 3 laser sheets with an offset of 120°, or 4 laser sheets with an offset of 90°.

Prior to scanning, the patient's ear must be rinsed to remove cerumen. In some cases it may also be advantageous to treat the surface of the ear canal if the appearance is too glossy. This can be done in the way described above for obtaining a *lambertian* surface.

One scan can be performed in less than 1 minute, and it is thus possible to record a number of scans of one ear, and ask the patient to deliberately vary the size of the ear canal by swallowing, yawning, chewing, and drinking. In this way a series of scans of the ear canal can be recorded and the magnitude of the variation of the patient's ear canal can be detected. In the end it is possible to superimpose these scans on one another to create a model, which will fit the patient's ear under all conditions. Such a model is naturally made as a compromise between the different sizes of the ear canal.

The improved fit of the hearing aid shells according to the present invention compared to prior art hearing aid shells means that the frequent problem of acoustic feedback in hearing aids is minimised.

References

[1] TSai, R. Y., "A versatile Camera Calibration Technique for High-Accuracy 3D Machine Vision Metrology Using Off-the-Shelf TV Cameras and Lenses", *IEEE Journal of Robotics and Automation*, pages 323-344, Vol. RA-3, No. 4, August 1987.

[2] *Machine vision product guide,* Melles Griot, 1998.

[3] Heikkila, J, "Geometric Camera Calibration Using Circular Control Points", IEEE Transactions on Pattern Analysis and Machine Intelligence, Vol. 22, No 10. pp. 1066-1077, Oct 2000

Claims

1. A three dimensional calibration object having at least one plane of symmetry and whereby at least part of at least one 3D object feature curve of each symmetric part is a continuous curve.

2. The object of claim 1, being rigid.

3. The object of claim 1, being manufactured from metal.

4. The object of claim 1, being manufactured from a material selected from the group consisting of alloy, stainless steel, aluminium, a plastic polymer, kevlar®, carbon, wood.

5. The object of claim 1, wherein at least part of the surface of the object is rough.

6. The object of claim 1, wherein at least part of the surface of the object is non-glossy.

7. The object of claim 1, wherein the continuous curves of the at least part of the at least one 3D object feature curve can be described by continuous mathematical functions.

8. The object of claim 7, whereby the mathematical functions each describe part of a spiral.

9. The object of claim 7, wherein the mathematical functions each describe part of an ellipse.

10. The object of claim 7, wherein the mathematical functions each describe part of a circle.

11. The object of claim 7, wherein the mathematical functions comprise trigonometric functions such as sinus, cosinus, tangens, cotangens.

12. The object of claim 1, wherein each symmetric part has two, three, four, six, or more 3D object feature curves being symmetric over the plane of symmetry.

13. The object of claim 12, wherein the distance between two 3D object feature curves of each symmetric part is constant.

14. The object of claim 12, wherein all distances between 3D object feature curves of each symmetric part are constant.

15. The object of claim 1, having an axis of rotation.

16. The object of claim 15, wherein the axis is essentially vertical.

17. The object of claim 15, wherein the axis is essentially horizontal.

18. The object of claim 1, having two axes of rotation.

19. The object of claim 1, having three, four, five or more axes of rotation.

20. The object of claims 15-19, wherein a mathematical combination of image feature points, being representations of 3D object feature curves and being detectable in images of the object recordable by a camera at discrete values of angle of rotation and/or translation, plotted as a function of the angle of rotation and/or translation produces an estimable mathematical function.

21. The object of claims 15-19, wherein the mathematical combination is the image feature point x co-ordinate.

22. The object of claims 15-19, wherein the mathematical combination is the image feature point y co-ordinate.

23. The object of claims 15-19, wherein the mathematical combination is a sum of the image feature points x and y co-ordinates.

24. The object of claims 15-19, wherein the mathematical combination is the product of image feature point x and y co-ordinates.

25. The object of claims 15-19, wherein the mathematical combination is any function of the image feature point x and y co-ordinates such as $x^n + y^n$, $x^n - y^n$, $y^n - x^n$, $x^n * y^n$, x/y, y/x, x^n/y^n, y^n/x^n, sinus $(x^n + y^n)$, cosinus $(x^n + y^n)$, tangens $(x^n + y^n)$, cotangens $(x^n + y^n)$, sinus $(x^n * y^n)$, cosinus $(x^n * y^n)$, tangens $(x^n * y^n)$, cotangens $(x^n * y^n)$, exp $(x^n * y^n)$, hyp $(x^n * y^n)$.

26. The object of claims 15-19, wherein the mathematical combination is derived from image feature point x and y co-ordinates such as the difference in rotation angle or translation between two symmetric points

27. The object of any of claims 20-26, wherein the estimable mathematical function can be modelled with a first order approximation.

28. The object of any of claims 20-26, whereby the estimable mathematical function can be modelled with a second order approximation.

29. The object of any of claims 20-26, whereby the estimable mathematical function can be modelled with a third, fourth, fifth, sixth, seventh, eighth, ninth, tenth, or n^{th} order approximation.

30. The object of claim 1, having a size corresponding to the size of the objects to be scanned later.

31. The object of claim 1, the linear size of which is between 50 and 150 % of the linear size of the object to be scanned later, such as between 60 and 140 %, for example between 70 and 130 %, such as between 75 and 125 %, such as between 80 and 120 %.

32. The object of claim 1, having a size corresponding to the camera field of view.

33. The object of claim 1, the linear size of which is at least 10% of the camera field of view, such as at least 20%, for example at least 30%, such as at least 40%,

for example at least 50%, such as at least 60%, for example at least 70%, such as at least 75%, for example at least 80%, such as at least 85%, for example at least 90%, such as at least 95%.

34. The object of claim 1, being hollow and having the 3D object feature curves on the inside.

35. A method for calibration of a three dimensional light scanner comprising the steps of

i) providing a three dimensional light scanner,

ii) providing a calibration object according to claims 1 to 34,

iii) scanning the calibration object,

iv) determining image feature co-ordinates being representations of at least one pair of 3D object feature curves for each of a discrete number of values of an angle of rotation and/or translation, a pair consisting of one 3D object feature curve in each symmetric part of the calibration object,

v) changing the calibration parameters to fit the calibration object.

36. The method according to claim 35. whereby a sheet of laser light is projected onto the calibration object producing 2D image feature curves.

37. The method according to claim 35, whereby the 2D image feature curves are determined using the Hough transformation.

38. The method according to claim 35, whereby 2D image feature co-ordinates are found as the intersection between image feature curves such as, the intersection between two n^{th} order curves, as the intersection between two first order curves, as the intersection between two second order curves, as the intersection between two third order curves, as the intersection between a fist order curve and a second order curve, as the intersection between a first order curve and a third order curve, or as the intersection between a second order curve and a third order curve.

39. The method according to claim 35, further comprising plotting of a mathematical combination of at least one 2D image feature co-ordinate being representations

of each pair of 3D object feature curves against the angle of rotation and/or translation of the calibration object.

40. The method according to claim 39, further comprising determination of the mean plane of symmetry in the plot.

41. The method according to claim 40, whereby the mean plane of symmetry is determined by calculating the mean angle of rotation and/or mean translation for pairs of angle of rotation having the same value in the mathematical combination.

42. The method according to any of claims 40 to 41, whereby the determined mean plane of symmetry is used to calibrate the encoder offset.

43. The method according to any of claims 40 to 41, whereby pairs of mean angle of rotation and/or mean translation are used to calibrate the laser sheet displacement.

44. The method according to any of claims 40 to 41, whereby pairs of mean angle of rotation and/or mean translation are used to calibrate the laser sheet angle.

45. The method according to any of claims 40 to 41, whereby laser sheet calibration comprises selecting symmetric points, plotting of the rotation angle and/or the translation for the first point against the difference in the rotation angle and/or the translation between the two symmetric point, deriving mathematical formula for the plotted lines and estimating α, d, and φ_0.

46. The method according to claim 35, whereby step v) comprises determination of 2D laser sheet co-ordinates of the 2D image feature curves corresponding to a discrete number of values of angle of rotation.

47. The method according to claim 46, whereby 2D co-ordinates of the 3D object feature curves are calculated from mathematical functions determining the 3D object feature curves for a discrete number of values of angle of rotation and/or translation.

48. The method according to claim 35, whereby step v) comprises comparison of pairs of 2D laser sheet co-ordinates to calculated 2D co-ordinates.

49. The method according to claim 35, whereby step v) comprises using the Tsai algorithm.

50. The method according to claim 35, whereby step v) comprises using the Heikkilä algorithm.

51. The method according to claim 35, whereby step v) comprises using direct linear transformation.

52. The method according to claim 35, whereby step v) comprises using direct non-linear matrix transformation.

53. The method according to claim 35, whereby step v) comprises an optimisation procedure such as least squares means to minimise the error.

54. The method according to claim 35, whereby outliers are excluded from step iv).

55. The method according to claim 35, whereby outliers are identified by back projection of image feature co-ordinates.

56. The method according to claim 55, whereby at least the 2% of the feature points deviating most from the back-projected 2D image feature curves are excluded from step iv).

57. The method according to claim 55, whereby the at least 3%, such as at least 5%, for example at least 10%, for example at least 12%, such as at least 15% for example at least 20, such as at least 25%, for example at least 30 %, such as at least 33 % are excluded.

58. The method according to claim 35, further comprising estimating initial calibration parameters.

59. The method according to claim 35, whereby the discrete number of values for an angle of rotation and/or translation is at least 100, preferably at least 240.

60. The method according to claim 35, whereby the discrete number of values for an angle of rotation and/or translation is at least 500, such as at least 750, for example at least 1000, such as at least 1200, for example at least 1500, such as at least 1800, for example at least 2000, such as at least 2400, for example at least 3000, for example at least 3600, such as at least 4200.

61. The method according to claim 35, whereby the laser intensity is varied depending on the surface and/or colour of the object to be scanned.

62. The method according to claim 61, whereby the laser intensity is determined automatically using automatic laser intensity calibration.

63. The method according to claim 35, whereby the calibration object is aligned manually using the cross-section between two laser sheets as a guiding reference.

64. The method according to claim 35, whereby the calibration object is mounted on mounting means.

65. The method according to claim 35, whereby the calibration object is mounted on a spike.

66. Method for three-dimensional scanning comprising the steps of

i) providing a three-dimensional light scanner

ii) calibrating the system,

iii) scanning an object determining image co-ordinates on the light contour projected on the object for each of a discrete number of values of an angle of rotation and/or translation,

iv) calculating three dimensional co-ordinates describing the surface of the object.

67. The method according to claim 66, whereby calibration comprises using a calibration object according to claims 1 to 34 in the method according to claims 35 to 65.

68. The method according to claim 66, whereby the three dimensional co-ordinates are calculated from image co-ordinates using the Tsai algorithm.

69. The method according to claim 66, whereby the three dimensional co-ordinates are calculated from image co-ordinates using the Heikkilä algorithm.

70. The method according to claim 66, whereby the three dimensional co-ordinates are calculated from the image co-ordinates using direct linear transformation.

71. The method according to claim 66, whereby the three dimensional co-ordinates are estimated using direct non-linear matrix transformation.

72. The method according to claim 66, whereby the image co-ordinates are determined using Hough transformation.

73. The method according to claim 66, whereby the image co-ordinates are determined using a method selected from the group consisting of filter search such as line or point filter search, max intensity, threshold, centre of gravity, derivatives.

74. The method according to claim 66, whereby the three-dimensional light scanner comprises at least two light sources and at least two cameras.

75. The method according to claim 66, whereby the three-dimensional light scanner comprises at least three light sources and at least three cameras.

76. The method according to claim 66, whereby the three-dimensional light scanner comprises three light sources and six cameras.

77. The method according to claim 66, whereby the object is rotated during scanning.

78. The method according to claim 66, whereby the object is translated during scanning.

79. The method according to claim 66, whereby the object is rotated and translated during scanning.

80. The method according to claim 66, whereby the camera and light source are rotated around the object during scanning.

81. The method according to claim 66, whereby the camera and light source are translated along the object during scanning.

82. The method according to claim 66, whereby the camera and light source are rotated and translated around the object during scanning.

83. The method according to claim 66, whereby the discrete number of values for an angle of rotation and/or translation is at least 100, preferably at least 240.

84. The method according to claim 66, whereby the discrete number of values for an angle of rotation and/or translation is at least 500, such as at least 750, for example at least 1000, such as at least 1200, for example at least 1500, such as at least 1800, for example at least 2000, such as at least 2400, for example at least 3000, for example at least 3600, such as at least 4200.

85. The method according to claim 66, whereby the laser intensity is varied depending on the surface and/or colour of the object to be scanned.

86. The method according to claim 85, whereby the laser intensity is determined automatically using automatic laser intensity calibration.

87. The method according to claim 66, whereby the object is aligned manually using the cross-section between two laser sheets as a guiding reference.

88. The method according to claim 66, whereby the object is mounted on mounting means.

89. The method according to claim 66, whereby the object is mounted on a spike.

90. Method for manufacturing a shell comprising a device for the ear of an individual comprising the steps of

i) providing three dimensional co-ordinates describing the surface of the ear and/or ear canal,

ii) modelling a three-dimensional model.

91. The method according to claim 90, whereby the data of step i) are provided using three-dimensional scanning according to claims 66 to 89.

92. The method according to claim 90 whereby the data of step i) are provided by scanning a model of the ear and/or ear canal of an individual.

93. The method according to claim 91, whereby the surface of the model is non-glossy.

94. The method according to claim 91 whereby the surface of the model is rough.

95. The method according to claim 90, whereby the data of step i) are provided by scanning the ear and/or ear canal of an individual.

96. The method according to claim 95, whereby the ear and/or ear canal is scanned a number of times.

97. The method according to any of claims 95 to 96, whereby the ear and/or ear canal is scanned a number of times under different conditions affecting the geometry of the ear and/or ear canal of the individual.

98. The method according to any of claims 96 to 97, further comprising computer modelling of the device for the ear by adjusting the model for the dynamic changes in the geometry of the ear and/or ear canal using scan data from different scans.

99. The method according to claim 90, whereby the three-dimensional model is modelled using milling.

100. The method according to claim 90, whereby the three dimensional model is modelled using 3-dimensional printing.

101. The method according to claim 90, whereby the three dimensional model is modelled using stereo lithography.

102. The method according to claim 90, whereby the three dimensional model is modelled using selective laser sintering.

103. The method according to claim 90, whereby the three dimensional model is modelled using laminated object modelling.

104. The method according to claim 90, whereby the three dimensional model is modelled using inkjet modelling.

105. The method according to claim 90, whereby the three dimensional model is modelled using fused deposition modelling.

106. The method according to claim 90, whereby the three dimensional model is modelled using nano-printing.

107. The method according to claim 90, whereby the device comprises a hearing aid.

108. The method according to claim 90, whereby the device comprises a mobile phone.

109. The method according to claim 90, whereby the device comprises a loud speaker.

110. The method according to claim 90, whereby the device comprises communication devices.

111. The method according to claim 90, whereby the device comprises a device capable of detecting vibrations in the scull and converting these into a transmittable signal.

112. The method according to claim 90, whereby the device comprises a tinnitus masker or a tinnitus masking device.

113. A device manufactured according to claims 90 to 112.

114. A method for manufacturing a dental implant for an individual comprising the steps of

i) providing three dimensional co-ordinates describing the surface of the dental implant,

ii) modelling a three-dimensional dental implant.

115. The method according to claim 114, whereby the data of step i) are provided using three-dimensional scanning according to claims 66 to 89.

116. The method according to claim 114, whereby the data of step i) are provided by scanning a model of the dental implant for the individual.

117. The method according to claim 115, whereby the surface of the model is non-glossy.

118. The method according to claim 115, whereby the surface of the model is rough.

119. The method according to claim 114, whereby the provision of data in step i) comprise scanning of a tooth of an individual.

120. The method according to claim 114, whereby provision of data of step i) comprise scanning of the oral cavity of the individual

121. The method according to claim 114, whereby the three-dimensional model is modelled using milling.

122. The method according to claim 114, whereby the three dimensional model is modelled using 3-dimensional printing.

123. The method according to claim 114, whereby the three dimensional model is modelled using stereo lithography.

124. The method according to claim 114, whereby the three dimensional model is modelled using selective laser sintering.

125. The method according to claim 114, whereby the three dimensional model is modelled using laminated object modelling.

126. The method according to claim 114, whereby the three dimensional model is modelled using inkjet modelling.

127. The method according to claim 114, whereby the three dimensional model is modelled using fused deposition modelling.

128. The method according to claim 114, whereby the three dimensional model is modelled using nano-printing.

129. A dental implant manufactured according to claims 114 to 128.

Figure 1

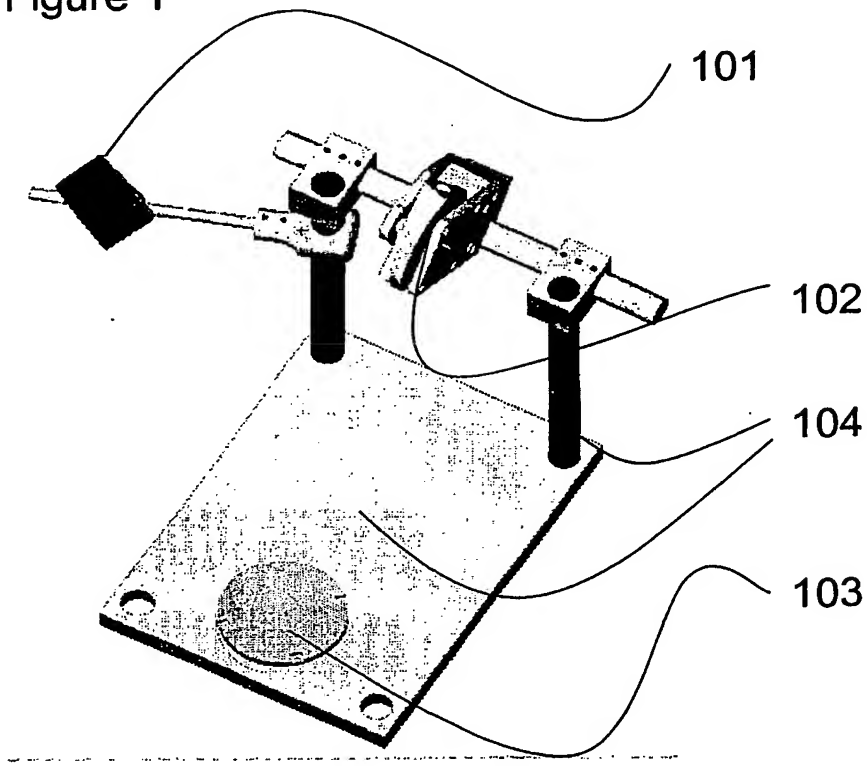

Figure 2

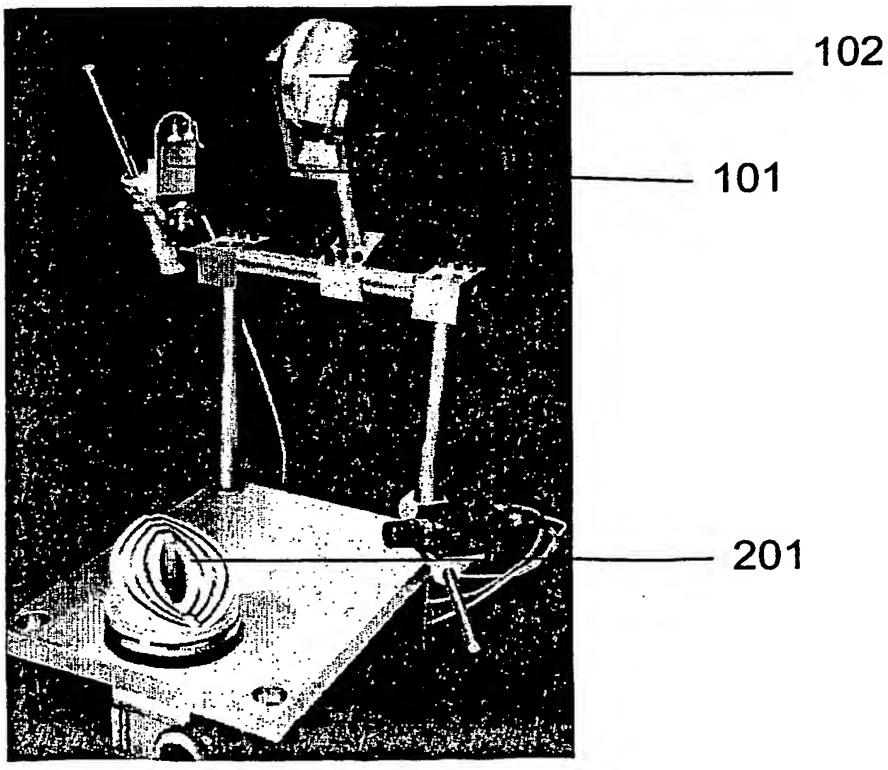

Figure 3

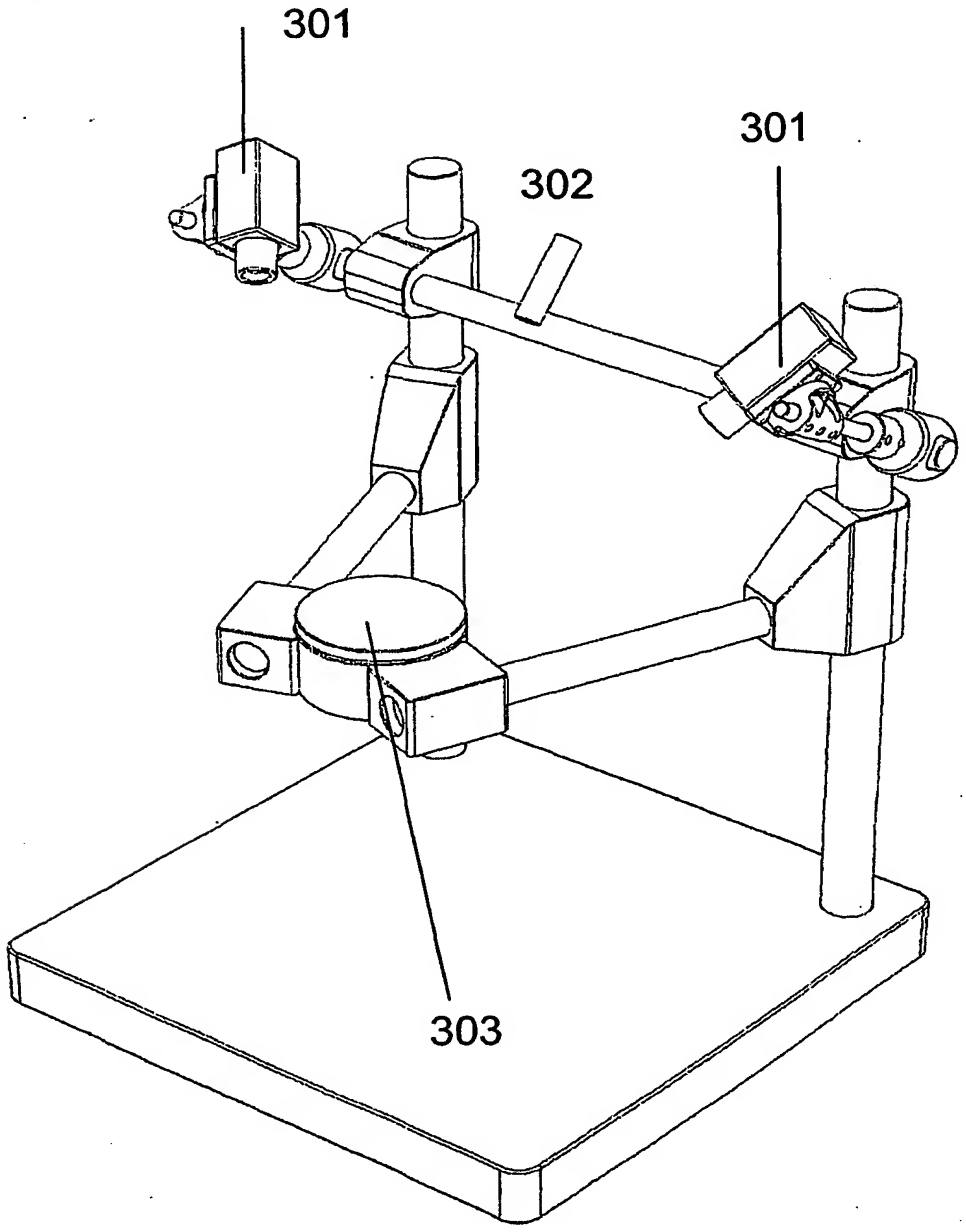

Figure 4

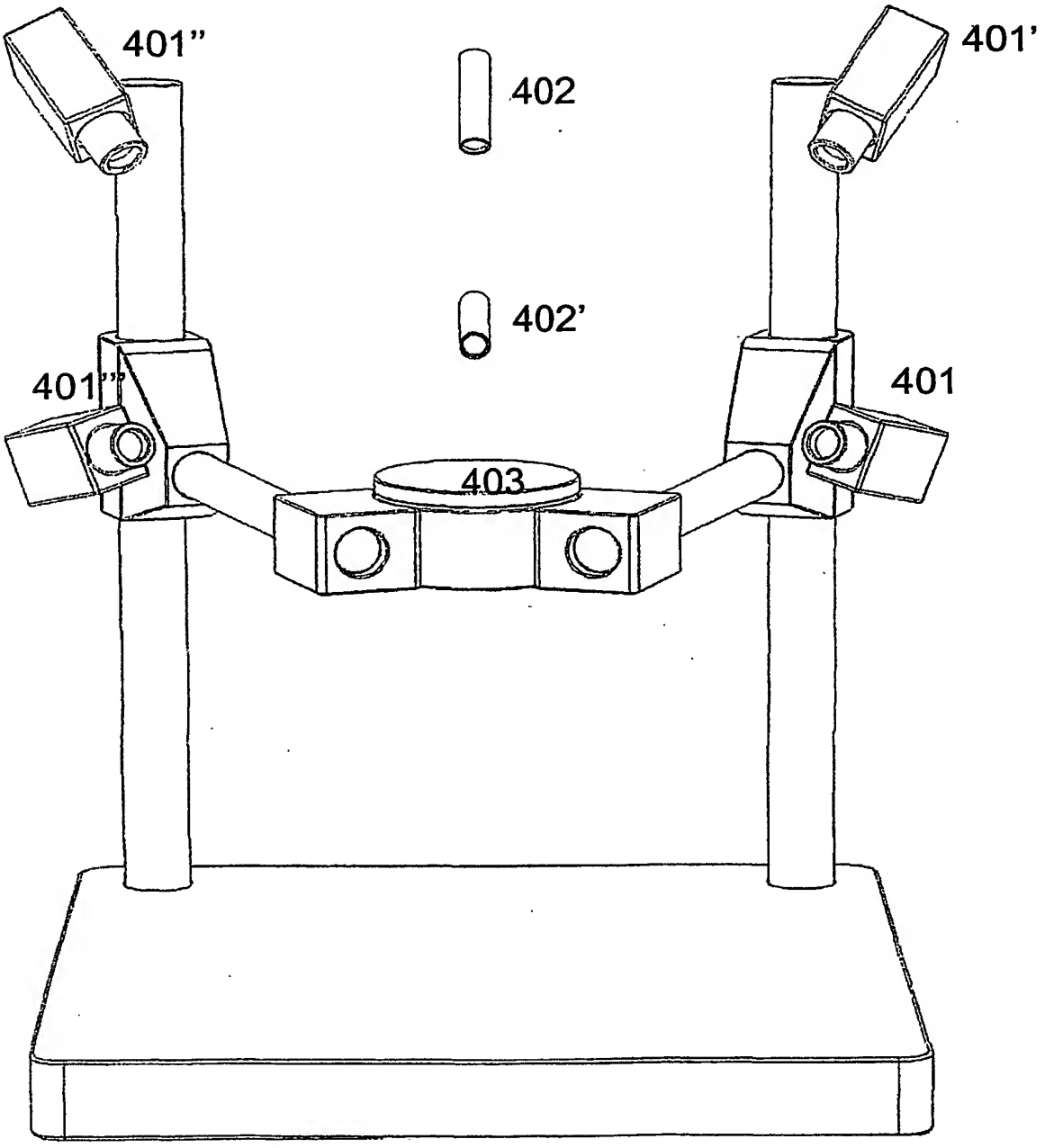

Figure 5

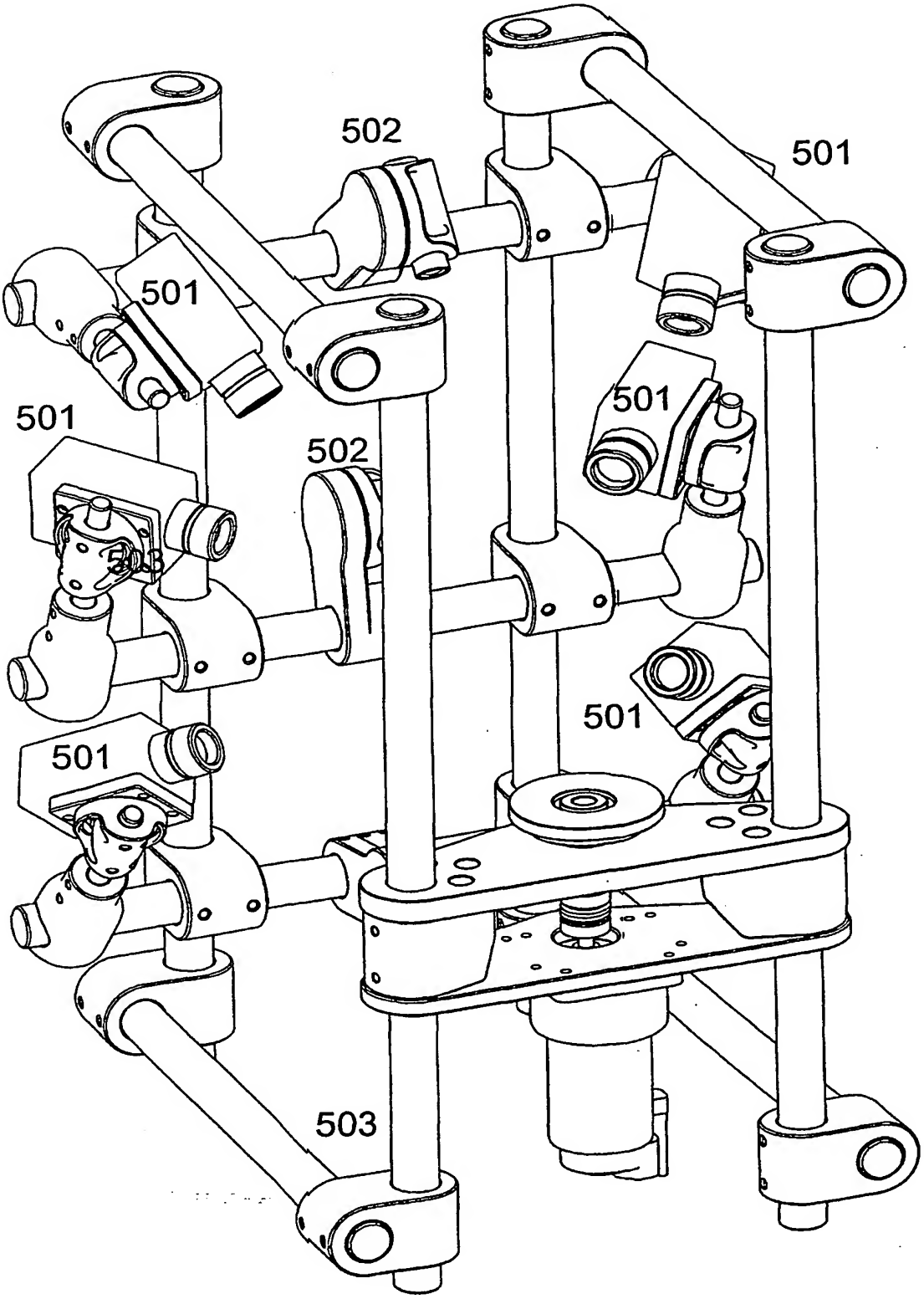

Figure 6

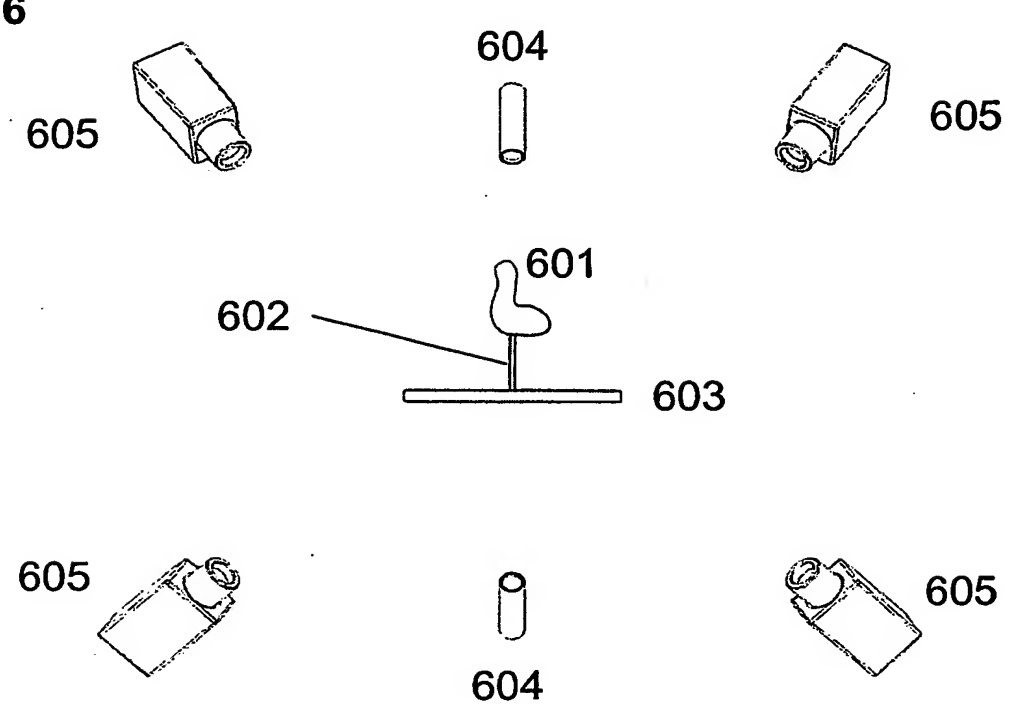

Figure 7

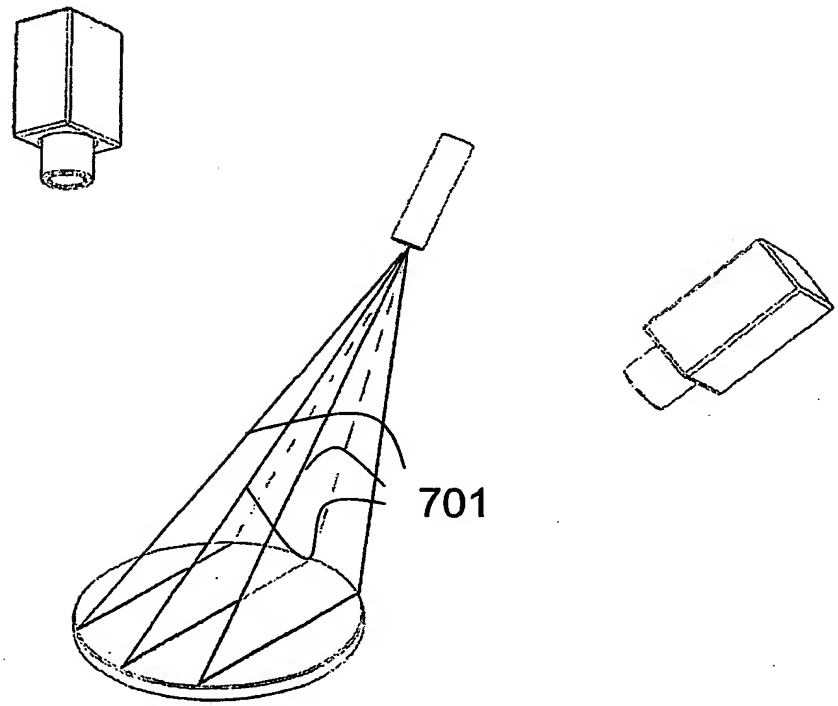

Figure 8

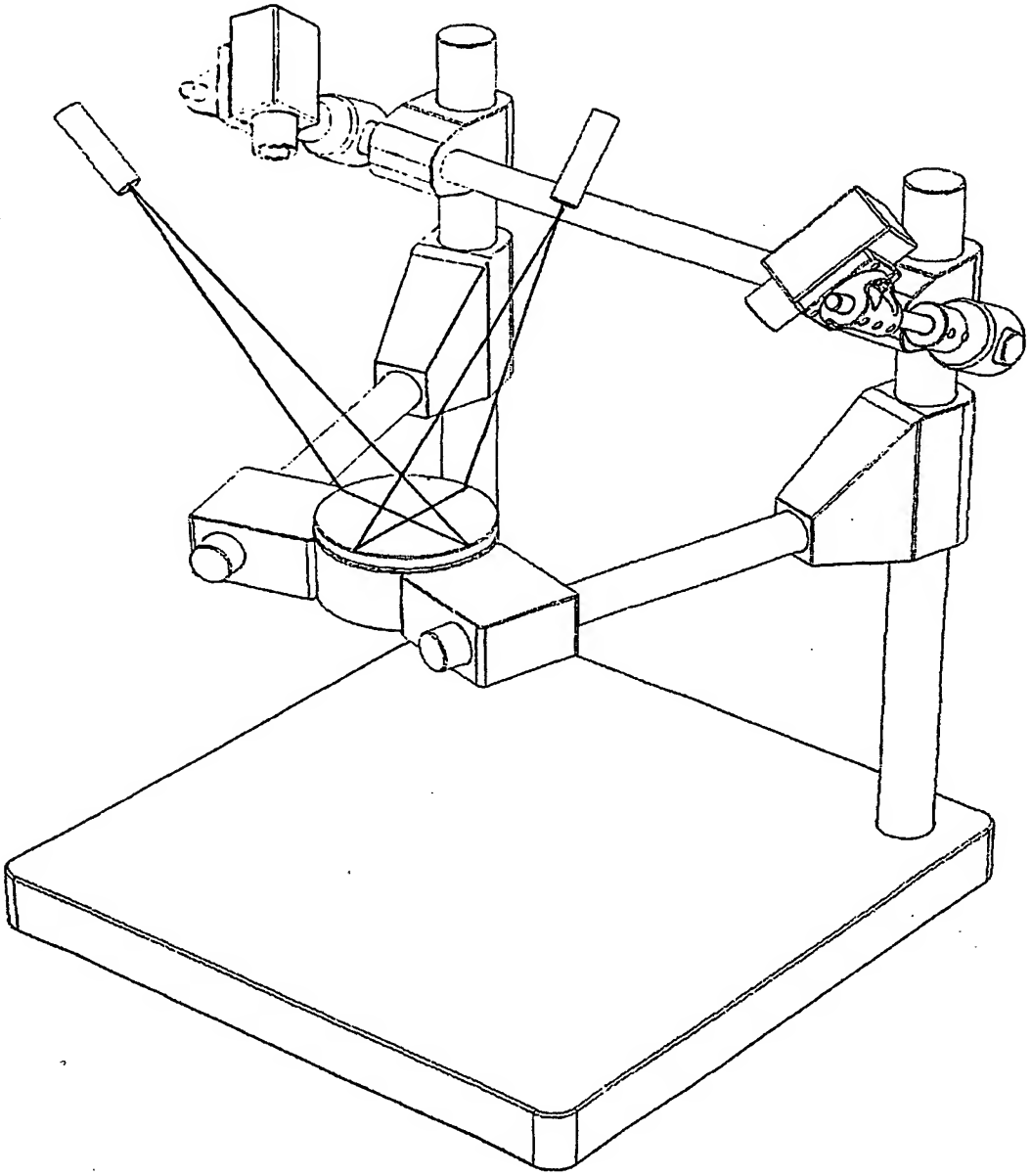

Figure 9

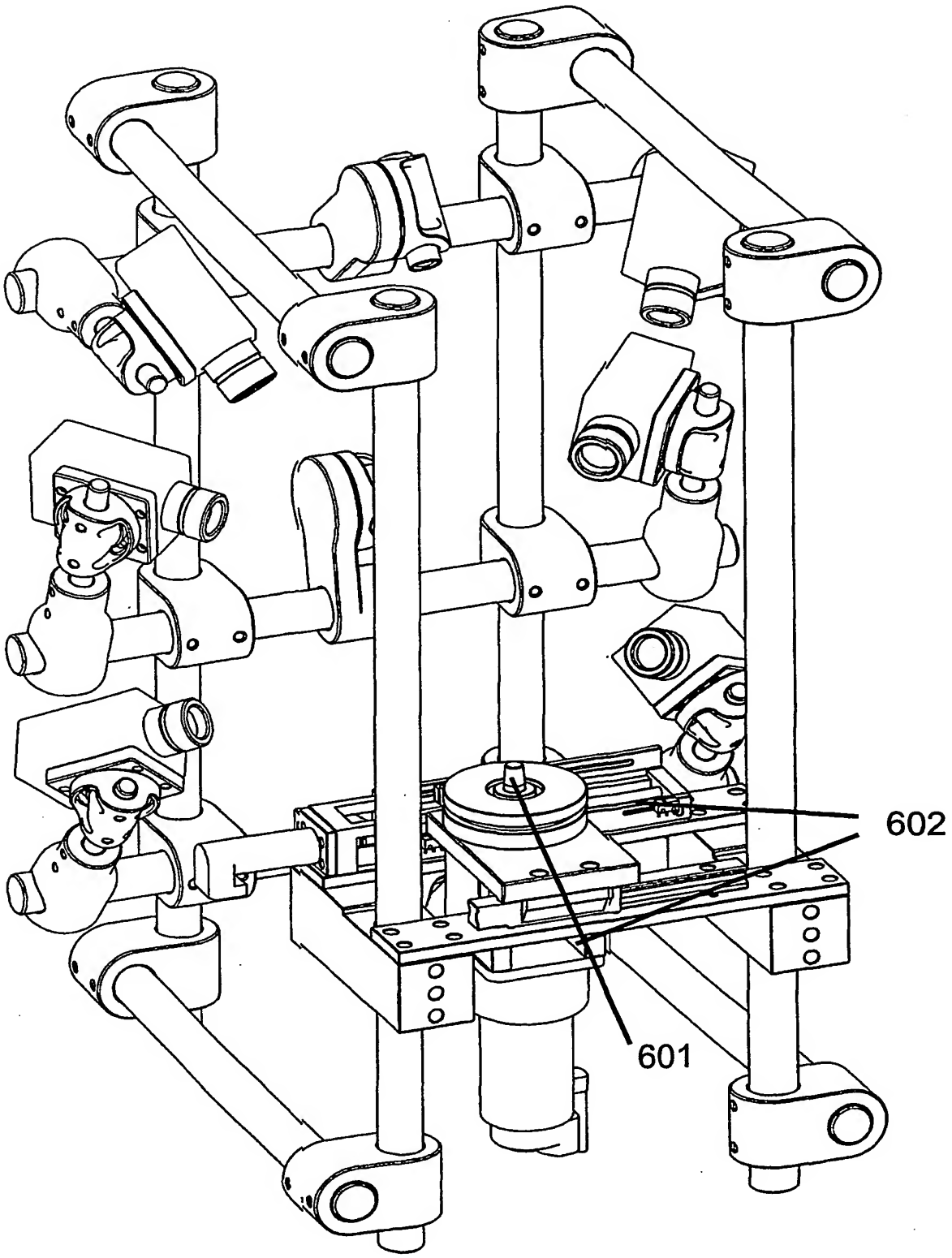

Figure 10

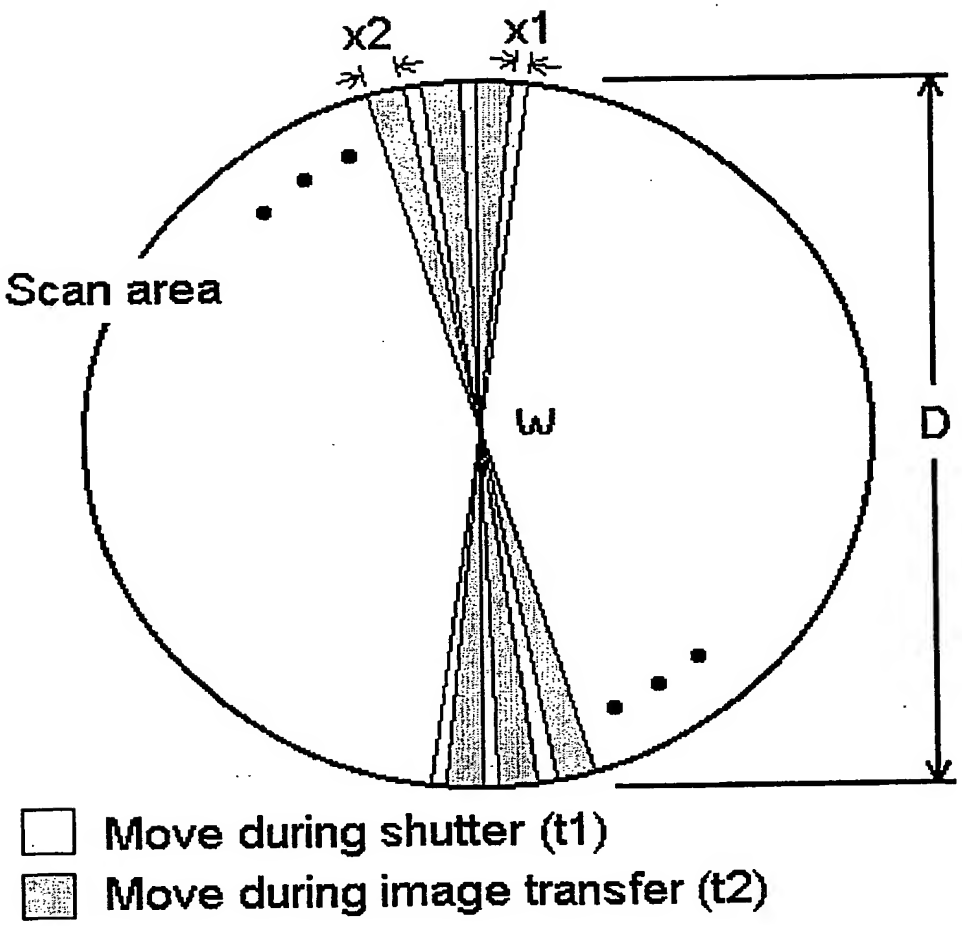
x2
x1
Scan area
W
D
Move during shutter (t1)
Move during image transfer (t2)

Figure 11

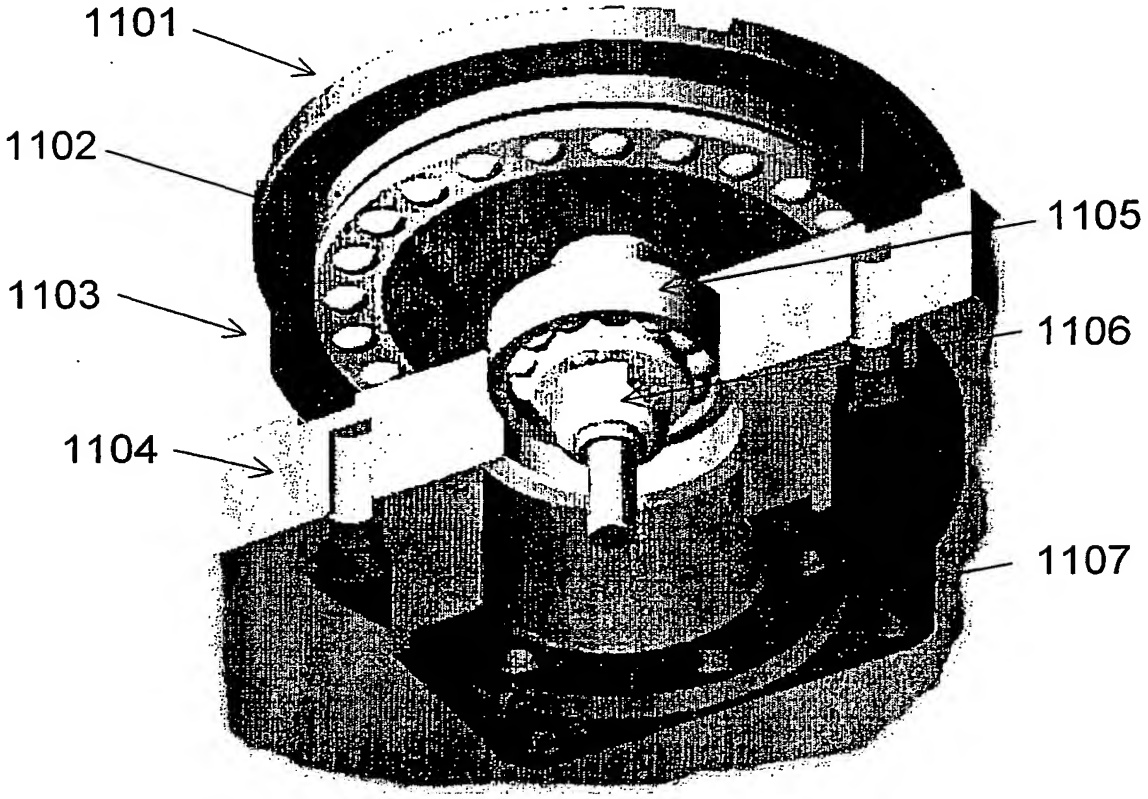

Figure 12

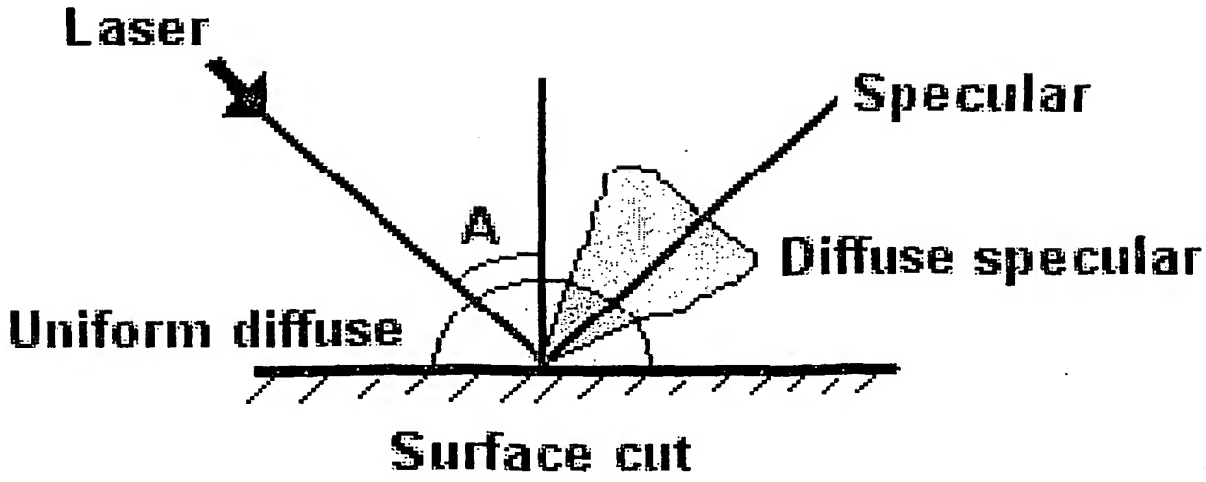

Figure 13

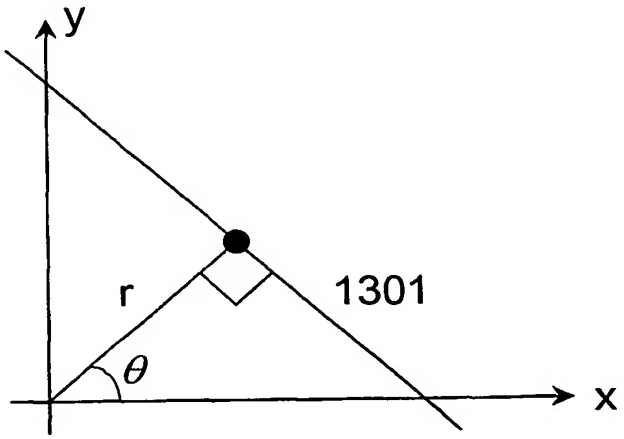

Figure 14

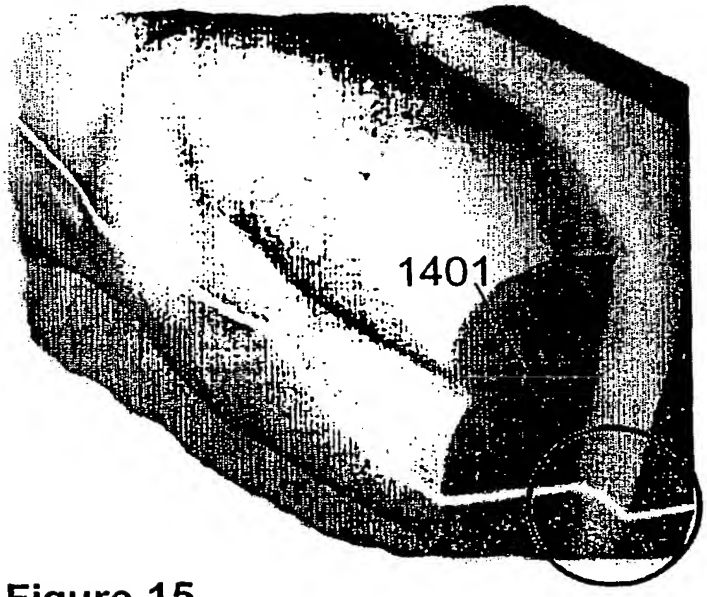

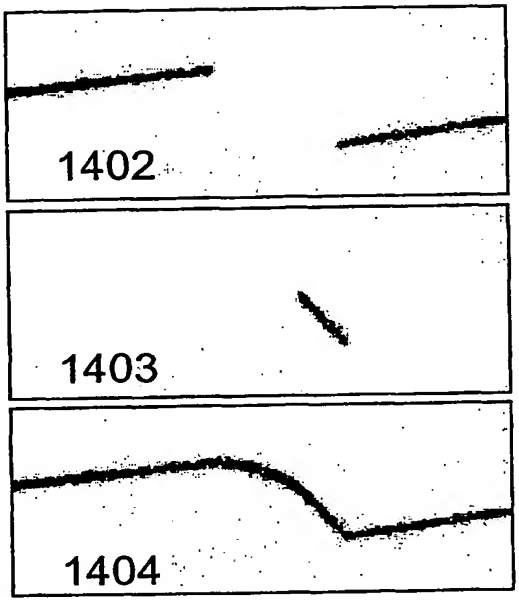

Figure 15

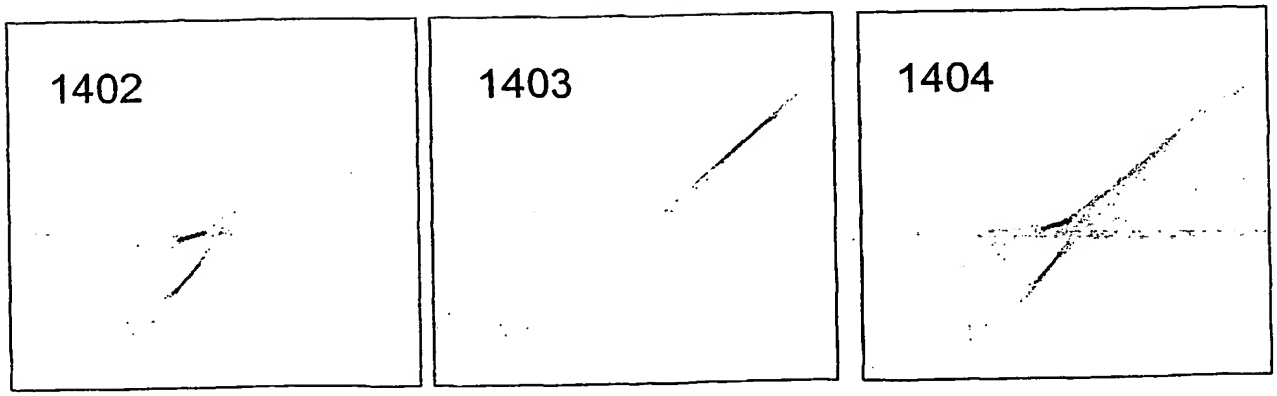

Figure 16

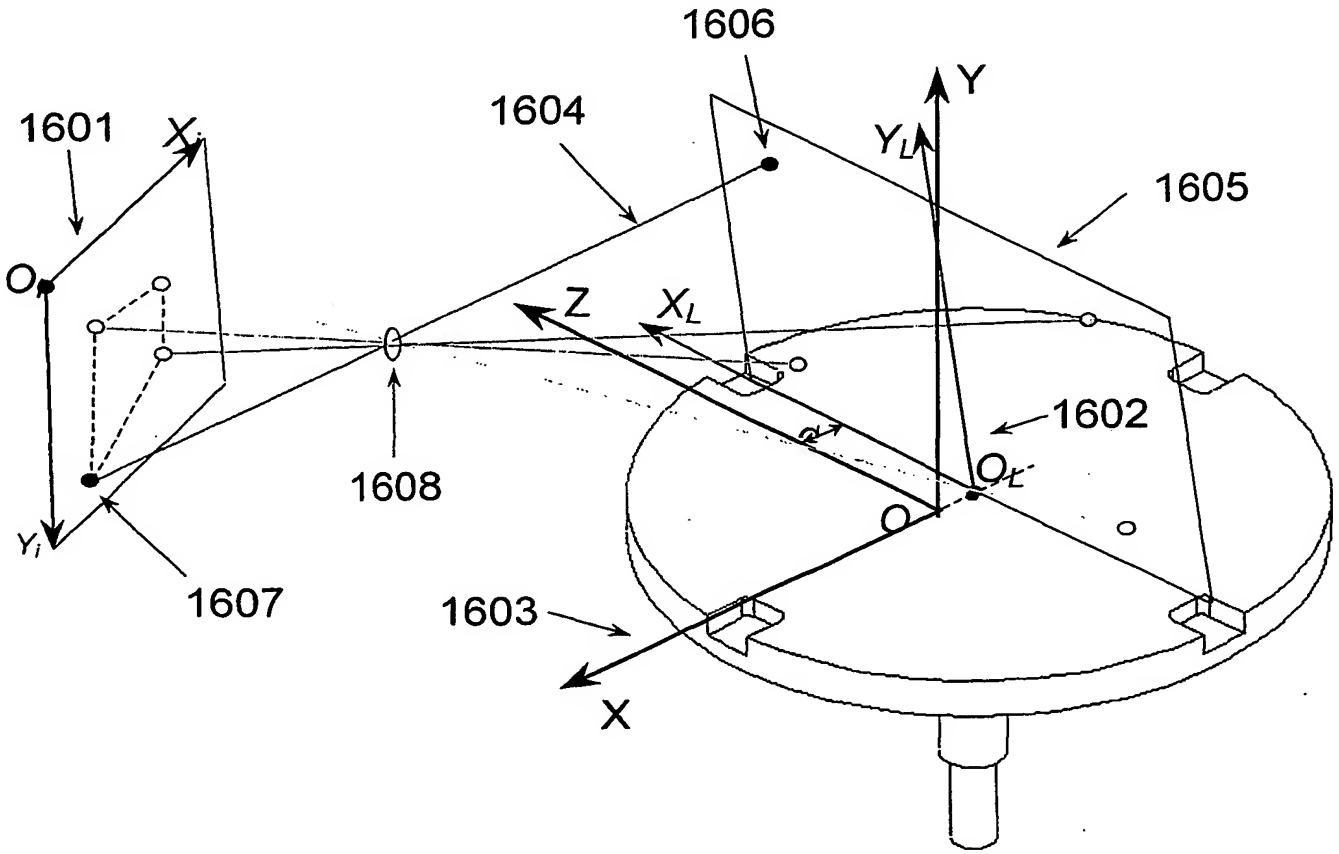

Figure 17

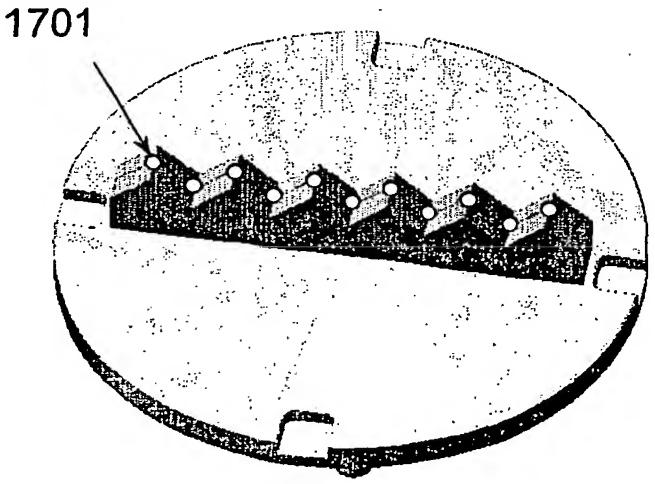

Figure 18

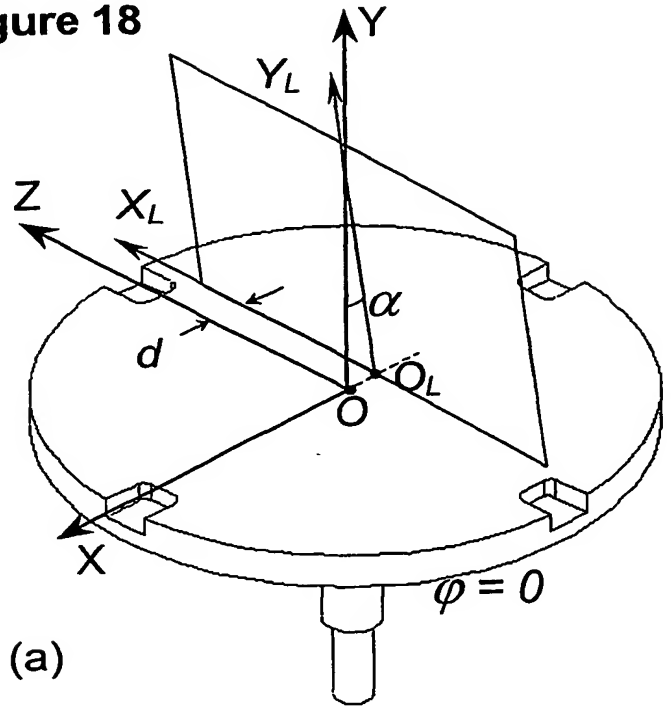

(a)

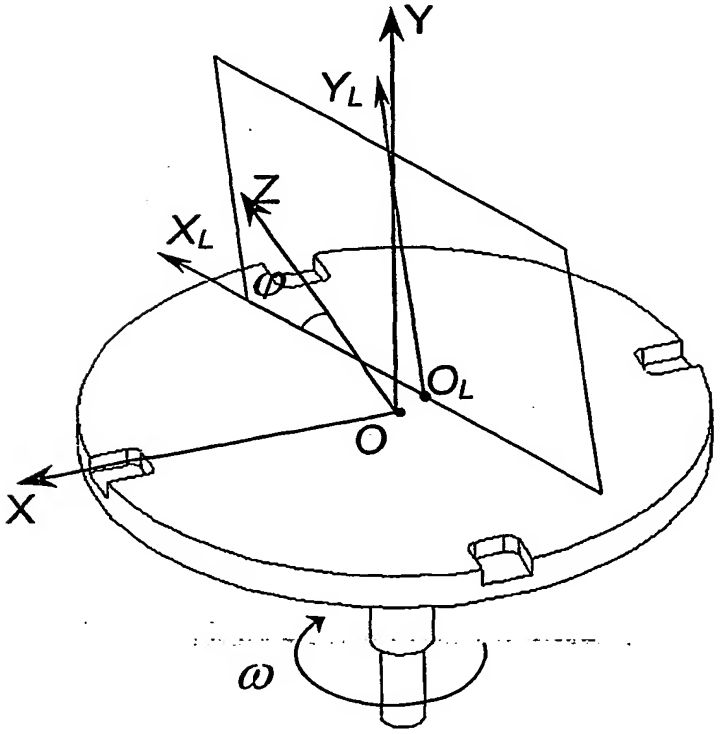

(b)

Figure 19

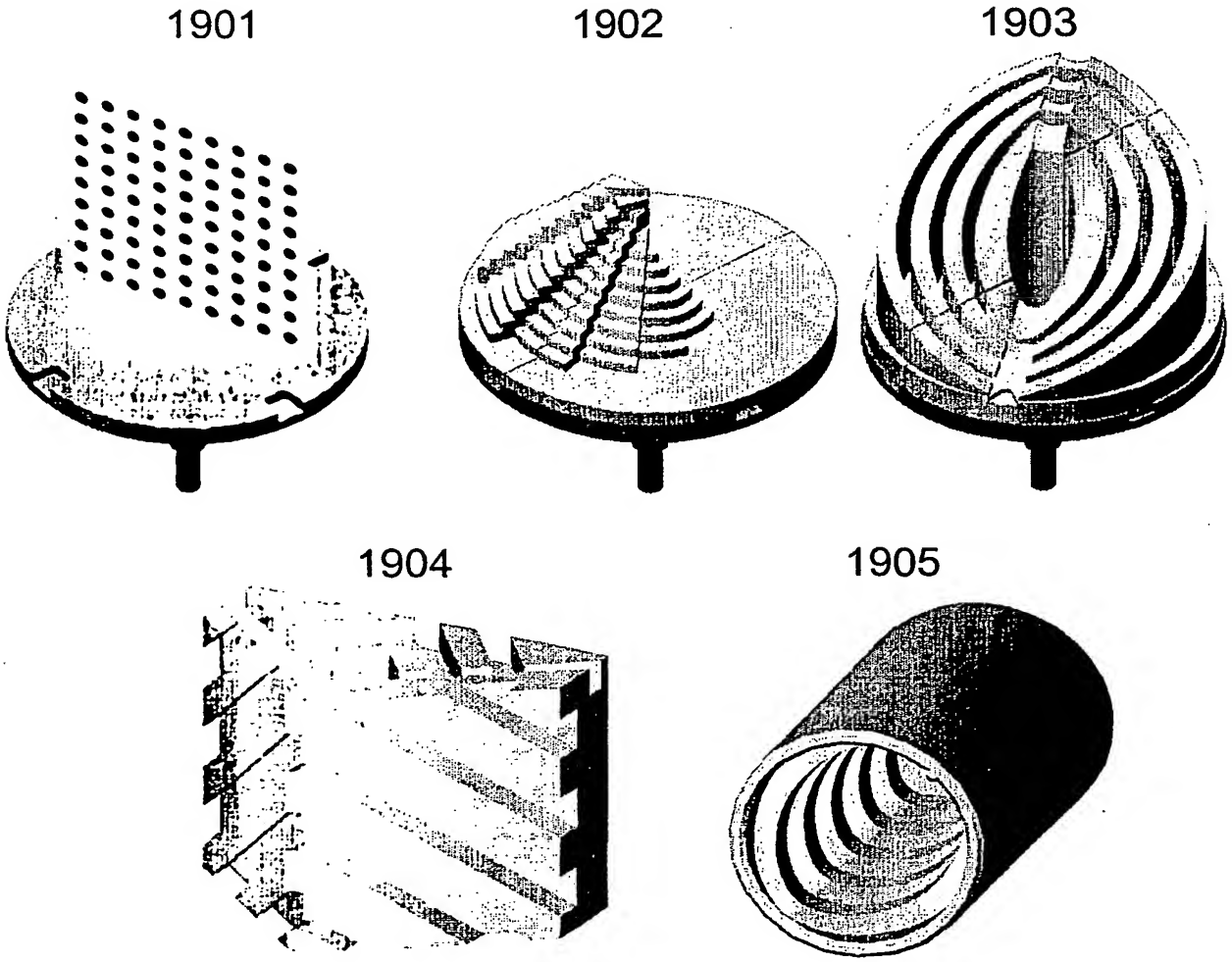

Figure 20

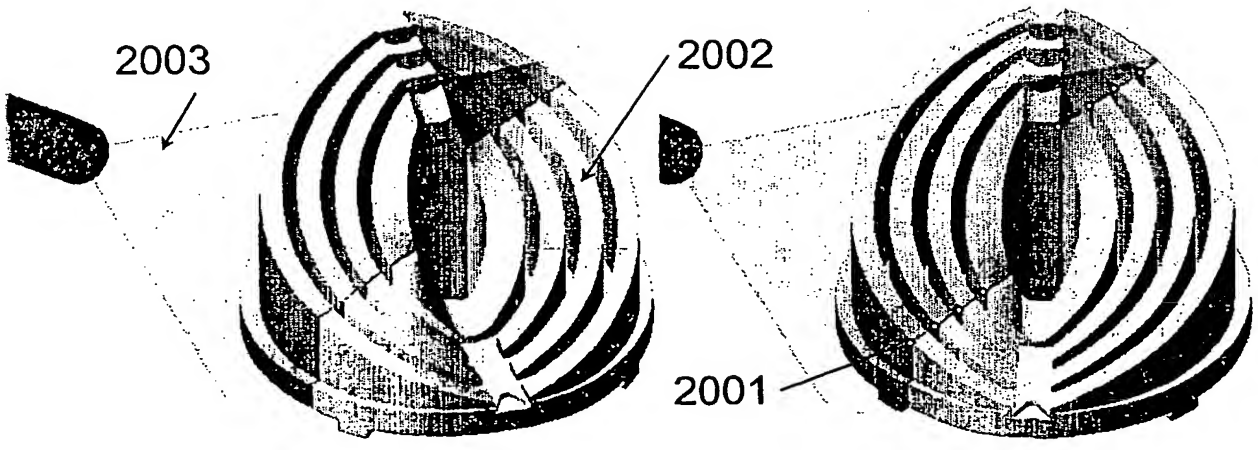

Figure 21

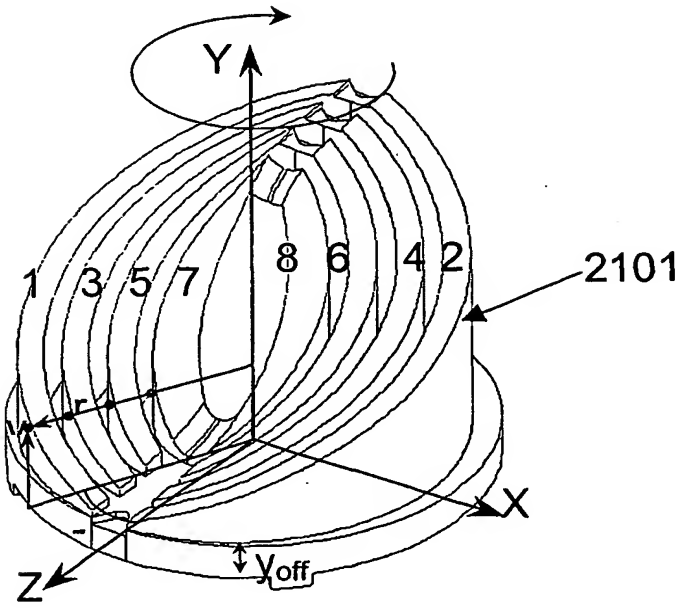

Figure 22

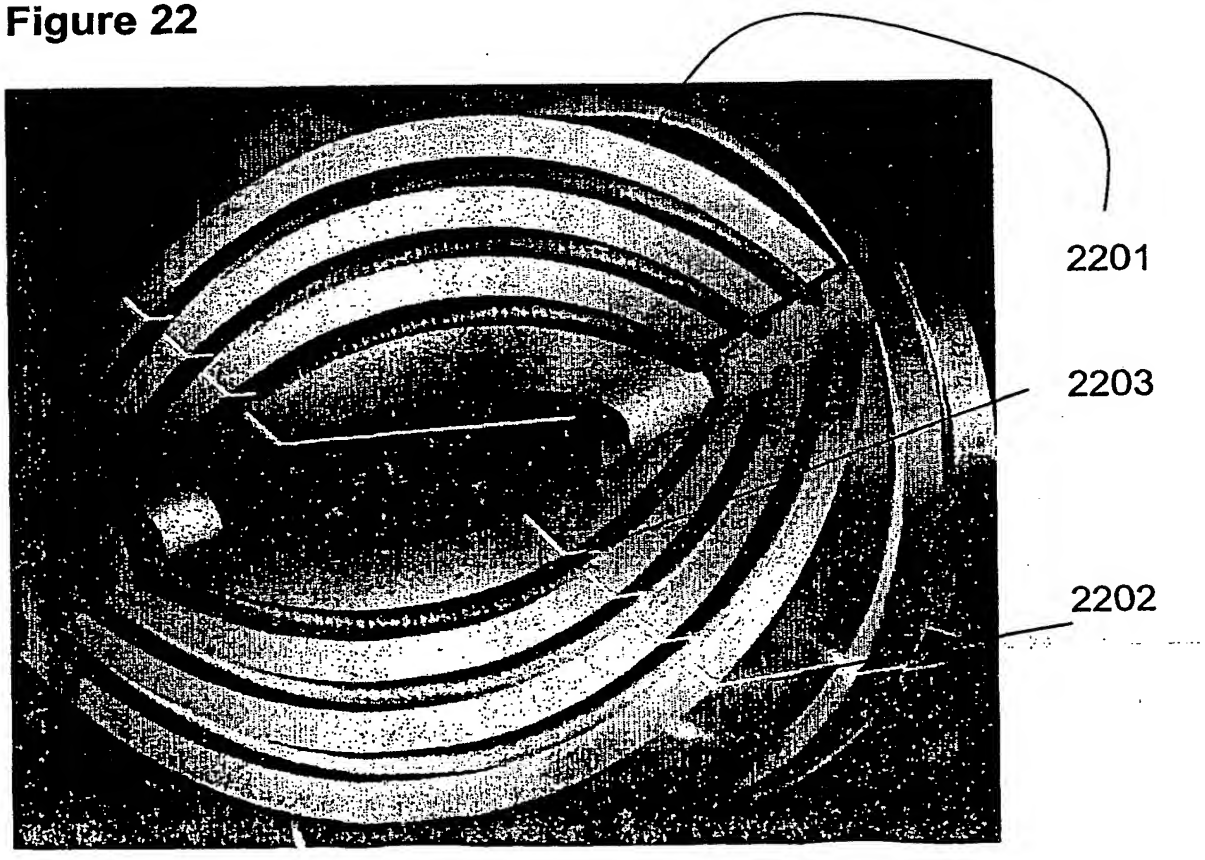

Figure 23

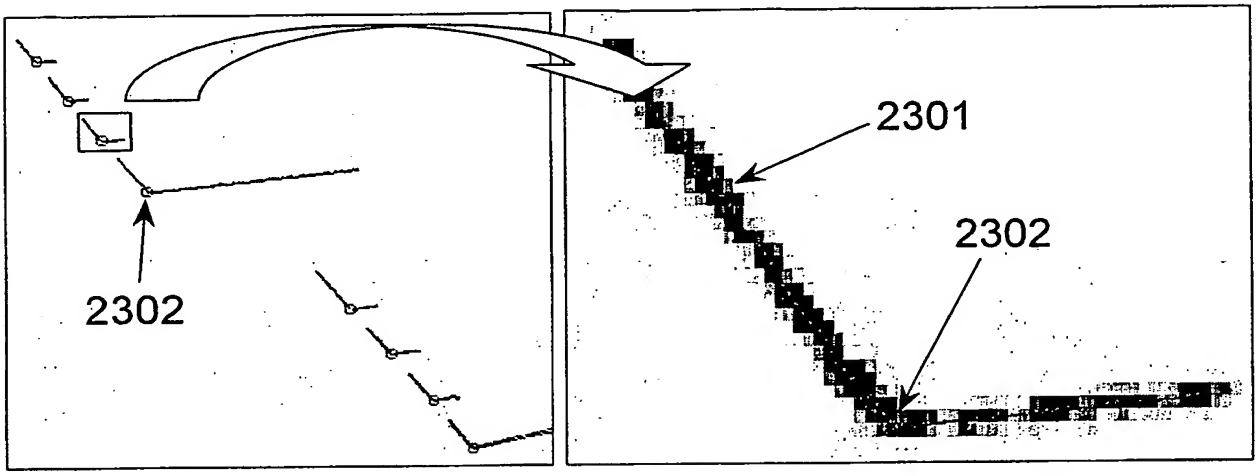

Figure 24

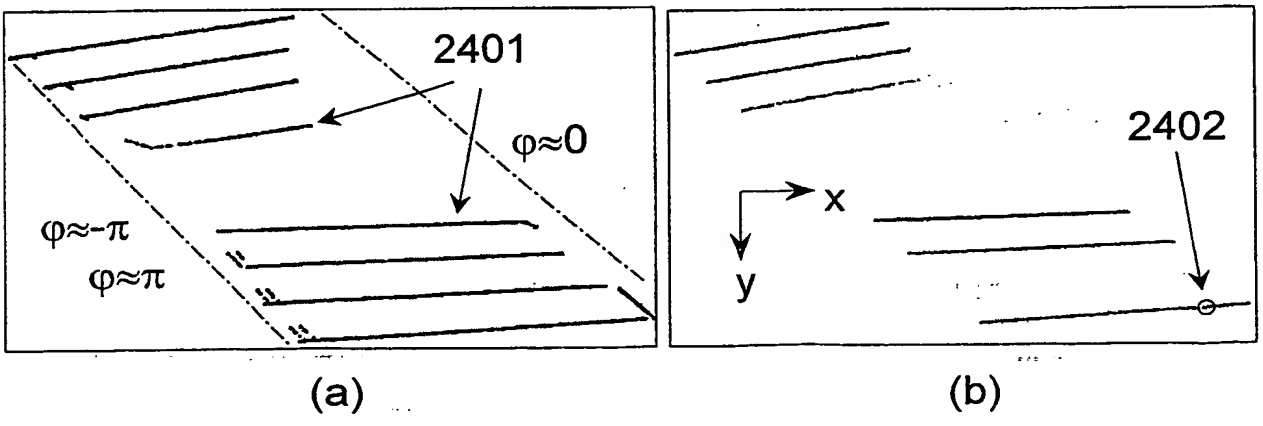

Figure 25

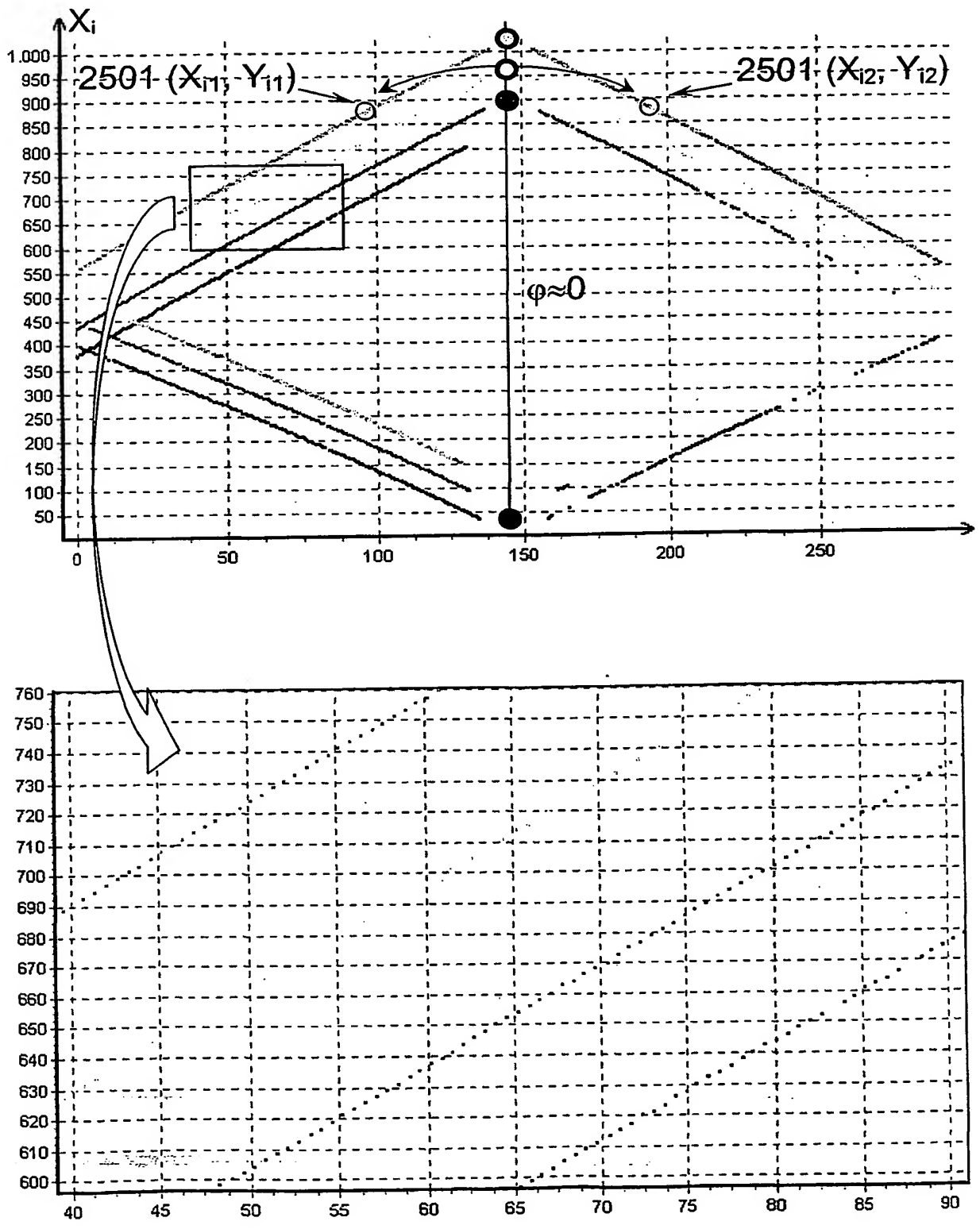
Xi
2501 (Xi1; Yi1)
2501 (Xi2; Yi2)
φ≈0
1.000
950
900
850
800
750
700
650
600
550
500
450
400
350
300
250
200
150
100
50
0
50
100
150
200
250
760
750
740
730
720
710
700
690
680
670
660
650
640
630
620
610
600
40
45
50
55
60
65
70
75
80
85
90

Figure 26

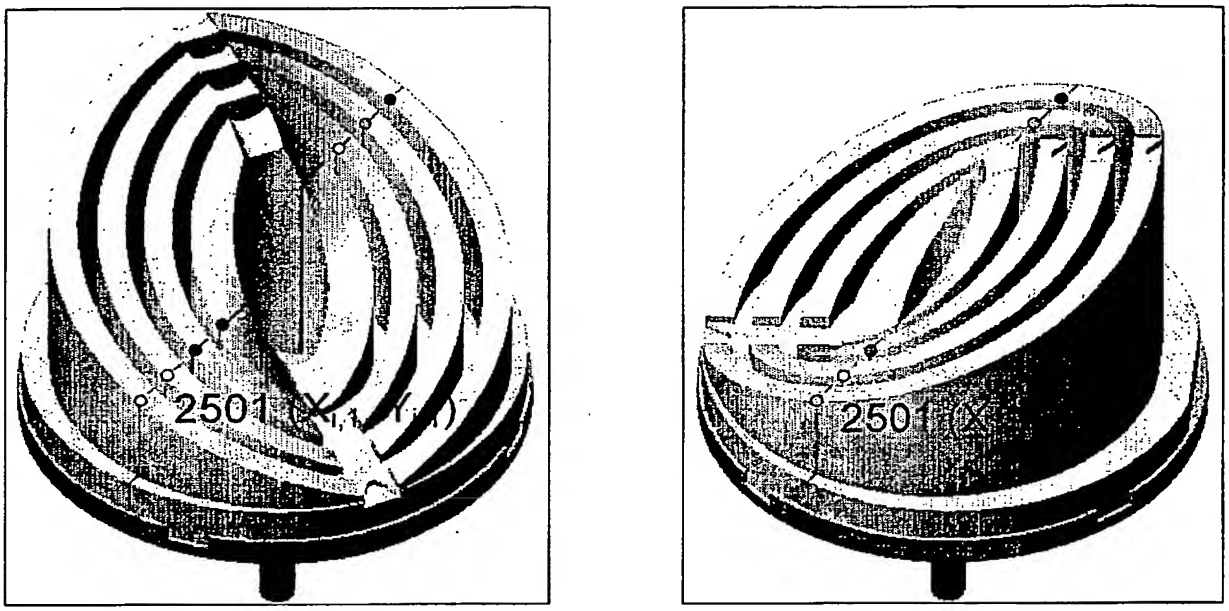

Figure 27

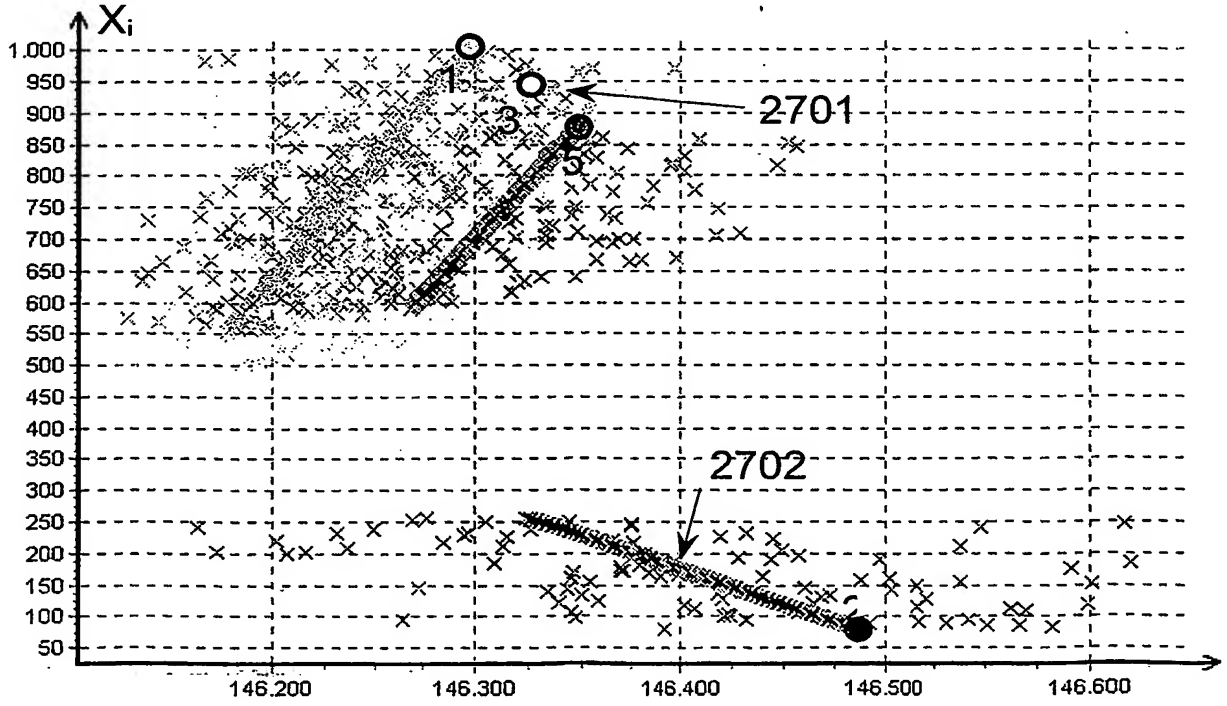

Figure 28

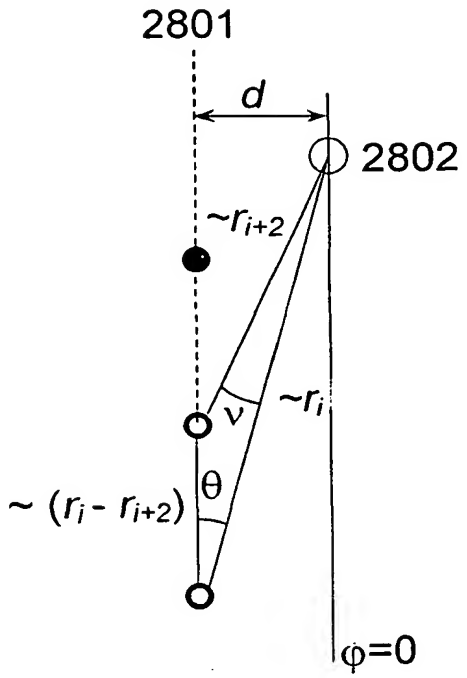

Figure 29

Figure 30

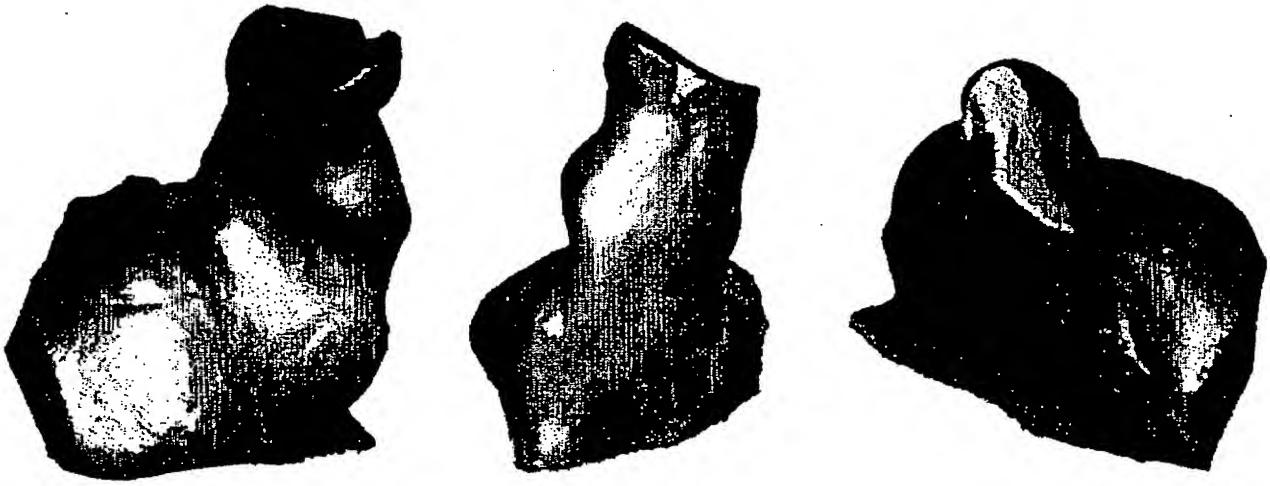

Figure 31

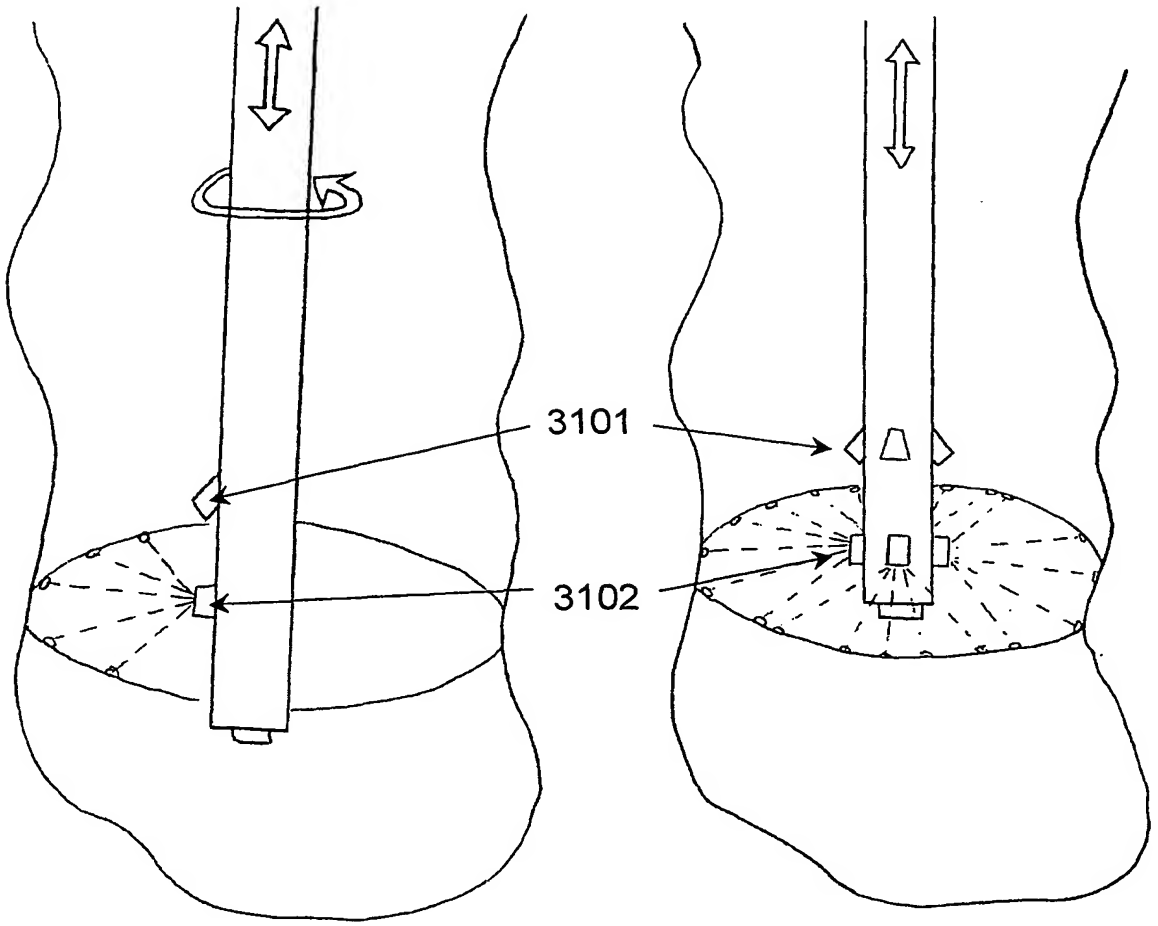

Figure 32

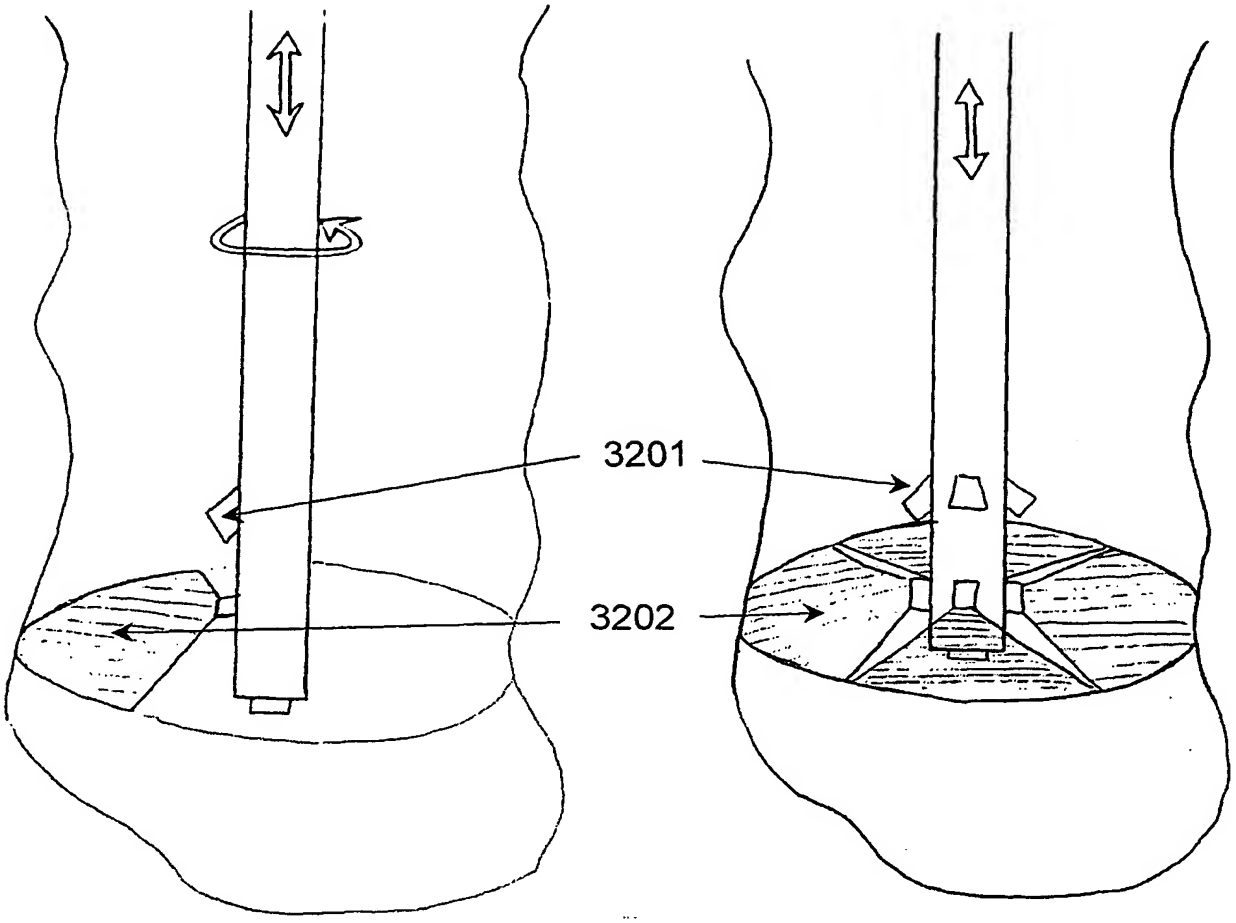

Figure 33

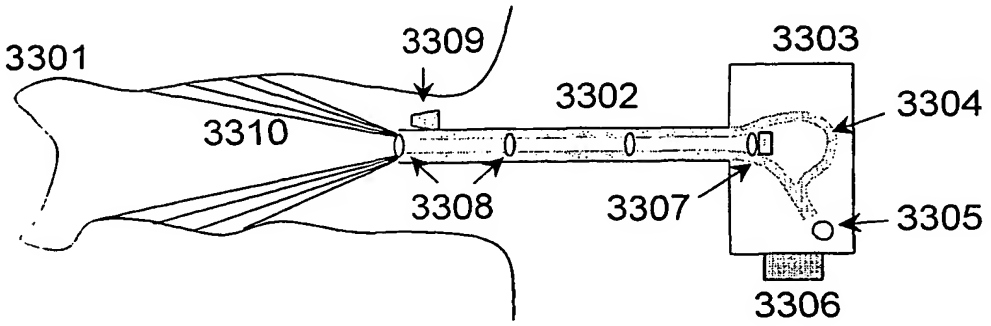

Figure 34

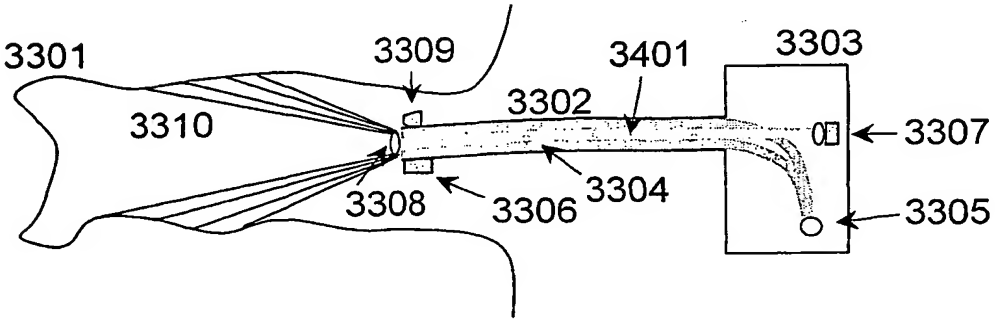

Figure 35

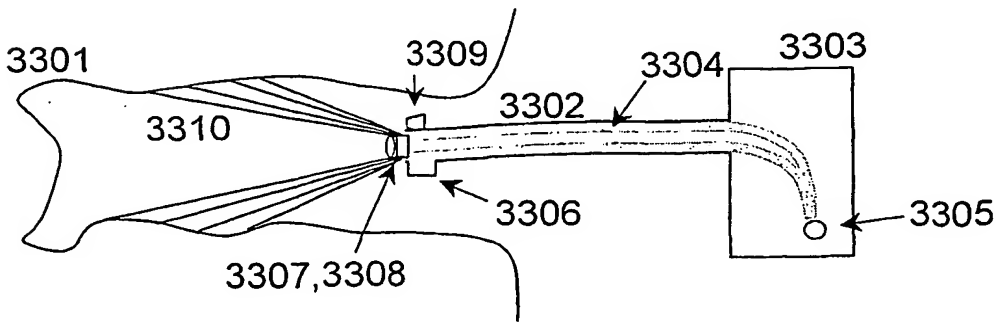

(12) INTERNATIONAL APPLICATION PUBLISHED UNDER THE PATENT COOPERATION TREATY (PCT)

(19) World Intellectual Property Organization
International Bureau

(43) International Publication Date
28 February 2002 (28.02.2002)

PCT

(10) International Publication Number
WO 02/16865 A3

(51) International Patent Classification[7]: G01B 11/25, 3/30

(21) International Application Number: PCT/DK01/00564

(22) International Filing Date: 24 August 2001 (24.08.2001)

(25) Filing Language: English

(26) Publication Language: English

(30) Priority Data:
PA 2000 01258 25 August 2000 (25.08.2000) DK
60/244561 31 October 2000 (31.10.2000) US

(71) Applicant *(for all designated States except US)*: 3SHAPE APS [DK/DK]; Bredgade 58; 2-3.sal, DK-1260 Copenhagen K (DK).

(72) Inventors; and

(75) Inventors/Applicants *(for US only)*: DEICHMANN, Nikolaj [DK/DK]; Kirsteinsgade 12, 1.sal, DK-2100 Copenhagen Ø (DK). CLAUSEN, Tais [DK/DK]; Viborggade 72A, 1.tv., DK-2100 København Ø (DK).

(74) Agent: HØIBERG APS; St. Kongensgade 59B, 4.sal, DK-1264 Copenhagen K (DK).

(81) Designated States *(national)*: AE, AG, AL, AM, AT, AT (utility model), AU, AZ, BA, BB, BG, BR, BY, BZ, CA, CH, CN, CO, CR, CU, CZ, CZ (utility model), DE, DE (utility model), DK, DK (utility model), DM, DZ, EC, EE, EE (utility model), ES, FI, FI (utility model), GB, GD, GE, GH, GM, HR, HU, ID, IL, IN, IS, JP, KE, KG, KP, KR, KZ, LC, LK, LR, LS, LT, LU, LV, MA, MD, MG, MK, MN, MW, MX, MZ, NO, NZ, PH, PL, PT, RO, RU, SD, SE, SG, SI, SK, SK (utility model), SL, TJ, TM, TR, TT, TZ, UA, UG, US, UZ, VN, YU, ZA, ZW.

(84) Designated States *(regional)*: ARIPO patent (GH, GM, KE, LS, MW, MZ, SD, SL, SZ, TZ, UG, ZW), Eurasian patent (AM, AZ, BY, KG, KZ, MD, RU, TJ, TM), European

[Continued on next page]

(54) Title: OBJECT AND METHOD FOR CALIBRATION OF A THREE-DIMENSIONAL LIGHT SCANNER

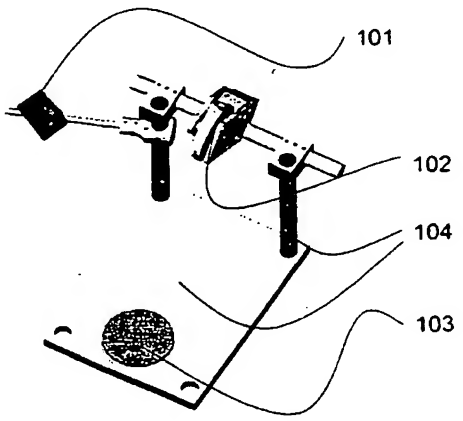

(57) Abstract: The invention relates to the field of precision calibration of three-dimensional light scanners. The invention specifically concerns a calibration object for calibration of all parameters of a three-dimensional light scanning system, the calibration object having at least one plane of symmetry and whereby at least one 3D object feature curve of each symmetric part is a continuous curve. The invention further relates to a method for calibration of a three-dimensional light scanner and a method for three-dimensional light scanning. Further specific embodiments for scanning of and modelling of objects for the ear and/or ear canal, and for scanning and modelling of dental implants are described.

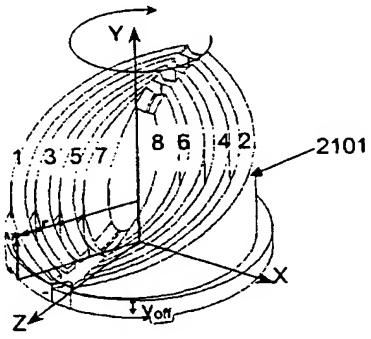

WO 02/16865 A3

patent (AT, BE, CH, CY, DE, DK, ES, FI, FR, GB, GR, IE, IT, LU, MC, NL, PT, SE, TR), OAPI patent (BF, BJ, CF, CG, CI, CM, GA, GN, GQ, GW, ML, MR, NE, SN, TD, TG).

Published:
— *with international search report*

(88) Date of publication of the international search report:
20 June 2002

For two-letter codes and other abbreviations, refer to the "Guidance Notes on Codes and Abbreviations" appearing at the beginning of each regular issue of the PCT Gazette.

INTERNATIONAL SEARCH REPORT

International Application No
PCT/DK 01/00564

A. CLASSIFICATION OF SUBJECT MATTER
IPC 7 G01B11/25 G01B3/30

According to International Patent Classification (IPC) or to both national classification and IPC

B. FIELDS SEARCHED

Minimum documentation searched (classification system followed by classification symbols)
IPC 7 G01B

Documentation searched other than minimum documentation to the extent that such documents are included in the fields searched

Electronic data base consulted during the international search (name of data base and, where practical, search terms used)

C. DOCUMENTS CONSIDERED TO BE RELEVANT

Category °	Citation of document, with indication, where appropriate, of the relevant passages	Relevant to claim No.
X	US 5 681 981 A (D.R.MACMURTRY) 28 October 1997 (1997-10-28) figures 1-14 * the whole document * ---	1-4,7, 12,15-17
A	US 4 185 918 A (P. DIMATTEO ET AL) 29 January 1980 (1980-01-29) column 3, line 44 -column 8, line 2; figures 1-9 column 9, line 42 -column 15, line 2; figures 15-19 --- -/--	1,2, 7-17, 20-23, 30,31, 34-36, 64,66, 67,77, 78,88

[X] Further documents are listed in the continuation of box C.

[X] Patent family members are listed in annex.

° Special categories of cited documents :

"A" document defining the general state of the art which is not considered to be of particular relevance

"E" earlier document but published on or after the international filing date

"L" document which may throw doubts on priority claim(s) or which is cited to establish the publication date of another citation or other special reason (as specified)

"O" document referring to an oral disclosure, use, exhibition or other means

"P" document published prior to the international filing date but later than the priority date claimed

"T" later document published after the international filing date or priority date and not in conflict with the application but cited to understand the principle or theory underlying the invention

"X" document of particular relevance; the claimed invention cannot be considered novel or cannot be considered to involve an inventive step when the document is taken alone

"Y" document of particular relevance; the claimed invention cannot be considered to involve an inventive step when the document is combined with one or more other such documents, such combination being obvious to a person skilled in the art.

"&" document member of the same patent family

Date of the actual completion of the international search	Date of mailing of the international search report
16 November 2001	05.03.02

Name and mailing address of the ISA	Authorized officer
European Patent Office, P.B. 5818 Patentlaan 2 NL - 2280 HV Rijswijk Tel. (+31-70) 340-2040, Tx. 31 651 epo nl, Fax: (+31-70) 340-3016	VISSER F.P.C.

1

Form PCT/ISA/210 (second sheet) (July 1992)

INTERNATIONAL SEARCH REPORT

International Application No
PCT/DK 01/00564

C.(Continuation) DOCUMENTS CONSIDERED TO BE RELEVANT

Category	Citation of document, with indication, where appropriate, of the relevant passages	Relevant to claim No.
A	US 5 506 683 A (YOON-MO YANG ET AL) 9 April 1996 (1996-04-09) * the whole document * figures 1-12	1-6,35, 37,64, 66-68, 70-72,78
A	GB 2 104 652 A (SRI INTERNATIONAL) 9 March 1983 (1983-03-09) page 3, line 3 -page 9, line 5; figures 1-15	35,36, 66-68, 70-72

Form PCT/ISA/210 (continuation of second sheet) (July 1992)

INTERNATIONAL SEARCH REPORT

national application No.
PCT/DK 01/00564

Box I Observations where certain claims were found unsearchable (Continuation of item 1 of first sheet)

This International Search Report has not been established in respect of certain claims under Article 17(2)(a) for the following reasons:

1. ☐ Claims Nos.:
because they relate to subject matter not required to be searched by this Authority, namely:

2. ☐ Claims Nos.:
because they relate to parts of the International Application that do not comply with the prescribed requirements to such an extent that no meaningful International Search can be carried out, specifically:

3. ☐ Claims Nos.:
because they are dependent claims and are not drafted in accordance with the second and third sentences of Rule 6.4(a).

Box II Observations where unity of invention is lacking (Continuation of item 2 of first sheet)

This International Searching Authority found multiple inventions in this international application, as follows:

see additional sheet

1. ☐ As all required additional search fees were timely paid by the applicant, this International Search Report covers all searchable claims.

2. ☐ As all searchable claims could be searched without effort justifying an additional fee, this Authority did not invite payment of any additional fee.

3. ☐ As only some of the required additional search fees were timely paid by the applicant, this International Search Report covers only those claims for which fees were paid, specifically claims Nos.:

4. ☒ No required additional search fees were timely paid by the applicant. Consequently, this International Search Report is restricted to the invention first mentioned in the claims; it is covered by claims Nos.:

1,35,66 and their subclaims

Remark on Protest

☐ The additional search fees were accompanied by the applicant's protest.

☐ No protest accompanied the payment of additional search fees.

FURTHER INFORMATION CONTINUED FROM PCT/ISA/ 210

This International Searching Authority found multiple (groups of) inventions in this international application, as follows:

1. Claims: 1,35,66 and their subclaims

   Claims 1-34, 35-65 and 66-89 treat a calibration object, the calibration of a three dimensional light scanner and the light scanner itself.

   1.1. Claim : 35 and its subclaims
   The subject matter treated in claims 35-65 concerns the calibration of a three dimensional light scanner

   1.2. Claim : 66 and its subclaims
   The subject matter treated in claims 66-89 concerns the light scanner itself.

2. Claim : 90 and subclaims

   Claims 90-113 describe a method for manufacturing a shell comprising a device for the ear of an individual

3. Claim : 114 and subclaims

   Claims 114-129 treat a method for manufacturing a dental implant for an individual

Please note that all inventions mentioned under item 1, although not necessarily linked by a common inventive concept, could be searched without effort justifying an additional fee.

INTERNATIONAL SEARCH REPORT

Information on patent family members

International Application No
PCT/DK 01/00564

Patent document cited in search report	Publication date	Patent family member(s)	Publication date
US 5681981 A	28-10-1997	DE 69513336 D	23-12-1999
		DE 69513336 T	02-03-2000
		EP 0692088 A	17-01-1996
		EP 0939295 A	01-09-1999
		WO 9520747 A	03-08-1995
		JP 8508579 T	10-09-1996
		US 2001042395 A	22-11-2001
		US 6226884 B	08-05-2001
US 4185918 A	29-01-1980	US 4508452 A	02-04-1985
US 5506683 A	09-04-1996	KR 9206740 B	17-08-1992
		KR 9206050 B	27-07-1992
		KR 9206741 B	17-08-1992
		KR 9308563 B	09-09-1993
		JP 7239219 A	12-09-1995
		US 5243872 A	14-09-1993
GB 2104652 A	09-03-1983	US 4412121 A	25-10-1983
		DE 3228014 A	10-03-1983
		DK 385982 A	01-03-1983
		FI 822967 A	01-03-1983
		FR 2511917 A	04-03-1983
		JP 58044972 A	16-03-1983
		NO 822589 A	01-03-1983
		SE 8204895 A	26-08-1982